Flood risk analysis of embanked river systems

Probabilistic systems approaches for the Rhine and Po rivers

Curran, A.N.

DOI
10.4233/uuid:3010a337-742c-4776-a747-2985085e981d

Publication date
2020

Document Version
Final published version

Citation (APA)
Curran, A. N. (2020). *Flood risk analysis of embanked river systems: Probabilistic systems approaches for the Rhine and Po rivers*. [Dissertation (TU Delft), Delft University of Technology].
https://doi.org/10.4233/uuid:3010a337-742c-4776-a747-2985085e981d

Important note
To cite this publication, please use the final published version (if applicable).
Please check the document version above.

FLOOD RISK ANALYSIS OF EMBANKED RIVER SYSTEMS

PROBABILISTIC SYSTEMS APPROACHES FOR THE RHINE AND PO RIVERS

FLOOD RISK ANALYSIS OF EMBANKED RIVER SYSTEMS

PROBABILISTIC SYSTEMS APPROACHES FOR THE RHINE AND PO RIVERS

Dissertation

for the purpose of obtaining the degree of doctor
at Delft University of Technology,
by the authority of the Rector Magnificus, Prof.dr.ir. T.H.J.J. van der Hagen,
chair of the Board for Doctorates,
to be defended publicly on
Friday 4 December 2020 at 12.30 hours

by

Alex CURRAN

Master of Science in Water Science and Engineering,
IHE Delft, Delft, The Netherlands,
born in Waterford, Ireland.

This dissertation has been approved by the promotors

promotor: Prof. dr. ir. M. Kok
copromotor: Dr. ir. K.M. De Bruijn

Composition of the doctoral committee:

Rector Magnificus,	chairman
Prof. dr. ir. M. Kok,	Delft University of Technology, promotor
Dr. ir. K.M. De Bruijn	Delft University of Technology, co-promotor

Onafhankelijke leden/Independent members:

Prof. dr. ir. S.N. Jonkman	Delft University of Technology
Prof. dr. A. Castellarin	University of Bologna
Prof. dr. F. Klijn,	Delft University of Technology
Prof. dr. B. Merz	GFZ German Research Centre for Geosciences
Dr. ir. R. Lammersen	Rijkswaterstaat

Reserve member:

Prof. dr. ir. P.H.A.J.M. van Gelder	Delft University of Technology

Keywords: Flood Risk, Uncertainty Analysis, Flood defences, System Behaviour, Rhine, Po

Printed by: Ipskamp Printing

Front & Back: Grasshopper Geography

ISBN 978-94-6421-121-4

An electronic version of this dissertation is available at
http://repository.tudelft.nl/.

No man is an island entire of itself;
Every man is a piece of the continent, a part of the main;
If a clod be washed away by the sea,
Europe is the less,
as well as if a promontory were,
as well as any manner of thy friends
or of thine own were;
Any man's death diminishes me,
because I am involved in mankind.
And therefore never send to know for whom the bell tolls;
It tolls for thee.

John Donne, 1623

CONTENTS

SUMMARY

Flooding causes more damage worldwide than any other natural disaster, and factors such as climate change and population growth are likely to increase future risk. Due to this increased threat, and as a reaction to some of the devastating floods seen in Europe in the early 21st century, the four year System-Risk project was initiated in 2015. The project consortium included academic, commercial and institutional partners, backed by the European Union's Horizon 2020 fund. Research from 15 PhDs was carried out on three system types relating to large-scale riverine flood risk; atmosphere-catchment systems, socio-economic systems, and river-dike-floodplain (or embanked river) systems, of which the latter is considered in the present study.

For anthropological reasons, the low-lying floodplains of embanked river systems are often densely populated with a high degree of assets and infrastructure exposed to inundation. While dikes reduce the probability of flooding, the sudden inundation caused by breaching of those dikes means that such events can often be catastrophic. To provide decision makers with information on flood impacts and to evaluate potential flood mitigation measures, 'risk-based' analyses are often carried out, where risk is considered to be a combination of probability and consequences.

In river systems with embankments, multiple branches or tributaries, flood inundation flows may originate from various sources, and take various pathways outside the main banks due to breaching and overflow. Flood risk analyses of such systems often miss or ignore these interactions and provide a limited understanding of the spatial and temporal dynamics of large-scale floods. Decisions and measures based on such risk analyses can be inefficient or transfer risk to other locations.

In embanked river systems, a 'systems approach' to flood risk analysis can be used to account for source and pathway interactions by integrating different hydrological, hydraulic and geotechnical components of the river-dike-floodplain system into a single model. In such an approach, the assessment of embankment failure is based on the reliability equation ($Z = R - S$), where failure occurs if the strength (or resistance - R) of the defence is lower than the hydraulic load (or solicitation - S) applied to it. These calculations are made over discretised sections of embankments and continually throughout the simulation period, meaning flooding resulting from failures at a given location will impact the rest of the (integrated) system being modelled. Probability distributions are generally adopted for the load and strength variables, and analyses are performed by simulating multiple events sampled from these distributions, i.e. the Monte Carlo method. Not only can this approach provide decision-makers with accurate estimates of local and system-wide risk, but it also provides a database of realistic simulations from which system understanding can be obtained.

The principal aim of this study was to build on the systems approach to flood risk analysis for embanked river systems. The approach was applied to two case studies which represent two of the most developed floodplain regions of Europe; the Po River

in Italy and the Dutch Rhine-Meuse delta. The systems approach has been utilised in studies by De Bruijn et al. (2014), Merz et al. (2016), Gouldby et al. (2012) and others, as it allows for flood risk management strategies that are effective for the entire basin. However, previous approaches have significant limitations and simplifications, both in terms of the methods used and the resulting information that can be provided for flood risk management decision-makers. Some of the most important limitations are briefly described below, followed by the methods and results of addressing them undertaken in this study.

- Insufficient representation of embankment strengths.
  The strengths of levees are often only characterised by their resistance to the high water level of an event, and not the duration of that event. Including this duration variable can impact both localised and system-wide estimates of risk.

- Insufficient representation of the river-dike-floodplain system and inundation patterns.
  Flood risk analyses should include all possible pathways for inundation. Existing systems approaches often ignore inundation pathways that flow back into the river or between compartmentalised regions in the floodplain.

- Lack of methods available to represent interdependent hydrological sources.
  In many cases, systems approaches are designed for simple river systems where only events originating in the main river channel are considered. In more complex systems the range of events caused by the interaction of multiple tributaries needs to be considered.

- Lack of methods providing decision makers useful flood risk information.
  Even with a well-developed analysis method for system behaviour, decision makers often require uncertainty and scenario analyses to accompany risk estimates. Methods to do so are lacking from current system behaviour studies.

As a first step, a method was developed to adapt existing probabilistic representations of dike strength in the Netherlands (fragility curves) to include duration as a variable (which has a large influence on piping and macrostability breach mechanisms). These were then used in a complete systems approach hazard analysis of the Rhine delta. Including the duration was expected to reduce the impact of the 'system behaviour' effect whereby upstream breaches reduce the discharge (and therefore risk) downstream. This is true at many locations, but the overall effect is more complex, and including the duration actually increases the expected number of breaches during extreme events compared to using existing fragility curves.

Next, a quasi-2D floodplain schematisation was developed to better represent the potential for 'negative' interdependencies in the Netherlands. Such interactions occur when the pathways of inundation 'shortcut' across floodplains between rivers or 'cascade' between protected floodplain compartments. This approach provided important understanding of inundation patterns and impacts in the floodplains, illustrated at three specific locations in the Dutch system. It also highlighted areas in which inundation

would cause significant pressures on secondary/regional defences or on the floodplain side of primary defences.

As a third step, a method to better represent interdependent hydrological sources was developed and applied to the complex network of tributaries on the Po River. In order to generate stochastic events for Monte Carlo simulations of the region, a statistical dependence model (a copula) was developed for these tributaries. The method produced accurate estimates of the distribution of flows and water levels in the region. A complete hazard analysis, including breaching, was also conducted, providing information that could be used to estimate the efficacy of large-scale mitigation measures (e.g. detention areas), as well as further evidence of the advantages of the overall systems approach.

The final aspect of this study was on generating risk information for use by decision-makers. Uncertainty and scenario analyses are all possible in a systems approach, but implementing them needs careful consideration of the relationships between components. To facilitate this, a framework on how to generate these analyses was developed and subsequently applied to the Dutch case study. The framework proved useful in generating this information, highlighting the importance and uncertainty of various components of the system. One of the most significant results for the case study showed that the expected annual damage due to riverine flooding in the Netherlands reduces from €85 - €64 million when calculated with a systems approach. This and other results demonstrate the importance of the framework for the decision making process.

In both case studies, a clear conclusion from the results is the importance of assessing the risk at a scale that can include all relevant processes and interdependencies. Doing so affects expected loads, failure probabilities, risk and has many implications for system understanding and future flood management decision making. It is also clear that the Monte Carlo method used in this systems approach is robust and provides a useful database of simulations which can be queried to facilitate better system understanding. Potential applications to other embanked river regions are also discussed, as well as limitations and recommendations for further research. It is expected that the developed components and overall approach will contribute to improved future flood risk analyses and thus flood risk management.

SAMENVATTING

Wereldwijd veroorzaken overstromingen meer schade dan alle andere natuurrampen samen, en factoren zoals klimaatverandering en bevolkingsgroei zullen het toekomstige risico waarschijnlijk doen toenemen. Naar aanleiding van deze verwachte risicotoename, en als reactie op een aantal grote overstromingen in Europa in het begin van de 21e eeuw, werd in 2015 het vierjarige EU System-Risk project opgestart. Het projectconsortium omvatte onderzoeksinstituten, overheden en bedrijven. Onderzoek van 15 PhDs werd uitgevoerd in drie werkpakketten met iedere hun eigen focus op een bepaald aspect van overstromingsrisico's van grote riviersystemen: interacties tussen atmosfeer en hydrologie; interacties tussen sociaal-economische en fysische systemen; en: interacties tussen rivier-dijk-achterland. De huidige studie is onderdeel van het laatst genoemde werkpakket.

De laaggelegen riviergebieden langs bedijkte rivieren zijn vaak dichtbevolkt en kennen een hoge dichtheid van bebouwing, infrastructuur en andere investeringen welke blootgesteld kunnen worden aan overstromingen. Waterkeringen beschermen het gebied tegen overstromingen en verkleinen dus de kans op en overstroming. Echter, een plotselinge overstroming veroorzaakt door het doorbreken van die waterkeringen kan rampzalige gevolgen hebben. Om beslissers van informatie te voorzien over de gevolgen van overstromingen en om mogelijke hoogwaterbeschermingsmaatregelen te beoordelen, worden vaak risico-analyses uitgevoerd, waarbij risico wordt beschouwd als een combinatie van overstromingskans en gevolgen van een overstroming. In bedijkte riviersystemen waarbij de rivieren splitsen in verschillende takken of juist bij elkaar komen vanuit verschilende zijrivieren, kunnen overstromingen verschillende oorzaken hebben, en kunnen dan ook verschillende patronen buiten de primaire waterkeringen volgen, als gevolg van het dijkdoorbraken en overlopen van dijken. Analyses van overstromingsrisico van zulke systemen missen of negeren vaak interacties tussen het rivier- en dijksysteem, en bieden een niet volledig inzicht in de ruimtelijke en temporele dynamiek van grootschalige overstromingen. Beslissingen en maatregelen op basis van deze risicoanalyses kunnen inefficiënt zijn of het risico naar andere gebieden overdragen.

Om rekening te houden met interacties in bedijkte riviersystemen, kan een 'systeembenadering' voor de analyse van overstromingsrisico worden gebruikt, door integratie in één enkel model van verschillende hydrologische, hydraulische en geotechnische componenten van het rivier-dijk-achterland systeem. Bij een dergelijke benadering is de beoordeling van dijkfalen gebaseerd op de betrouwbaarheidstheorie (Z = R - S), waarbij een falen optreedt als de sterkte (of 'resistance' - R) van de kering lager is dan de hydraulische belasting (of 'solicitation' - S). Deze berekeningen worden voor meerdere dijkvakken gemaakt en voortdurende tijdens de simulatie aangepast, en dit betekent dat overstromingen als gevolg van dijkdoorbaken op één bepaalde locatie de rest van het (geïntegreerde) gemodelleerde systeem beïnvloeden. Kansverdelingen worden, in het algemeen, gebruikt voor de belastings- en sterktevariabelen, en analyses worden uitge-

voerd door het simuleren van meerdere gebeurtenissen die uit deze kansverdelingen zijn getrokken (Monte Carlo-methode). Deze benadering kan niet alleen beslissers nauwkeurige schattingen geven van lokale en systeem-brede risico's, maar biedt ook een database met realistische simulaties waaruit systeeminzicht kan worden verkregen.

Het belangrijkste doel van deze studie was om de systeembenadering van het overstromingsrisico analyse voor bedijkte riviersystemen verder uit te bouwen. De benadering is toegepast op casestudy's die twee van de meest ontwikkelde gebieden langs riviersystemen van Europa vertegenwoordigen: de Po in Italië en de Nederlandse Rijn-Maasdelta. De systeembenadering is toegepast in studies van De Bruijn et al. (2014), B. Merz et al. (2016), Gouldby et al. (2012) en andere. Deze systeembenadering maakt het mogelijk om beheersplannen voor overstromingsrisico's te ontwikkelen die effectief zijn voor het hele stroomgebied. Vele andere benaderingen hebben echter aanzienlijke beperkingen en vereenvoudigingen, zowel wat betreft de gebruikte methoden als de daaruit voortvloeiende informatie die kan worden verstrekt aan beslissers voor het beheersen van overstromingsrisico's. Enkele van de belangrijkste beperkingen worden hieronder kort beschreven, gevolgd door de methoden en resultaten van het aanpakken ervan die in deze studie ontwikkeld zijn.

- Onvoldoende weergave van de sterkte van dijken.
  De sterkte van dijken wordt vaak alleen weergegeven door hun weerstand tegen de hoogste waterstand van een gebeurtenis, en niet tegen de duur van die gebeurtenis. Het opnemen van deze duur kan zowel lokale als systeem-brede risicoschattingen beinvloeden.

- Onvoldoende weergave van het rivier-dijk-achterland systeem en overstromingspatronen.
  Overstromingsrisico analyses omvatten in principe alle mogelijke routes voor overstromingen. Bestaande systeembenaderingen negeren vaak overstromingen die terugstromen in de rivier of tussen gecompartimenteerde gebieden in het achterland.

- Gebrek aan methoden om de onderlinge afhankelijkheid van hydrologische gebeurtenissen weer te geven.
  Vaak worden systeem benaderingen ontworpen voor eenvoudige riviersystemen waarbij alleen gebeurtenissen die afkomstig zijn uit het hoofdrivier worden beschouwd. In complexere systemen wordt rekening gehouden met de reeks van gebeurtenissen die worden veroorzaakt door de interactie van meerdere zijrivieren.

- Gebrek aan methoden die beslissers nuttige informatie over overstromingsrisico's bieden.
  Zelfs met een goed ontwikkelde analysemethode voor systeemwerking, hebben beslissers vaak onzekerheid- en scenarioanalyses nodig bij risicoschattingen. Methoden om deze analyses te maken ontbreken in de huidige studies over systeemwerking.

Als eerste stap werd in dit onderzoek een methode ontwikkeld om bestaande Nederlandse probabilistische inschatting van dijksterkte (fragility curves) aan te passen om

ook de duur van het hoogwater als variabele op te nemen. De duur van een hoogwatergolf is met name belangrijk voor de mechanismen 'piping' en 'macrostabiliteit'. Deze aanpassing werd vervolgens toegepast in een systeembenadering van de Rijndelta met dijkdoorbraken. Het opnemen van de duur zou naar verwachting de invloed van 'systeemwerking' verminderen, omdat stroomopwaartse dijkdoorbraken de afvoer (en dus het risico) stroomafwaarts verminderen. Dit geldt op veel locaties, maar het totale effect is complexer, en het opnemen van de duur verhoogt zelfs het verwachte aantal dijkdoorbraken tijdens extreme gebeurtenissen ten opzichte van het gebruik van bestaande fragility curves.

Vervolgens werd een quasi-2D schematisering van het achterland ontwikkeld om 'negatieve' onderlinge afhankelijkheden in Nederland te onderzoeken. Dergelijke interacties treden op wanneer een overstroming een 'shortcut' over het achterland tussen verschillende rivieren veroorzaakt, of dat er een 'cascade effect' optreedt tussen bedijkte compartimenten. Deze benadering levert belangrijk inzicht op over overstromingspatronen en effecten in het acherland, geïllustreerd op drie specifieke locaties in het Nederlandse rivierensysteem. Het gaf ook de gebieden aan waar een overstroming een aanzienlijke extra belasting op secundaire / regionale waterkeringen of op de achterlandzijde van primaire waterkeringen zou veroorzaken.

Als derde stap werd een methode ontwikkeld om onderlinge afhankelijke hydrologische gebeurtenissen beter weer te geven. Deze methode werd vervolgens toegepast op het complexe netwerk van de zijrivieren van de Po-rivier. Om stochastische gebeurtenissen voor Monte Carlo simulaties van dit gebied te genereren, werd een statistisch afhankelijkheidsmodel (een copula) ontwikkeld voor deze zijrivieren. De methode verschafte nauwkeurige schattingen op van de verdeling van afvoeren en waterstanden in het gebied. Er werd ook een volledige risico-analyse uitgevoerd, met inbegrip van dijkdoorbraken, waarbij informatie werd verschaft die zou kunnen worden gebruikt om de efectiviteit van grootschalige maatregelen (bijv. retentiegebieden) in te schatten, één van de voordelen van de systeembenadering.

Het laatste aspect van dit onderzoek was het genereren van risico-informatie voor gebruik door beslissers. Onzekerheid- en scenario-analyses zijn allemaal mogelijk in een systeembenadering, maar het gebruik daarvan vereist een zorgvuldige beschouwing van de relaties tussen de verschillende onderdelen van het systeem. Om dit mogelijk te maken, is een kader (framework) ontwikkeld voor het uitvoeren van deze analyses. Deze is vervolgens toegepast op de Nederlandse casestudie. Het kader bleek nuttig bij het genereren van deze informatie en benadrukte het belang en de gevoeligheid van verschillende onderdelen van het systeem. Een van de belangrijkste resultaten toonde aan dat de verwachte jaarlijkse schade door overstromingsrisico's in Nederlandse rivieren vermindert van €85 tot € 64 miljoen, berekend met een systeembenadering. Deze en andere resultaten tonen het belang van het kader voor het besluitvormingsproces aan.

Een duidelijke conclusie uit de resultaten van beide casestudies is dat het van belang is om de schaal van de relevante processen en onderlinge afhankelijkheden goed in te schatten. Dit heeft gevolgen voor hydraulische belastingen, faalkansen, risico's en heeft veel implicaties voor het begrip van het systeem en de besluitvorming over overstromingen. Het is ook duidelijk dat de Monte Carlo-methode die in deze systeembenadering wordt gebruikt, robuust is, en een nuttige database met simulaties oplevert. Mogelijke

toepassingen naar andere bedijkte riviergebieden zijn ook aangegeven, evenals beperkingen en aanbevelingen voor verder onderzoek. Verwacht wordt dat de ontwikkelde onderdelen en de integrale aanpak bij zullen dragen aan betere analyses van het toekomstige overstromingsrisico en dus ook aan de beheersing van het overstromingsrisico.

1

INTRODUCTION

1.1. FLOOD RISK ANALYSIS (FRA)

1.1.1. FRA BASICS

The first human civilizations primarily developed around riverine regions (such as the Indus valley and Mesopotamia) due to the availability of transport, food and fertile floodplains. However, as these societies grew, controlling the course of the river and protecting against floods became more important, and so man-made embankments such as levees[1] were deemed necessary. Examples of the construction of levees as a large-scale societal project are seen on the Yellow River in China as far back as the 5th century B.C.E. (Chen et al., 2012). The water management provided by these constructions helped fuel the growth of the societies, but also created dynamic 'socio-hydrological' phenomena between the rivers and societies such as the 'levee effect' (Di Baldassarre et al., 2015), in which an increase in population and assets (and thus risk) in the floodplains is sometimes caused by the increased protection afforded by building a levee.

This levee effect has continued with the explosion in population over the last century, and an estimated 1 billion people (Di Baldassarre et al., 2013) now live in riverine floodplains, with 21 million people affected by flooding every year on average (Winsemius et al., 2016). Economically, flooding is known to be the most costly of all natural hazards, with over $30 billion of damage per year (The OFDA/CRED International Disaster Database, 2014). Climate change effects may also exacerbate the problem, as a 2°C increase in global temperatures could cause significant changes in both damage and the number of people affected by flooding (as seen in Figure 1.1 - Alfieri et al. 2017).

During the second half of the 20th century, in order to prioritise regions vulnerable to flooding and to evaluate the effectiveness of measures to protect them, the concept of flood risk as a calculable value was promoted, and given the following definition by the United Nations (UN-DHA, 1992);

[1] 'Dikes' and 'levees' are not made distinct in this study, and the terms are used interchangeably. Embankments are used more generally to describe any protective structure on the river bank, including levees or walls.

1

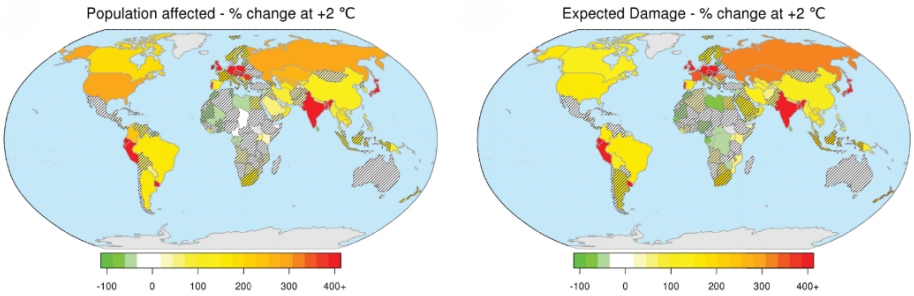

Figure 1.1: Expected increase in people affected by riverine floods due to a 2 degree in global surface temperatures(Alfieri et al., 2017).

> *Risk is the expected loss (of lives, persons injured, property damaged, and economic activity disrupted) due to a particular hazard for a given area and reference period.*

Methods to evaluate this risk can either be qualitative (using subjective classes to delineate categories of risk) or quantitative (where an indicator of risk is calculated, such as expected economic damage or people affected). However, when using flood risk (or the reduction in risk) as the basis for the evaluation of large, costly defence projects, quantitative assessments are usually preferable, so as to clearly demonstrate the benefit to society. For this reason, the definition is often made more mathematically explicit by using the equation $Risk = Probability * Consequence$ (Klijn et al., 2015), where risk is defined over a certain period. For a single event, the consequences (e.g. economic damage, number of deaths) are the combination of flood event hazard characteristics (water depth, extent, etc.) and the vulnerability (how much loss is caused by those hazards). An extensive literature review on methods to relate these two aspects (hazard and vulnerability) has been performed by Merz et al. (2010). The probability is the likelihood of experiencing or exceeding those event consequences during the defined period.

The total risk from all possible events over a certain period can be defined as the expected damage, or more generally, expected consequences, $E(C)$. This can be calculated by integrating all possible consequences (C) over their corresponding probability density function $f_c(C)$;

$$TotalRisk = E(C) = \int C f_c(C) dC \tag{1.1}$$

For the flood risk analysis of a given area, the formula requires calculating the consequences associated with various exceedance probabilities (for example: the economic damage that has an annual exceedance probability of 0.01). Extreme-value theory (EVT - Gumbel and Lieblein 1954) is a useful statistical tool in this regard. EVT is often used to create distributions of flood hazard metrics in 'flood frequency analyses', which in turn can be used as inputs for flood risk analyses. The distributions are generally applied as hydrological boundaries to the area of interest and, using multiple simulations and various statistical methods (e.g. Monte Carlo method, as discussed in subsection 1.6.1), the distribution of consequences resulting from the flood hazard variables can be calculated.

In the set-up of such a risk analysis, it is crucial to ensure that the complete range of possible flood events can occur within the area of the model, including all major sources and pathways for the inundation.

1.1.2. INTERDEPENDENCY PROBLEMS

In terms of the potential sources of flooding, Vorogushyn et al. (2017) highlight the problem of 'spatiotemporal dependencies' not being accounted for in many flood risk analyses. This is observed when analyses derive flood maps and other datasets that assume flood hazards of a particular exceedance probability occur synchronously and homogeneously across the whole region of interest. Estimating risk based on such datasets ignores the dependencies between areas in the overall system. As the size of the area of interest increases, and more variability is introduced by rainfall patterns and different branches and tributaries, this omission will have a greater impact on the calculated risk.

For the pathways of inundation, it is important to consider how risk is distributed and transferred in the region of interest. In an embanked system, as the severity of an event increases (and the probability decreases), flows from the river channel to the floodplain[2] become more likely, due to the overflow of the river into floodplains and 'breaching', in which the structural failure of an embankment allows flow to pass through it. When such an event changes the temporal or spatial distribution of risk at another location, it is considered to be part of a range of effects studied in relation to flood risk, variously called 'system behaviour' (De Bruijn et al., 2014) or 'load interdependencies', and described in section 1.2.

The present work tries to address these two (inter)dependency problems (loads and spatiotemporal) with a 'systems approach' Leonard and Beer (1994) to flood risk modelling of large-scale embanked river systems. The general need for such approaches in FRA is highlighted by Vorogushyn et al. (2017), and the present study provides a framework for doing so as well as developing and improving various components of the approach. The two interdependency effects are often poorly represented in flood risk analyses, (and therefore also in risk management decisions), most likely due to the complexity and uncertainty of breaching and tributary dependencies. However, as well as the improved accuracy of risk estimates when the dependencies are included, the system understanding achieved by modelling these processes can allow for new effective solutions to be developed that reduce overall risk. By incorporating a systems approach with a better understanding of natural and man-made processes, as well as utilising increased computational power, future flood risk assessments can start to incorporate these interactions and provide improved estimates of risk for decision-makers.

The systems approach used in this study is described below, along with knowledge gaps of existing implementations of this approach. The two main variable inputs for the approach (hydrological loads and defence strengths) are then described, followed by the case studies and tools. Finally, a summary of the research objectives and outline of the rest of the thesis is given.

[2] The term 'floodplain' is here used to denote areas vulnerable to flooding due to a breach. This is in contrast to the use of the term in the Netherlands, where the floodplain is usually in between the embankments and river channel

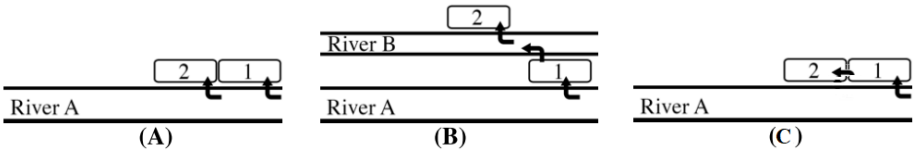

Figure 1.2: Hypothetical examples of positive (A) and negative (B and C) system behaviour (adapted from Dupuits et al.)

1.2. SYSTEMS APPROACH TO FRA

1.2.1. GENERAL APPROACH

The definition of risk given by the UN-DHA in section 1.1 states that the risk should be evaluated for a 'given area' and 'reference period'. For riverine flood risk, the reference period must be sufficiently long to ensure that one meteorological event (e.g. a rainstorm) or hydrological event (e.g. spring snow melt) is not considered to be the cause of multiple distinct floods. For this reason, the risk for future unknown events is usually calculated for a calendar or hydrological year. This can then be easily expanded to estimate risk over longer time periods, for example over the life-cycle of a structure. The definition of a 'given area' is, however, more difficult to clarify, and necessitates an approach where interactions between different processes (hydrological, hydraulic and geotechnical, amongst others) are accounted for.

For a risk assessment of river flooding, a simple option would be to set the 'given area' or region of interest to the river catchment boundary. This ensures that any given flood event develops entirely within this region and can be characterised by processes or systems within it (e.g. hydrological or geotechnical). Analysis at these scales is therefore a core aspect of a systems approach. However, larger catchments are less likely to coincide with administrative boundaries, and the authorities responsible for flood protection of a certain region are less interested in the flooding outside of that region. For this reason, practical decisions must be made as to the boundaries of the system, based on available knowledge.

With temporal and spatial boundaries of the risk analysis set, the modelled system must then include all sources and pathways for flooding, considering the dependency problems highlighted in section 1.1. Concepts similar to 'System behaviour' include 'load interdependencies' (Klerk, 2013), 'river system behaviour' (Van Mierlo et al., 2003) and 'system-risk' (Gouldby et al., 2012). In essence, the effect being described in these definitions relates to the temporal or spatial change in risk at one location due to flooding that originates at another location. 'Positive' or 'negative' system behaviour effects relate to situations that reduce or increase risk respectively (Dupuits et al., 2016). For example, in Figure 1.2A, flooding at location 1 would reduce the discharge (and therefore risk) at location 2, creating a positive dependency. In Figure 1.2B, however, flooding at location 1 might actually increase the risk at location 2 by 'shortcutting' flood flows from one river to another, creating a negative dependency.

A third aspect that may need to be included in a risk analysis is the phenomenon of 'cascading' flows. System behaviour is usually more applicable to large river systems

with low-lying floodplains which are often 'compartmentalised' by human infrastructure and defences (Alkema and Middelkoop, 2005). Such divisions are seen on major European rivers such as the Po (Castellarin et al., 2011) and Rhine (Klijn et al., 2010), as well as the Mississippi (Jonkman and Kok, 2008). While a compartment connected to the river is at risk of flooding from the river directly, it is also possible that flooding flows from one compartment to the next, for example in Figure 1.2C. In this case the upstream flooding would be considered to have a negative effect on the risk downstream. All three interactions can be accounted for by analysing the complete system, and this is a principal goal of Chapter 3 of this study.

Using a large-scale systems approach can also help account for the spatiotemporal dependencies of flood events (Vorogushyn et al., 2017). Over a large system, a single meteorological event can cause flows with varying severities and timings in the different river channels and tributaries. By modelling the entire system, and using the complete range of sources of flooding, the spatiotemporal patterns of flooding appear 'naturally' within the system, as shown for the case study in Chapter 4.

As described above, large-scale analyses can account for dependencies by including the dependencies occurring within the river system (breaches etc.) and the hydrological system (correlated flows etc.). Therefore, a practical approach for the FRA of embanked river systems is to create a model of the system of interest that includes important subprocesses like the routing network and defences, and to input uncertainty distributions that try to account for every flooding possibility. In doing so, the distribution of consequences can be obtained for use in Equation 1.1.

This approach is used in the present study, and can be roughly summarised by the diagram in Figure 1.3. The two main inputs (hydrological loads and defence strengths) are given respective letter designations to relate them to the reliability equation ($Z = R–S$), as discussed in section 1.4. These inputs are used to generate multiple simulations of the overall system, and the aggregation of those simulations provide hazard distributions. In the present study, the relationship between hazard and impact is not a primary focus, so vulnerability is considered to be a deterministic property of the floodplain system. This means that risk can be directly calculated from hazard.

1.2.2. KNOWLEDGE GAPS

Similar implementations of the systems approach given in Figure 1.3 have been used to solve load and spatiotemporal dependency problems for embanked river systems in the works of De Bruijn et al. (2014), Merz et al. (2016), Gouldby et al. (2012) and others. However, these works have various limitations, both in terms of the methods used and the resulting information that can be provided for flood risk management decision-makers. Some of the limitations are briefly described below, with reference to (where applicable) subsequent sections that provide a more detailed literature review. The limitations include;

– No methods available to represent hydrological dependence (section 1.3).
  In many cases, systems approaches are designed for simple river systems with the only source of possible inundation coming from one river channel. In more complex systems the spatiotemporal dependencies of multiple tributaries need to be included in the hydrological load distribution (Figure 1.3).

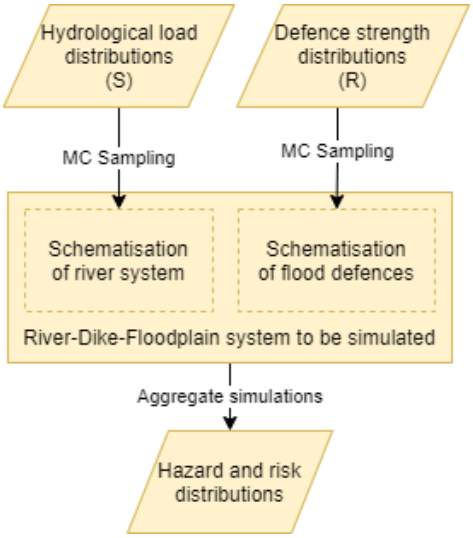

Figure 1.3: Basic Monte Carlo process for system behaviour risk assessment.

– Insufficient representation of defence strengths (subsection 1.4.1 and subsection 1.4.2). Often, the defence strength distribution used as an input for the simulated system (Figure 1.3) does not account for the duration of time required for a breach to initiate during high-water events. Including this duration is likely to impact the spatial distribution of risk.

– Insufficient representation of the river-dike-floodplain system (subsection 1.4.3). As discussed above, the modelled system (Figure 1.3) must be able to simulate all sources and pathways for flooding. Existing systems approaches often ignore the negative load dependencies described by the diagrams in Figure 1.3A and B, which are, in many systems, substantial.

– Insufficient methods to provide decision makers with relevant information with regard to system behaviour.
Even with a well-developed analysis method for system behaviour, decision makers often require uncertainty and scenario analyses to accompany risk estimates. Methods to do so are lacking from current system behaviour studies.

The above limitations of current systems approach have been addressed in this study and the methods and results from doing so are the core work of this thesis. The different components all contribute to an improved systems approach, and thus to improved flood risk analyses for embanked river systems. However, for a better appreciation of these methods, an understanding of the complex hydrological and geotechnical processes in embanked river systems is required. These are therefore described and reviewed below, with the specific work done in this thesis highlighted by reference to subsequent chapters. These innovations and developments are then again summarised in the section 1.7: research objectives and outline.

1.3. INPUT: HYDROLOGICAL LOADS

From Figure 1.2A it can be reasoned that the risk at location 2 depends not only on location 1, but on locations further upstream which, in turn, are dependent on others. This raises the question as to how to define the extent or upstream boundary of the system. Three broad methods to generate the range of all possible hydraulic events required for a risk assessment are explained here.

The first method is to apply a chain of models (a weather generator, a hydrological model and a hydraulic model) to the entire catchment. This has been performed in Germany on the Elbe River(Merz et al., 2016) and Rhine river until Lobith on the Dutch-German border (Hegnauer et al., 2014), in the USA on the Mississippi river (Dunn et al., 2016) and in Japan (Assteerawatt et al., 2016). In the latter study, the method even allows for the combination of fluvial (riverine) and pluvial (rainfall generated) flooding. Another benefit of the approach is the generation of realistic flood waves that can, for example, include the effects of antecedent soil moisture. However, if the complete dynamics of the upstream hydrological system are not relevant, other methods can be utilised that are more computationally efficient and less data intensive.

Another option is to use the results (either raw data or derived statistics) of other analyses in which system behaviour is accounted for (such as the first method). This would be required for studies in which the area of interest is known to be affected by upstream hydraulic system behaviour, but the actual flooding pattern is not relevant to the study. For example it was noted in the study by Courage et al. (2013)that previous studies of system behaviour on the Rhine (Lammersen, 2004) limit the maximum possible river flow that can enter the Netherlands. This phenomenon led to the development of GRADE, (Generator of Rainfall and Discharge Extremes, Hegnauer et al. 2014) to estimate the flows expected in the Netherlands from the Rhine and Meuse rivers. GRADE simulated 50,000 years of events in these catchments, under various scenarios, and the resulting discharge distributions are used in many studies in the Netherlands. Hydrological distributions from the GRADE datasets are also used in the present study in Chapters 2, 3 and 5.

The third option to get the range of possible flood events in a system would be to use a probability distribution of one or more flood descriptors at the boundaries of the system. In this case the location of this boundary must be chosen so that upstream system effects are deemed negligible. For example, in a system behaviour analysis of the Rhine River by Apel et al. (2009), Cologne is selected as a starting point for the simulations as the area upstream is mountainous and naturally defended, and judged not prone to system behaviour effects. Most often this flood descriptor would be discharge, but could also include a variable to describe the shape of the floodwave that enters the system. The discharge probability distributions resulting from extreme value theory may need to combine high discharges originating from separate upstream processes (for example spring melting of ice or winter storms), each of which can follow different individual distributions (Merz and Blöschl, 2008).

In systems with complex tributary networks, the first option (a weather generator model) is preferable. However, if such data is not available, then probability distributions summarising the inputs of the various tributaries (the third option) can be used but they must then include a dependence model. This ensures the spatiotemporal dependencies

of the network are accounted for. Such a method is developed in this study as part of a study on the Po River (see section 7.2) in Chapter 4.

If the downstream extents of the river system are not resistance dominated (i.e. backwater effects or external loads are possible), then the compound effect of river discharge and high water levels may need to be accounted for. Such effects are not addressed in the present study, but methods to include this have been developed by Diermanse et al. (2014) and Khanal et al. (2018), and these are discussed in the Chapter 6. Other boundary condition or initial state variables that could be considered important in a system behaviour analysis are wind setup and direction, soil-moisture levels in the floodplain and lake storage volumes (Courage et al., 2013). Wind setup is included in the uncertainty ranges defined in the fragility curves, but floodplain soil moisture and lake storage volumes are ignored in the analysis as they are not considered significant for inundation modelling. The limitations of these omissions are discussed in Chapter 6.

1.4. INPUT: DEFENCE STRENGTHS

In a flood risk analysis that allows for system behaviour, it is vital that embankment strengths (or ability to resist overflow and failure) are sufficiently represented. With accurate crest-height data, well established hydrodynamic tools can be used to model overflow of the river banks or embankments, and some of these are discussed in subsection 1.6.2. The failure mechanisms of the embankment or defences, however, can be highly complex and uncertain, and require specific approaches to be incorporated into the assessment. They will have an impact at both the location of the failure and (if enough water leaves the river) other locations in the system.

Operational failures of controllable defences, such as those included in a system behaviour by Diermanse et al. (2014), are not taken into account in the present study, nor are human interventions in embankment failures such as sandbag belts around piping 'boils' (Mazzoleni et al., 2014b). These can be considered 'real-time' or 'dynamic' changes to the system and the limitations introduced by not including them are discussed in the Chapter 6. As the present study is concerned with protected river systems, the primary failure considered here are levee breaches. Depending on the system analysed, these failures are likely to be one of the largest contributors to overall flood risk but are difficult to predict due to their variability in space, time, and the uncertainty surrounding growth and initiation mechanism. Many aspects of these variables are discussed in the introduction or literature review of subsequent chapters, but an overall summary is given below.

1.4.1. BREACHES IN SYSTEM BEHAVIOUR ASSESSMENT

System behaviour risk assessments are generally based on multiple simulations of flood events. This requires methods to determine the failure state of a potential breach location in the simulations. The most common method used to assess whether a section of dike has failed or not is the reliability or limit-state equation given in Equation 1.2. This relates the loads (S) at a given moment, to the resistance or strength (R), such that $Z < 0$ describes a failed state of the dike section. Failure state checks are made continually throughout simulations, and at multiple discretised sections of dike, meaning a failure

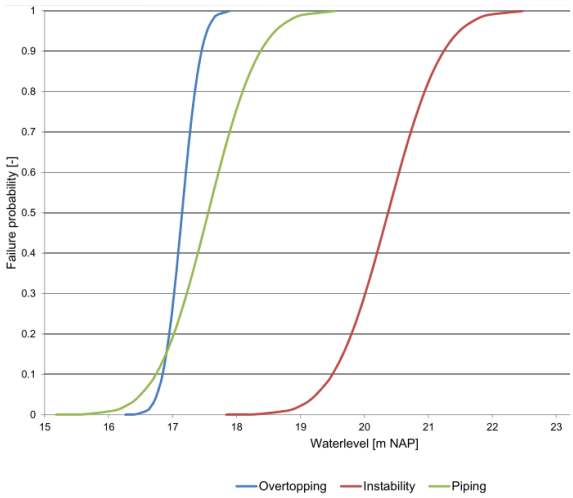

Figure 1.4: Example of fragility curves (Wojciechowska et al., 2015)

at one location has the potential to impact the rest of the system.

$$Z = R - S \tag{1.2}$$

Given the complexities and uncertainties surrounding breaching, probabilistic distributions of each these variables are usually used. Thus, the probability of failure becomes $P_f = P(Z < 0)$, and statistical approaches can be used to determine it. Various methods have been developed to generate densities relating the load variables to the probability of failure, of which 'fragility curves' (relating probability to water-level) are the most common (Bachmann et al., 2013).

The principal breaching mechanisms (as described in subsection 1.4.2) can be represented by fragility curves, describing the conditional probability of failure given a water level. However, in system behaviour assessment this distribution is often used to determine the water level at which the dike fails, and the range of uncertainty for this level can become quite large. For example, in Figure 1.4, the 90% confidence interval for the water level leading to piping failure is 2 m, which (in most river systems) is an enormous difference in terms of return period flow. Larger failure uncertainty ranges generally require more simulations to achieve convergence in Monte Carlo approaches, such as the one used in this study. Also, the resulting outputs will have larger uncertainties, making them less useful in decision-making. Some of the issues related to dike fragility assessment specific to the Netherlands are described in more detail in Chapter 6.

The principle reasons for the uncertainty in fragility curves are; the effect of other load variables, the variable compositions and maintenance states of the dikes, and incomplete knowledge of the processes leading to failure. An important load variable not included is the shape of the floodwave the dike is exposed to. Including this aspect is complex as the dike can be considered to be subjected to multiple loads as the flood-

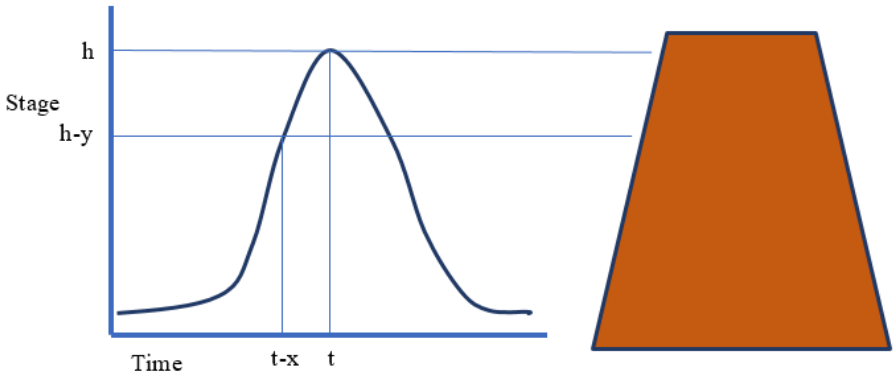

Figure 1.5: Time-dependent loading on dikes

wave passes. An example of this is given in Figure 1.5. At the moment of the peak of the flood wave, the dike is subjected to a maximum hydraulic load h for an instant. It has also been subjected to a hydraulic load $h - y$ for a period of x, and this smaller load will continue after the peak. Methods to account for this duration dependent failure are developed in Chapter 2, based on the expansion of fragility curves into a 'fragility surface' that includes duration as a dependent variable.

1.4.2. BREACH FAILURE MECHANISMS

A non-exhaustive list of potential failure mechanisms, including liquefaction and collision, is given by Vrijling (2001), from which Van Mierlo et al. (2003) considers overtopping, piping and slope failure and erosion to be the most important. Of these, the mechanisms of inner and outer sliding can be grouped under the title 'macro-stability', and thus piping, overtopping and macrostability are often considered to be the most relevant, for example in the study of De Bruijn et al. (2014). A brief description of these three mechanism is given below, but more complete details are available in the provided references as well as overviews by Vorogushyn et al. (2009), Steenbergen et al. (2004), Vrouwenvelder et al. (2010) amongst others.

Piping is the process in which channels develop inside a dike due to seepage within a permeable layer, such as sand. The channels originate at the downstream side of the dike (where phreatic surfaces converge) due to the pressures induced by the water level on the river-side. The steps involved in the process are given in Figure 1.6. A timeline of the research into this phenomenon is provided by Schweckendiek et al. (2014), illustrating the empirical approaches developed by Bligh (1915) and Lane (1935), before a process-based approach was developed by Sellmeijer (1988) and updated by Sellmeijer et al. (2011).

Like piping, macrostability also initiates due to seepage in a sandy permeable layer but results in the uplift, heave or sliding of a large section of the dike due to the pressures created. This is caused by the reduced shear stress between the layers as shown in Figure 1.7, below, and is often described using the models of Bishop (1955) or Van et al. (2005).

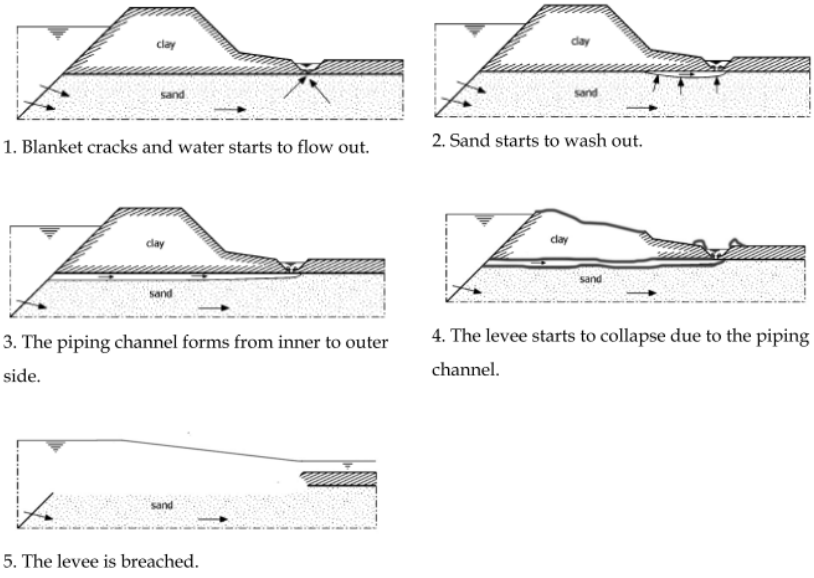

Figure 1.6: Steps in the process of piping (Schweckendiek et al., 2014)

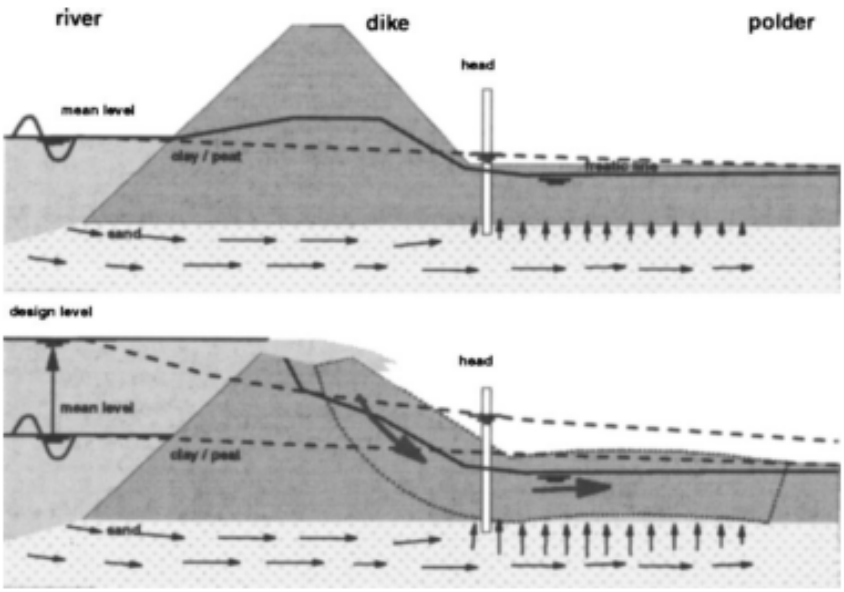

Figure 1.7: Schematic of macro-instability failure (Van et al., 2005)

Overtopping as a mechanism does not require permeation but is instead caused by erosion due to wave overtopping or overflow of the dike on the 'hinterland' or floodplain side. van der Meer et al. (2008) tested 6-hour overtopping discharges on sea-dikes, based on the expected duration of storms, but river discharges are likely to have significantly different durations and wave-sizes. Experimental failures under conditions more closely related to river dikes are provided by Schmocker and Hager (2009). The dependence on duration of inundation is noted for all failure mechanisms that are used by De Bruijn et al. (2014), and methods to try and account for this are therefore developed in Chapter 2.

1.4.3. BREACH LOCATION

Dike breaches are generally possible at any location along a dike stretch, and breaches that develop independently could potentially merge or interact with each other. However, in system behaviour risk analyses, breaches are usually represented as individual events that are each possible over a discretised section of the river dike system. Deciding on the length of these sections can be difficult. For fragility assessments, Vergeer (1990) suggested a 500 m discretisation of dike sections, and this has been adopted in studies by Vorogushyn et al. (2010), Apel et al. (2009) and many others. Steenbergen et al. (2004) suggests the process of subdividing the flood defence system should attempt to maintain similar physical characteristics and relevant loading conditions, meaning that section divisions may differ depending on breaching mechanisms.

In the Netherlands, the VNK2 project (Jongejan et al., 2013) discretised dike sections that were 'statistically homogeneous', based on dike features and assumed composition, with these sections further grouped based on simulated inundation patterns resulting from breaches. For practical purposes, the discretisation is often based on available cross-section data, for example in system behaviour studies on the Po river (Domeneghetti et al., 2013) and the Koshi river in Nepal (Oliver et al., 2018). Within the dike sections, the choice for the actual initiation point of the breach can be subjective. Studies on the Po River (Castellarin et al., 2011) chose locations on the Po River based on comparisons of the longitudinal profiles of the dike crest and a steady state water level, while the VNK2 project mentioned above chose 'conservative' locations through which the most damage would be caused by a breach.

To account for the possibility of 'shortcutting' of flows across floodplains from one river stretch to another (see Figure 1.2B), breach locations on the floodplain side may also need to be identified. Possible examples of locations for shortcutting have been identified in the Netherlands (there termed 'polder-side' breach locations) by Courage et al. (2013) and Klerk (2013), and are discussed in more detail in Chapter 2, alongside an analysis of shortcutting effects.

Related to floodplain side or (or as sometimes called 'polder side') breaching is the idea of 'cascading' floodplain flows (see section 1.2) between compartmentalised floodplain regions. In such regions, the pathways for flood inundation will also be heavily influenced by breaches occurring from one compartment to the next. As with polder side breaches, knowledge on this topic is limited, although it is discussed in relation to the Netherlands by Van der Most and Klijn (2013). Methods to account for cascading are also developed and demonstrated in Chapter 3.

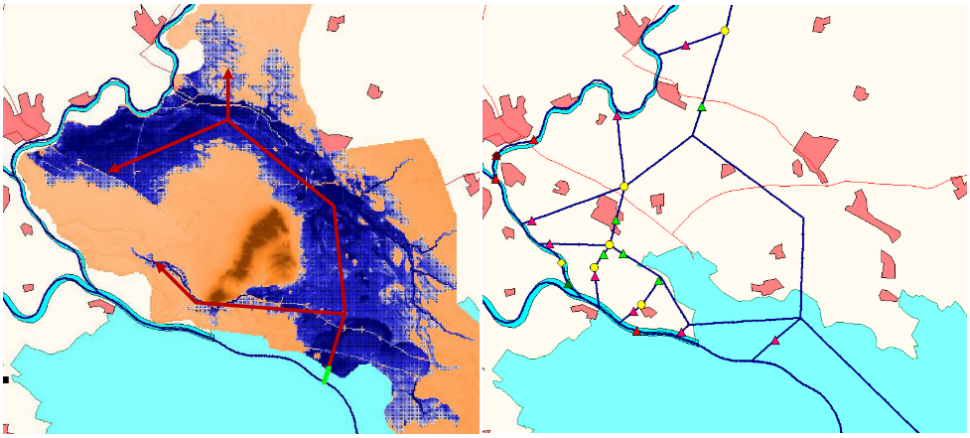

Figure 1.8: Example shortcutting 1D schematisation of the German Rhine to the IJssel (Klerk, 2013)

1.4.4. BREACH DEVELOPMENT AND SIZE

Once a breach begins to develop, the outflow will be determined by the growth and size of the breach, as well as the topography of the inundation area. Depending on the schematisation or scale of the system behaviour analysis, breach growth or final size may not be considered necessary, for example in the large-scale system analysis performed for Japan by Assteerawatt et al. (2016). In general, however, statistical or empirical functions are usually used to model the growth and / or the final size of breaches, and thus (indirectly) estimate the flow through the breach over time.

Due to their uncertainty and rarity, historical breach data may not always be available, accurate or representative of the current system. To overcome this challenge in a risk analysis, the final width of a simulated breach is often considered a stochastic variable that follows a certain distribution. In this case, multiple simulations can be run (such statistical methods are almost always used for system behaviour analyses - see subsection 1.6.1) where the final width or other growth parameters are sampled from distributions. For example, in a system behaviour analysis of the upper Rhine, Apel et al. (2009) used a normal distribution based on historical data. For the Po River, Mazzoleni et al. (2014a) based the width and depth of breaches on statistics from 200 years of historical observations (Govi and Turitto, 2000). Interestingly, breach width statistics collected in this study and by Vorogushyn et al. (2010) both approximate the final width with a lognormal distribution, as seen in Figure 1.9.

In this latter study the authors consider the uncertainty relating to the breach development rate to be minor in comparison to the uncertainty in final width. In the Netherlands, the breach growth rate formula developed by Verheij and der Knaap (2002) is used as standard, in favour of simpler functions for the growth of a breach to a final width, such as by (Dawson and Hall, 2006; Vaskinn et al., 2003). The Verheij and der Knaap formula, or adaptations of it, have been utilised by van Mierlo et al. (2007), Vrouwenvelder et al. (2010) and Bruijn et al. (2016). The relative importance of these parameters and others are discussed in Chapter 6. The breach width B is given by the below formula,

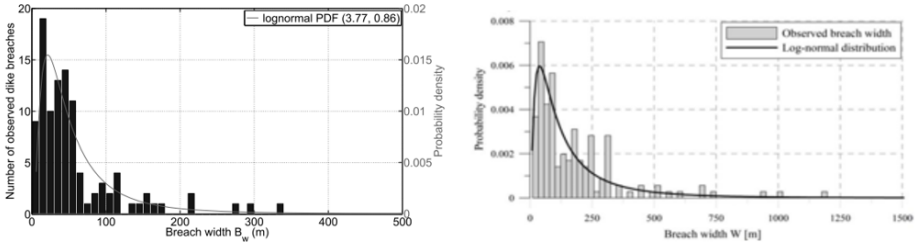

Figure 1.9: Breach width statistics approximated by lognormal distribution; Vorogushyn et al. (2010) (left) and Govi and Turitto (2000) (right)

where H is the difference in water levels either side of the dike, g is the gravitational constant, and t is the time in hours since the start of the breach. u_c is the 'critical velocity' parameter, which can be adjusted for clayey or sandy dikes. The growth is highly sensitive to this parameter and its importance in large scale risk assessments is evaluated in Chapter 5.

$$B = 1.3 \frac{g^{0.5} H^{1.5}}{u_c} log\left(1 + \frac{0.04g}{u_c} t\right) \tag{1.3}$$

1.5. CASE STUDIES

The two primary case studies examined in this work are the Rhine-Meuse River system of the Netherlands, and the Po River in Italy. Brief descriptions of these locations are given as a background in subsequent chapters, but an overall summary of these locations and why they were chosen is here provided. The basic criteria for selection were;

- That the river systems were large and embanked, and therefore aspects of system behaviour and / or spatial consistency were relevant for flood risk analysis.
- That information was readily available for the locations, or mediums existed to obtain it.
- That the systems were applicable to the EU System-Risk project that funded the study, making rivers from countries in which consortium partners were based more desirable.

System behaviour is possible in any river system but becomes more relevant in larger, lowland river basins. In these areas, the volume of out-of-bank flows tends to be more significant, and thus has a bigger impact on the spatial and temporal variability of risk in a system. As mentioned, protected systems are also more prone to system behaviour effects due to the larger impacts of breaches. Worldwide, many locations could have been selected for the study. System behaviour risk assessments have been conducted on the Mississippi river (Remo et al., 2012) and in Japan (Tanaka et al., 2017) and studies of large-scale events that caused breaching and system behaviour effects were performed

on the Indus river (Syvitski and Robert Brakenridge, 2013), Pearl river (Zhang et al., 2013) and Mekong River (Thanh et al., 2019), amongst others.

Protected river systems in Europe were preferable for the study due to the second and third criteria mentioned above. The 2005 EU floods directive has put the generation of flood maps and risk assessments on the agenda of EU countries, and the effects of river levee breaching are shown to be relevant to studies on the Garonne (Bertrand et al., 2018), Rhône (Arnaud-Fassetta, 2013), Tisza (Kiss et al., 2015), Danube (Posner, 2015) and many others large rivers. The Elbe River has also been well studied, especially since the flood and breaching events in 2002 and 2013. Many of the topics discussed in this thesis can be related to studies on the Elbe such as the 'Regional flood model' (Falter et al., 2016) and system behaviour effects (Vorogushyn et al., 2011). The applicability of this study to the Elbe and other locations in Europe and worldwide is discussed in the conclusions.

The Netherlands has a long history of flood protection, and risk-based management has been in place since the 1960s, primarily as a reaction to the 1953 flood disaster (Bubeck et al., 2017). Almost 60% of the country surface area is flood prone, with a similar percentage of the population living in these areas. Given this large exposure, flood protection is generally considered a government responsibility and various laws on protection have been implemented that instigated detailed research into national risk assessments. This focus on large-scale flood risk means that understanding system behaviour effects has become important. However, the large computational effort required to run such analyses limited their development until the 21st century, when the studies of van Mierlo et al. (2007) and Vrouwenvelder (2006) highlighted their potential importance to flood risk.

The two largest rivers flowing into the Netherlands are the Rhine and the Meuse, and many of the dikerings[3] in the country are situated adjacent to these rivers. The Rhine has a catchment area of ~185,000 km^2 (Figure 1.9), with an average flow of about 2,200 m^3/s. It splits into the three branches of the Waal, Lek and IJssel, which route roughly 2/3, 2/9 and 1/9 of the flows from the main river respectively. Although the disaster in 1953 was primarily due to a storm surge, it initiated the drive for risk-based management of all flooding types, including riverine. A major flooding event occurred on the Rhine in 1926, and despite events in 1993 and 1995 having very similar discharge discharge peaks (~12,000 m^3/s), these latter events did not cause any breaches to fully develop. Instead, the flooding was mostly on the Meuse river, for which extreme flows are very often correlated to those on the Rhine (Diermanse, 2002).

The Meuse has a smaller catchment size of ~34,000 km^2 (Figure 1.10), with an average flow of about 350 m^3/s. As well as being correlated, the flows on the Meuse and Rhine are at some points physically close; the Waal branch of the Rhine comes within 1 km of the Meuse as they flow towards the Rhine/Meuse lower river region ('benedenrivierengebied'). System behaviour studies by Courage et al. (2013) identified the 'Land van Maas en Waal' (Land of Meuse and Waal in Dutch) dikering between the rivers as a potential location for 'shortcutting' of flows across the floodplain, and this possibility is further explored in Chapter 3. Given the close connection between these rivers, and the fact that they represent the majority of the riverine flood threat to the Nether-

[3] In the Netherlands, a dike-ring is an uninterrupted ring of water defences, like dikes, dunes or high grounds.

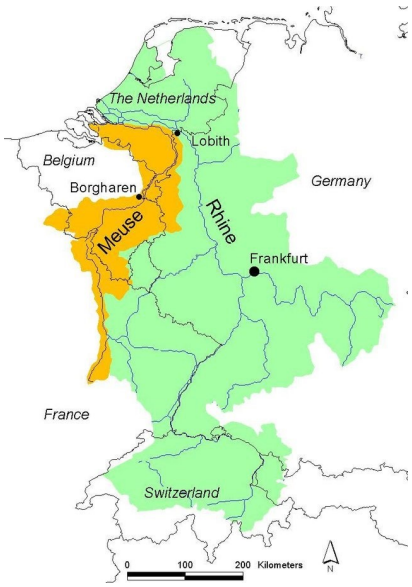

Figure 1.10: Rhine and Meuse catchments (Kwadijk, 2007)

lands, it makes sense to consider them as one system in a risk analysis. As mentioned in section 1.3, the Rhine/Meuse lower river region is excluded from the system as well as the related tidal and storm surge dynamics. The limitations incurred due to this are discussed in the Chapter 6.

Another idea that follows from section 1.3 is that system behaviour analyses could (and perhaps should) be extended upstream beyond the border with Germany, even up to Switzerland. This is not done in the present study for three main reasons. First, the administrative boundary delineates a new group of decision makers, and thus risk analyses specific to one country are preferable. Second, system behaviour is assumed to be less prevalent on the river further upstream, as flows at many locations are expected to re-join the main channel further downstream. Finally, the GRADE study (Hegnauer et al., 2014) provides upstream boundary conditions specifically for the purpose of analysing risk in the Netherlands and includes aspects of system behaviour in Germany.

The Po River is located in northern Italy, with the ~74,000 km^2 catchment situated between the Alp and Apennine mountain ranges (Figure 1.11). As the catchment is entirely within the administrative boundary of Italy, it makes sense to analyse the system as a whole. The river is less branched than the Rhine and Meuse in the Netherlands, and system behaviour effects such as shortcutting are therefore unlikely. However, the floodplains along the main channel are compartmentalised, and so the first and third aspects of system behaviour described (Figure 1.2A and C) are possible. In fact, many breaches have been recorded in the region, such as those during floods in 1951 and October 2000. As well as the possibility of aspects of system behaviour due to breaching, the complicated tributary system could be subject to the problems of spatiotemporal dependencies (see Chapter 4), making the application of large-scale risk analyses very

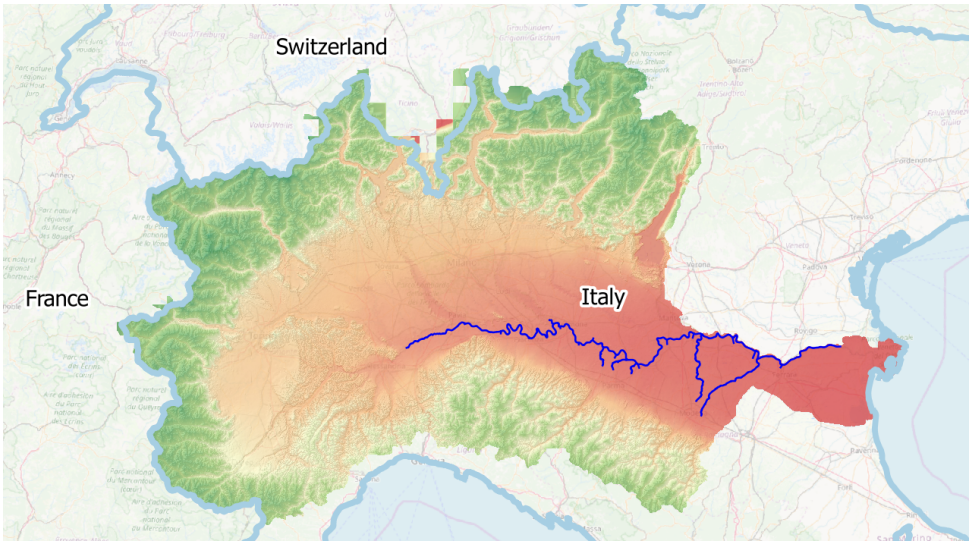

Figure 1.11: Po river catchment in Northern Italy

useful for the region.

As well as the interesting river dynamics and flood protection aspects of these two case studies, they are also closely associated with partners of the System-Risk project (Deltares, University of Bologna, TU Delft and GeoForschung Zentrum), and information and data could be easily obtained to assist the research.

1.6. TOOLS

The primary focus of the study is a systems approach to flood risk assessment in the two case studies described above. In order to undertake these assessments, however, various mathematical and computational methods are required. Information about minor methods are generally provided in accompanying references, but brief descriptions of four important components of risk assessments (statistical, hydrodynamic, geotechnical and impact models) are given below.

1.6.1. STATISTICAL MODELLING

Given the uncertainties in both the load and dike strength, probabilistic formulations of the reliability equation are required in risk analyses that include breaching. Three main methods of doing so are discussed by Diermanse et al. (2014): Numerical integration, FORM (First-order reliability method - Rackwitz and Flessler 1978) and Monte Carlo sampling. Using the criteria of efficiency, accuracy and robustness (Grooteman, 2011), Diermanse et al. describe how Monte Carlo approaches provide the best trade-off of these metrics when analysing systems with many random variables, such as a river and levee system discretised into multiple sections.

For this reason, system behaviour analyses by Apel et al. (2009), Vorogushyn et al.

(2010), De Bruijn et al. (2014) and van Mierlo et al. (2007) have all used Monte Carlo approaches. In each of these cases, dike strengths are sampled from their underlying uncertainty distributions at various locations on the river, and hydraulic loads are sampled for the boundaries of the system. With these conditions in place, the system is simulated over a defined period to model both the hydrodynamic and geotechnical (breaching) development of the flood event. With repeated simulations, the probabilities of certain event features (e.g. flooding at a certain location, breaching of a levee section) can be estimated.

Monte Carlo approaches can, however, be inefficient. For example, if a section of levee has a very low failure probability, the amount of simulations required for this to be apparent (i.e. for the probability to 'converge') will become very large. To account for this, various sampling procedures have been developed that are more selective than the so-called 'crude' Monte Carlo approach. These include Latin hypercube sampling (McKay et al., 1979), directional sampling (Ditlevsen et al., 1990) and importance sampling (Engelund and Rackwitz, 1993). Diermanse et al. (2014) argue that the latter is the preferred option for protected river systems with many potential breach locations. The general idea is to sample values which are in a region of the sample space that is more likely to be of interest to the required output. For example, when using a distribution of annual maximum flood events as a boundary condition, it will often be more relevant to sample events that have an exceedance probability less than 0.5 (i.e. larger events).

An important caveat of using the Monte Carlo approach with multiple distributions is to understand the dependence (if any) between the distributions. Failures of nearby levee sections are, of course, mutually dependant on the hydraulic loads they experience, but this problem is overcome by using simulations of flood events that route loads over the entire system. Adjacent levee section failures may also be correlated due to having similar compositions and geometries, and the potential importance of this is discussed in Chapter 6. A commonly modelled dependence in flood risk analysis is the correlation between hydraulic loads originating from adjacent rivers or tributaries to a larger river. To model such a dependence, the two most common approaches are Copulas (Renard and Lang, 2007), and the model of Heffernan and Tawn (2004). The former is used in this study for the tributaries of the Po river (Chapter 4) and the correlation between the Meuse and Rhine (Chapters 3 and 5).

Importance sampling, copulas and a number of other statistical tools can be implemented in the Probabilistic Toolkit software developed at Deltares. It can be used to 'wrap' the multiple simulations required for Monte Carlo analysis, and can also 'parallelise' the simulations, meaning they can be run simultaneously on multiple cores of a machine. For these reasons the software was used extensively in this study.

1.6.2. HYDRODYNAMIC MODELLING

Within each flood event simulation of the Monte Carlo analysis, the hydraulic loads must be routed through the system. Simulating channel and overland flows is traditionally achieved using 1D or 2D numerical implementations of the St. Venant equations (Teng et al., 2017) such as those found in software packages like MIKE (DHI, 2002), Sobek (Dhondia and Stelling, 2004), HEC-RAS (DHI, 2002) and TUFLOW (Syme, 2001). However, the 2D components of these numerical solvers can often be time-consuming, es-

pecially for the multiple large-scale simulations required in system behaviour analysis. Methods to improve the 2D computational efficiency include the use of (Stelling, 2012), GPU modelling (Kalyanapu et al., 2011) and quasi-2D approaches (Bates and De Roo, 2000; Lhomme et al., 2008). An implementation of the Quasi-2D approach is developed for Sobek in Chapter 3, and an existing HEC-Ras version is used in Chapter 4.

HEC-Ras and Sobek have been utilised in the present study for the Po and Netherlands case studies respectively, primarily due to the availability of existing calibrated models already built in these software packages. Both software packages allow for parallelisation and provide user-interfaces for model development. HEC-Ras offers the added advantage of pre-defined failure functions for hydraulic structures, while this feature was developed as part of this study for Sobek.

1.6.3. GEOTECHNICAL FAILURE MODELLING

As described in section 1.4, this study primarily utilises existing geotechnical studies that have been summarised in the form of fragility curves. In the Netherlands, the methods through which impact assessments are conducted by waterboards and provincial authorities are set out in the 'Legal assessment tools' (Slomp et al., 2016). Within these tools, the Hydra-Ring suite of models (Diermanse et al., 2013), the successor to PC-Ring (Steenbergen et al., 2004), is the most commonly used calculation tool for dike failure probabilities. However, Hydra-ring relies on a database of hydraulic boundary conditions to the dike stretches and separate probabilistic models of sub-systems (Hydra-K -coast, etc.). Therefore, it cannot be used to consider interactions in the larger system.

As Hydra-ring cannot conduct national-scale system behaviour assessments, and does not include an unsteady hydraulic component, the method of including dike fragility curves employed De Bruijn et al. (2016) is more suited for large-scale risk assessment. This method depends on fragility curves (Wojciechowska et al., 2015) that relate the failure probabilities to hydraulic variables. These fragility curves are based on pre-existing models, such as those used in Hydra-Ring or similar. Fragility curves are available from the WV21 project (Kind, 2011), however the set of curves developed in the OKADER project (van der Meij et al., 2016) are more comprehensive, providing information for three failure mechanisms (overtopping, piping and macrostability) at sections of about ~1 km each. On the Po, the fragility curves were built as part of the work on this case study, based on the work of (Mazzoleni et al., 2014b).

1.6.4. IMPACT MODELLING

As mentioned above, an important step in a risk analysis it to quantify the impact of the expected hazard. Traditionally, flood impacts have been categorised into those that are tangible (can be quantified in some way, such as monetary damage) and intangible (cannot be easily quantified, e.g. psychological impact). The most common metrics of tangible impacts are economic cost and fatalities, but other metrics could include lost work hours and number of people affected. Finally, the tangible effects can be further divided into direct damages (those caused directly by the flood inundation) and indirect damages (for example loss of business during the recovery period).

The principal method to calculate direct economic impacts involves relating flood hazard variables (e.g. water depth and velocity) to damages using 'depth-damage' func-

tions, usually through GIS (Geographical Information System) computation. One such implementation is the 'flood impact analysis tool' (FIAT - Slager et al. 2016) and its specific Netherlands application SSM-2017 (Slager and Wagenaar, 2017). The latter has been used for damage calculations in the present study in Chapter 5. Direct economic damages are well suited to GIS calculation as the majority of vulnerable features remain fixed in place during the event (buildings, infrastructure etc.). Fatality and indirect damage modelling, however, will generally involve dynamic actions such as evacuation or relocation of non-fixed items, and such methods are used in Chapter 5.

1.7. RESEARCH OBJECTIVES AND OUTLINE

Risk analysis is an important aspect of flood management. Flood risk analyses of large embanked river systems often require a systems approach due to the presence of 'system behaviour' interactions and 'spatiotemporal dependencies'. The main objective of this work, therefore, is to present such an analysis method to account for these effects, improving and developing upon the limitations of previous approaches. Doing so is likely to have a positive impact on flood management decision making and understanding. This aim can be adapted into the form of the following research question;

How can system dependencies and interactions be incorporated into the flood risk analyses of large-scale embanked river systems? What are the outcomes of doing so, in general, and for the Dutch Rhine and Po river case studies?

However, in order to achieve this, a number of limitations in existing approaches must be addressed, which can be considered secondary objectives. Some of these secondary objectives are alluded to in the previous sections. Firstly, methods to schematise and trigger breaches that are duration dependent must be developed and incorporated into system behaviour approaches (Chapter 2). Such approaches should be expanded to allow for load interdependencies (Chapter 3) and spatiotemporal dependencies (Chapter 4) that occur between components of a system. Finally, methods must be developed to allow for scenario and uncertainty analyses in system behaviour risk assessments, providing clearer information for decision-makers (Chapter 5). As well as the general methods developed, in each of these chapters specific results relating to the case studies are also provided. The rough 'position' of these steps / chapters in relation to the overall approach is provided in Figure 1.12, and a summary of the work done, and research questions addressed, is given below.

This dissertation is outlined as follows;

- Chapter 1 - Introduction

This chapter gives an introduction to flood risk analysis and dependency problems and suggests a systems approach to tackle these problems. Limitations of this approach are described in relation to a literature review of the two main inputs to the proposed approach (defence strengths and hydrologic loads). The chapter also provides a summary

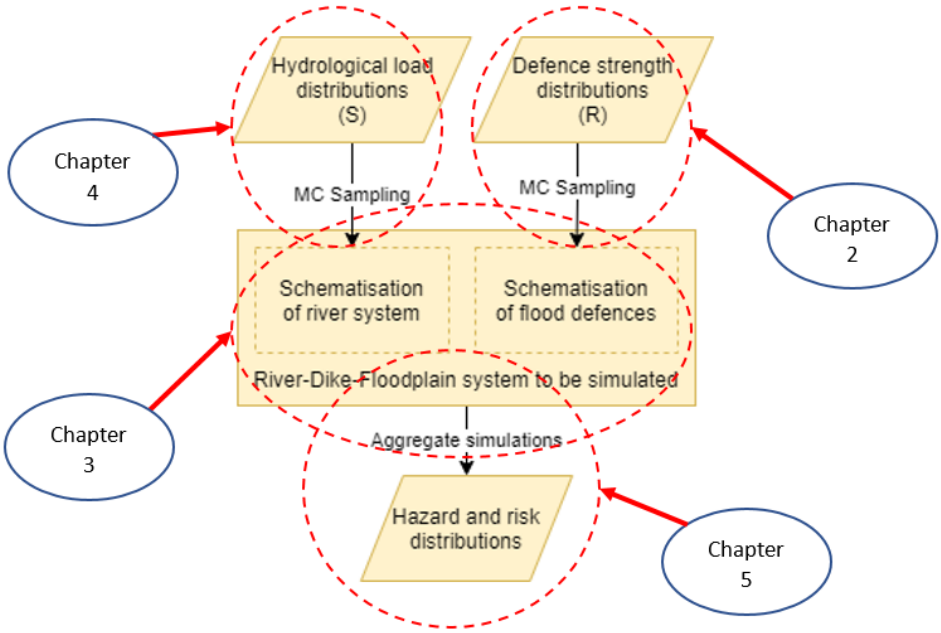

Figure 1.12: General innovation focus of each chapter in relation to Monte Carlo analysis method for system behaviour

of the case studies and main tools used in the study.

- Chapter 2 – Floodwave duration impact on system behaviour

Research Question: For system behaviour analysis, how can the resistance to floodwave duration be included in representations of dike strengths, and what is the impact of including this component?

As discussed in subsection 1.4.1, conventional approaches in system behaviour assessments do not include the duration of floodwaves as a factor in triggering breaches. This can have a large impact on both the spatiotemporal pattern of risk as well as the overall risk. In this chapter, a method to represent the time duration aspects of different breach mechanisms in a system behaviour analysis is developed. The chapter shows the impact of applying such a method compared to the conventional method used for the Netherlands case study. In relation to Figure 1.12, Chapter 2 focuses on the dike fragility component of the overall method.

- Chapter 3 – Spatial interdependencies of inundation in system behaviour

Research Question: How can load interdependencies related to floodplain flows be incorporated into system behaviour risk analyses? What are the results of including them?

As discussed in subsection 1.4.2, the systems approach can be utilised to account for load interdependencies in a river network. However, to account for the various interactions in a practical and computationally efficient manner requires specific aspects to be considered, such as floodplain or 'polder' side breaching (subsection 1.4.3) and floodplain schematisations (subsection 1.6.2). In this chapter, spatial patterns of risk transfers in the Netherlands case study are analysed by building a quasi-2D model that includes interactions between rivers and river branches. It also allows for the possibility of polder-side breaching. Specific interactions and risk transfers observed due to the analysis are highlighted in the results. In Figure 1.12, this work focuses on the overall schematisation of floodplains in system behaviour.

- Chapter 4 – System behaviour on the Po River

Research Question: How can the complex spatiotemporal dependencies of systems with multiple rivers or tributaries be accounted for in a system behaviour analysis, and what insights does this bring?

As discussed in section 1.3, the systems approach used in this study requires hydrological boundary conditions that are coherent in space and time. In this chapter, a system behaviour analysis for the Po river case study is developed, addressing the dependency problems caused by the complex tributary system using a copula. New fragility curves are also developed for the region allowing for a complete system behaviour analysis that includes breaching. In Figure 1.12, this work looks at the problem of dependent load distributions, but is also an application of the overall process to another case study.

- Chapter 5 – Uncertainty and scenario analysis through system behaviour

Research Question: How can risk assessments using a systems approach provide useful information and analysis for decision makers? What are the results of such analysis for the Netherlands case study?

This chapter considers system behaviour assessments in general, and how such assessments should be structured to provide useful information for decision makers on uncertainties and scenarios. This is done by developing an overall assessment framework to generate uncertainty and scenario analyses, and applying it to the Netherlands. In Figure 1.12, this chapter can be seen as addressing the outputs part of the process, but does so by testing aspects of the inputs.

- Chapter 6 – Discussion, limitations and recommendations

Within each of the previous chapters, the limitations and recommendations specific to the approach and case study being addressed are considered. Within Chapter 6, however, these limitations and recommendations are summarised in terms of the components of the general approach, again referencing the flow chart in Figure 1.3. Limitations of the general approach are also discussed, as well as specific discussion points about flood-risk analysis in the case studies.

- Chapter 7 – Conclusions

This chapter summarises the conclusions of the preceding chapters, both in terms of their results for the case studies and the for the systems approach in general, before the overall research question is considered. Implications of this study for the case studies are discussed, as well as possible future research and applications.

2

FLOODWAVE DURATION IMPACT ON SYSTEM BEHAVIOUR

ABSTRACT

Hazard analysis is a crucial step in flood risk management, and for rivers, the effects of breaches need to be taken into account. Hazard analyses that incorporate this overall "system behaviour" have become increasingly popular in flood risk assessment. Methods to perform such analyses often focus on high water levels as a trigger for dike breaching. However, the duration of high water levels is known to be another important failure criterion. This study aims to investigate the effect of including this duration dependency in system behaviour analyses, using a computational framework in which two dike breach triggering methods are compared. The first triggers dike breaches based on water levels, and the second one based on both water-level and duration. The comparison is made for the Dutch Rhine system, where the dike failure probabilities are assumed to conform to the new Dutch standards of protection. The results show that including the duration as a breach triggering variable has an effect on the hydraulic loads and overall behaviour in the system, therefore influencing the risk. Although further work is required to fully understand the potential impact, the study suggests that including this duration dependency is important for future hazard risk analyses.

A slightly modified version of this chapter has been published in *Georisk* as *Influence of water level duration on dike breach triggering, focusing on system behaviour hazard analyses in lowland rivers* (Curran et al., 2018).

2.1. INTRODUCTION

Risk analysis is vital for the flood risk management of lowland river systems. It requires the analysis of hazard, exposure and vulnerability at a system level (Vorogushyn et al., 2017). To assess hazards, extreme value analysis of peak discharges is often used, from which flood frequency distributions can be generated. However as noted by Apel et al. (2009), the extrapolation to extreme events used in this analysis may fail to consider processes not present in recorded data, such as out-of-bank flows. Furthermore, extreme value analysis is applicable only to the location from which the observations are drawn, and cannot be applied to an entire system. Due to these deficiencies, system behaviour analyses have become increasingly popular in flood hazard estimation.

Hydrodynamic system behaviour considers the behaviour of the river system when out-of-bank flows are included, and is most often used in the estimation of extreme flows in low-land or delta river systems. The concept has, in recent literature, been called 'river system behaviour', (van Mierlo et al., 2007), 'load interdependencies' (De Bruijn et al., 2014; Dupuits et al., 2016; Klerk, 2013), or simply 'system behaviour', (Bachmann et al., 2013). Various studies (including those mentioned above), have demonstrated its importance in the Netherlands (De Bruijn et al., 2014, 2016), and its relevance internationally has grown with studies in Germany (Falter, 2016; Vorogushyn et al., 2010), U.S.A. (Dunn et al., 2016) and Japan (Assteerawatt et al., 2016).

Studies of this type are often in relation to protected systems, where out-of-bank flows are primarily due to defence failures such as dike breaching. The temporal and spatial occurrence of dike breaches are highly uncertain and therefore probabilistic approaches to assess flood risk have been proposed by Apel et al. (2009), Vorogushyn et al. (2010), De Bruijn et al. (2014) and van Mierlo et al. (2007) amongst others. In each of these approaches, a Monte Carlo framework is used to sample variables such as loads, dike strengths and potential impacts for various locations on the river. Hydrodynamic simulations of a schematised area are then run multiple times and output variables (such as hydraulic loads, damages and system risks), can be inferred from the results. In these frameworks, sampled dike strengths will determine the conditions under which a dike breach is initiated or 'triggered' in a simulation. The geotechnical complexity of this breach triggering and growth process usually requires a number of simplifications to be made.

One common simplification is to assume the triggering of a dike breach is due to water level alone, as done by Apel et al. (2009), De Bruijn et al. (2016), Assteerawatt et al. (2016) and various others. The prevalence of this approach is partly due to the availability of 'fragility curves' in many countries, which relate water level to probability of failure for a dike section, according to various failure mechanisms. A consequence of using water level from the curves as a breaching trigger is that breaching within a simulation can only occur before (or directly at), the peak of the floodwave. Although this approach is reasonable for overtopping, other dominant failure mechanisms such as piping and macrostability have been shown to have a strong dependency on the duration of the floodwave (i.e. the period of time the water level is above certain thresholds) as well as the water level itself.

This paper attempts to investigate the effect of floodwave duration in flood hazard analyses that include system behaviour, for the case study of the lower Rhine River in

the Netherlands. The paper starts with a short review of existing system behaviour approaches and their application to the lower Rhine, as well as an overview of the mechanics of breaching. The methodology, results and conclusions are given in the proceeding sections.

2.2. EXISTING APPROACHES

2.2.1. SYSTEM BEHAVIOUR

The studies on system behaviour mentioned above are primarily academic, and rarely used directly in Flood Risk Management (FRM), policy making. One of the main reasons for this is the difficulty in validating the analyses against the extreme events that they attempt to model. In the Netherlands, the newly introduced national risk standards (Kok et al., 2017), require flood fatality to be assessed at a national level. This policy has precipitated more detailed studies that can account for assessments at the national scale, and thus system behaviour analyses have become more relevant.

An assessment of the expected hydraulic loads coming into the Netherlands from the Rhine and Meuse is given by the 'Generator of Rainfall and Discharge Extremes' (GRADE, Hegnauer et al. 2014). This study is an example of accounting for system behaviour, as the distributions of hydraulic variables for the Rhine resulting from this study (such as water level and discharge), take into account potential dike breaches upstream of the Dutch border. However, these breaches were considered in a deterministic way, occurring when certain water level thresholds related to overtopping were surpassed. Despite this simplification, the discharge and wave-shape distributions have been used in both legal policies and research on the Dutch Rhine, for example in the 'Legal safety assessment 2017', (Dutch acronym: WBI 2017, Slomp 2016).

The VNK2 project Jongejan et al. (2011), gives quantitative risk estimates for each dike ring within the Netherlands, accounting for uncertainties relating to loading conditions, resistances, and physical models. Within the VNK2 project, sections of dike on the dikerings were defined in such a way that breaches anywhere along these sections are likely to cause similar inundation extents. However, the possibility of hydraulic system behaviour between the dike rings was not accounted for. System behaviour research related to specific regions of dikerings in the Netherlands has been performed by Courage et al. (2013) and Klerk (2013), whereas analyses for simplified/hypothetical dikerings have been done by van Mierlo et al. (2007) and Dupuits et al. (2016). For the downstream boundary conditions in the Rhine delta, sea level distributions that include tidal variability have been used in system behaviour research by (Diermanse et al., 2014). National-scale system behaviour analyses for the Netherlands have been applied to flood fatality risk De Bruijn et al. (2014), and to hydrodynamic behaviour, De Bruijn et al. (2016). However, these studies assumed breach triggering based on high water levels alone. As explained below, this simplification is unrealistic in relation to known breaching mechanisms.

2.2.2. DIKE FAILURE

The system behaviour studies mentioned above all utilise the concept of the reliability or limit-state equation; $Z = R–S$. Failure is said to occur when $Z < 0$, i.e. when the load

or solicitation (S) is greater than the strength or resistance (R). In the case of a dike, the resistance is related to its composition and geometry whereas the loads relate to the hydraulic variables such as water-level, duration and discharge. For probabilistic failure analyses, both the strength and load variables are given in terms of distributions of these variables.

Distributions of dike strength are usually expressed in terms of their failure probability according to various mechanisms. A non-exhaustive list of failure mechanisms including liquefaction and collision is proposed by Vrijling (2001), and this is reduced to the principle mechanisms of overtopping, piping, slope failure and erosion by Van Mierlo et al. (2003). Of these mechanisms, slope erosion and inner and outer slope failure are often grouped under the title macro-stability, leading to the system behaviour analysis of De Bruijn et al. (2014) which focuses on piping, overtopping and macrostability. When these mechanisms are represented by fragility curves, the failure probabilities are generally assumed to be dependent on water level alone.

A dependence on the water level duration for each of these mechanisms is described by (Sellmeijer, 2006), (piping), (Van et al., 2005), (macrostability) and (Vorogushyn et al., 2010), (overtopping). Van et al. noted significant movement of a test dike after being exerted to high pore pressures for about 2 days, with the delay being due to the gradual evolution of the phreatic surface. Sellmeijer observed critical heads leading to piping failure in a test dike after effects after 30-60 hours, with the delay being due to the time required for a pipe to form in the permeable layer due to backwards erosion. The full geotechnics of these mechanisms are not described here, but more detail is provided in section subsection 1.4.2, the provided references and overviews by Vorogushyn et al. (2009), Steenbergen et al. (2004), Vrouwenvelder et al. (2010) and others.

These studies demonstrate that sustained water levels impact breaching probability and will therefore affect system behaviour analyses as described above. However, the models describing failure in this literature require detailed data inputs and are often technically complex, thus making them difficult to apply at a system level. A method to include a simplified duration dependency in a system behaviour analysis has been implemented by (Vorogushyn et al., 2010), but still requires extensive geotechnical knowledge, and cannot be applied to the currently available data for the Dutch dike system. A system behaviour analysis that includes water level duration as a variable for breach triggering has not been performed for the Netherlands, and an objective of this study is to determine its effects on the hydrodynamic system behaviour and potential flood hazards on the Rhine.

2.3. METHODOLOGY AND APPLICATION

2.3.1. COMPUTATIONAL FRAMEWORK

The presented research compares two dike-breach triggering methods for a hydrodynamic system behaviour analysis, using the Rhine case study. The comparison uses the concept of the reliability equation to trigger dike breaches probabilistically, where 'S' is the distributions of hydraulic loads (peak discharge and wave-shape), and 'R' is the distributions of dike strengths. These distributions are sampled in a Monte Carlo framework, and the resulting values are used as inputs to a hydrodynamic simulation of the

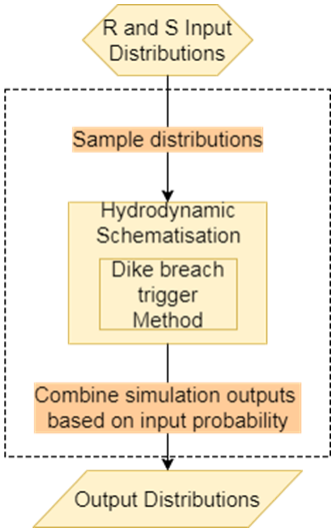

Figure 2.1: Probabilistic framework schematisation.

system. The hydraulic output variables of interest from each simulation, (such as water level and discharge), are combined into distributions based on the original input probabilities taken from the sampled values. The probabilistic framework for modelling each scenario has been adapted from De Bruijn et al. (2014), and is given in Figure 2.1, below.

For the loads, S, the discharges at the upstream boundary are sampled using an importance sampling procedure giving preference to higher discharges, whereas the wave-shape and dike strengths are sampled using crude Monte Carlo sampling. In all tested implementations of this framework, (termed scenarios), the input load distributions are the same. The dike strengths, R, are distributions of failure probability that relate to either water level or both water level and duration of exceedance of that water level. These two strength distributions have been termed 'fragility curves' and 'fragility surfaces' respectively, and 'fragility functions' collectively. Their formation is described for the specific case-study below.

The process given in Figure 2.1 is repeated for 3 system behaviour scenarios. In scenario 0, system behaviour is not implemented, (i.e. no out of bank flow occurs), and this is used to gauge the effect of the system behaviour scenarios. The frequency of breaching that would have occurred using both fragility curves and surfaces is recorded in scenario 0. In scenarios 1 and 2 (distinction explained in subsection 2.3.4) breaches are simulated and thus affect the river discharges. In all scenarios, the fragility functions are adjusted to ensure the resulting failure probabilities correspond to the probabilities required in the new protection standards when system behaviour is not considered.

2.3.2. APPLICATION TO LOWER RHINE RIVER

The presented case study area is the lower Rhine region along its three branches in the Netherlands; the Waal, the Nederrijn/Lek and the IJssel. The study is delimited upstream

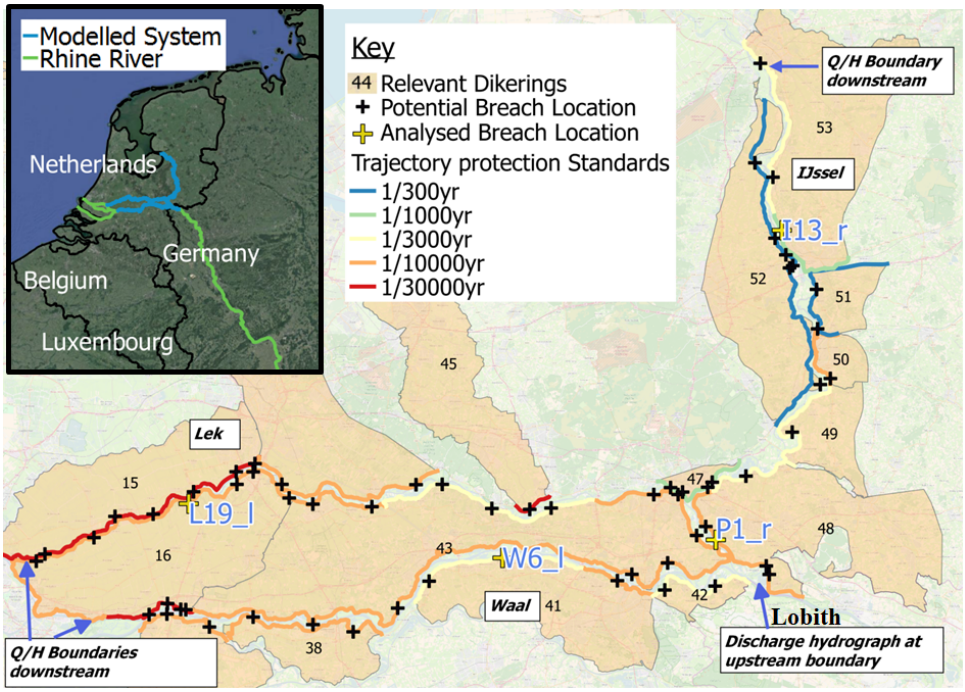

Figure 2.2: Top left map show case study location within the Netherlands. Indicated on larger map are the breach locations including the ones analysed in detail, as well as dike rings, river branches and the protection standards (failure probabilities of the embankment) associated with each dike trajectory.

at Lobith on the German border, a location for which for which data is available for the distribution of hydraulic variables. The flow in the system is heavily dominated by the upstream flow, and therefore smaller inflows within the Netherlands are not considered. The river network is almost completely defended with dikes employing different protection standards. Tidal effects on the Lek and Waal (or Merwede as it is called downstream) are observed as far upstream as Nieuwegein and Gorinchem respectively, but considered dominant downstream of Dordrecht and Rotterdam. For this reason, these latter locations delimit the case-study downstream; along with the IJsselmeer Lake (see Figure 2.2). The results at four locations of interest were chosen to illustrate the overall behaviour, and are labelled in Figure 2.2. The labels refer to a naming convention which describes the breach location on the branch, (Rhine, Pannerden Canal, Waal, Nederrijn/Lek or IJssel; $R, P, W, L, or I$, respectively). For example, ''$W2\_r$' is the second breach location on the Waal going downstream, and the breach is located on the right hand side. The location of all breaches is given in section 2.B.

The case-study was modelled as a 1D Sobek3 schematisation, adapted from a benchmarked model developed for Rijkswaterstaat. 62 predetermined breach locations were included to represent sections of dike as shown in Figure 2.2. These sections are based on a sub-discretisation of the dike 'trajecten' or trajectories, for which protection standards are described by Dutch law (Slomp, 2016). Given these trajectory protection standards,

the design failure probabilities for each dike breach section can be estimated, by assuming every meter embankment contributes equally to the overall failure probability of the trajectory section.

Within the Sobek model, each breach location is schematised as a weir that flows to a reservoir that represents the capacity of the adjacent dike-ring (see Figure 2.2). In scenarios where system behaviour is implemented, the weir is triggered by exceedance of the sampled water level threshold or water level-duration threshold. If a breach is triggered, it will start to grow in length and depth according to the Verheij and Van der Knaap (2003), breach growth formula, using default parameters (section 2.A). In the model, water will then flow from the river through the breach into the dike-ring which means the river discharge downstream is reduced.

2.3.3. HYDRAULIC LOADS

The principal load is the river inflow coming from Germany, schematised as a discharge hydrograph boundary condition at Lobith, near the Dutch-German border (Figure 2.2). This hydrograph is generated by combining discharge peak and wave-shape values sampled from distributions at this location, taken from GRADE, (Hegnauer et al., 2014). GRADE uses a combination of models to derive these distributions, such as a weather generator, a hydrological model and a hydraulic model for the entire river Rhine catchment upstream of Lobith. Different wave-shape distributions are assigned to hydrographs according to their peak value in the study, and these distributions were maintained for the present study (Figure 2.3). The downstream boundary conditions on all 3 branches were modelled using discharge-water levels ($Q-H$) relationships, meaning no tidal effects are considered. Given the focus of the study on dike-breaching mechanisms in system behaviour, this simplification was considered acceptable.

2.3.4. DIKE STRENGTHS / RESISTANCE

In the present study, breaches occur when the river water levels (scenario 1), or river water level durations (scenario 2), surpass a threshold. Recently developed fragility curves for overtopping, piping and macrostability (Levelt et al., 2017) are used as the basis for those thresholds in both scenarios. These curves have been generated for small dike sections on the entire Rhine/Meuse system, and were combined analytically to represent the breach locations given in Figure 2.2, assuming independence between the constituent curves. The standard deviations of these curves were maintained, but the mean values were adjusted so that failure probabilities in scenario 0 (without system behaviour) conform to the new protection standards. This constraint ensures the inclusion of water level duration as a breaching criterion does not severely affect the overall failure probability of the system, instead allowing for changes in system behaviour effects become apparent, such as breaching characteristics. This adjustment is done using a method similar to that described by De Bruijn et al. (2014). The design probabilities per location and calculated probabilities are given in section 2.A.

In scenario 1, sampled probabilities are transformed into threshold water levels using the fragility curves, and the lowest water level is used as the threshold for failure at that location. In scenario 2, breaching occurs due to a combination of water-level and the duration of time that level is exceeded in a simulation. The duration of exceedance of

Table 2.1: Factors to adjust fragility curves for certain durations, as suggested by 3 different dike fragility experts, and overall averages.

Expert	1 hr	24 hr	168 hr	720 hr
		Overtopping		
A	0.005	0.2	0.8	0.9
B	0.1	1.3	2	2
C	1	10	50	50
Average	0.37	3.83	17.6	17.63
		Piping		
A	0.0005	0.05	0.8	0.9
B	0.2	1	2	2.5
C	0.01	1	10	20
Average	0.07	0.68	4.27	7.8
		Macrostability		
A	0.02	0.1	0.6	0.9
B	0.7	1.3	1.8	2
C	0.01	1	10	20
Average	0.24	0.8	4.13	7.63

water levels was therefore added as a second variable to the fragility curves creating the example fragility surface shown in Figure 2.3. In practice, this means that Sampled probabilities applied to this surface give an incremental range of water levels and associated exceedance durations for which failure would occur according to that probability. The example sampled probability of 0.7 in the fragility surface in Figure 2.3 results in a set of thresholds whereby failure occurs if the water level exceeds 10 m for 48 hrs, or 10.2 m for 36 hrs, etc.. At each location, the ranges resulting from each mechanism were combined using the smallest duration for the incremental water level height, resulting in a single set of failure criteria.

To include the duration as a dependent variable in these surfaces, adjustment factors for the fragility curves for certain durations of water levels were elicited via the opinion of three dike failure experts. These values and the averages that were used are given in Table 2.1. The factors describe how the curve probabilities should be increased / decreased based on the durations. For example, a factor of 0.5 halves the probabilities described by the fragility curves for the corresponding duration, signifying the expert believes the fragility curves over-estimate the risk at this duration. Interpolating between these estimates creates surfaces similar to the example in Figure 2.3. This process was carried out for each breach mechanism and location in the model. Sampling values from each of the curves for a simulated event lead to the relationship between duration and water level for which failure would occur, as seen in the cyan line in Figure 2.3. As with the fragility curves, these surfaces were then adjusted to conform to the new protection standards. The original and adjusted curve data is given in section 2.C.

It can be seen that all experts agree that the existing fragility curves represent the uncertainty for some duration, as a factor of 1 lies within each range given, and this was generally the basis of the experts' decision making. The steady increases in the factors

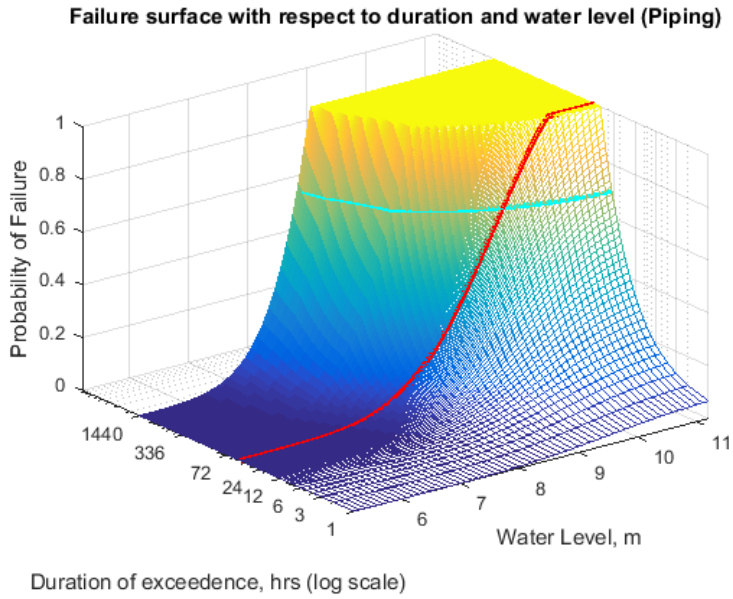

Figure 2.3: Example fragility surface for piping mechanism. Line in red shows original fragility curve, for which a duration of 48 hrs is considered most applicable by the experts. The cyan line shows the resulting threshold due to a sampling value of 0.7

with respect to duration show a clear dependency on this variable. However, the factors offered by experts differ greatly. This could be for numerous reasons, such as prior knowledge of the development of the curves, or a difference between understanding of the terms 'breaching' and 'failure'.

The sensitivity of these factors on the hydraulic results was not considered due to the demonstrative nature of this work, However, it should be noted that using these factors for scenario 2 factors represent a best-estimate between the extremes represented by scenario 0 (no system behaviour) and scenario 1 (system behaviour based on water level alone). In scenario 1, embankments will fail in the rising limb of the floodwave, ensuring large breach volumes are removed from the river system. In scenario 2, no breach volumes are removed from the river. Accounting for duration in scenario 2, embankments may also fail later which reduces the effect of the breach downstream.

While the use of different factors is likely to have an effect on the specific breaching estimates quantified in the results, it is recommended that a more structured expert judgement analysis to elicit duration dependency be prioritised over sensitivity analyses for future studies.

2.3.5. PROBABILISTIC ANALYSIS

Using the load and strength distribution probabilities described above, multiple simulations were run, and output variables of interest were recorded to compute probability distributions. In order to track and compute the input and output variables used in

each simulation, and their associated probabilities, the Probabilistic Toolkit© was used to 'wrap' the simulations. This tool collected and analysed the output data, referencing the input probabilities that had been used in that simulation. Sample probabilities were generated using importance sampling based around 16,000 m^3/s for the discharge, with a maximum of 20,000 m^3/s. The dike strengths and wave shapes were sampled with crude Monte Carlo sampling. 15000 simulations were run for each scenario, based on the convergence of the breaching failure probabilities. The scenarios were analysed in terms of hydraulic loads in the system, failure probabilities, and breaching data per location. The outcomes are discussed in the following section.

2.4. RESULTS AND DISCUSSION

2.4.1. HYDRAULIC LOADS

The calculated return period water levels for the four selected locations of interest are compared in Figure 2.4. It is immediately apparent that system behaviour leads to a reduction in the water levels, which is to be expected at all downstream locations, with the difference only being observed at higher return periods. Although it is small, a reduction of this impact is seen in scenario 2, due to the lower abstraction from the river when failure occurs after the peak of the flood wave. At less extreme flows, scenario 2 conforms more closely to scenario 0. In this scenario, breaches still occur, but many of the breaches are coming late in the flood wave, reducing the impact of system behaviour. At location $I13\_r$, the impact of system behaviour is observed at smaller return periods, and is greater than the other locations, but it should be noted that the scales on the x-axis are different for all locations. This larger impact is principally due to the lower protection standards on the IJssel.

An interesting aspect of system behaviour is noted when the corresponding discharges at these locations are assessed. At location $P1\_r$ the difference in discharges is negligible for all scenarios, despite having breach locations upstream of that location. This is due to a 'drawdown' effect of breaches downstream causing a water level gradient and pulling water downstream, and a similar effect is seen at location $W6\_l$. An extreme example of this is observed at $L19\_l$, where the large breach volume that occurs at that location causes higher peak discharges than the scenario without system behaviour. This effect has been observed by Kiss et al. (2015), who noted increases in water stream slope and power in river stretches upstream of breaches. In this instance, scenario 2 increases this effect, which is probably due to the increased water levels experienced at this location, which cause higher drawdowns and therefore larger discharges. The severity of this effect may be due to the simplification of using a 1D reservoir to represent the floodplain behind the breach, but the underlying principal behind it will still occur even with a more advanced schematisation. At location $I13\_r$ on the IJssel the reduction in discharge more closely corresponds to the water level distribution, and as with the water levels, breach triggering using duration as a variable mitigates the effect of system behaviour.

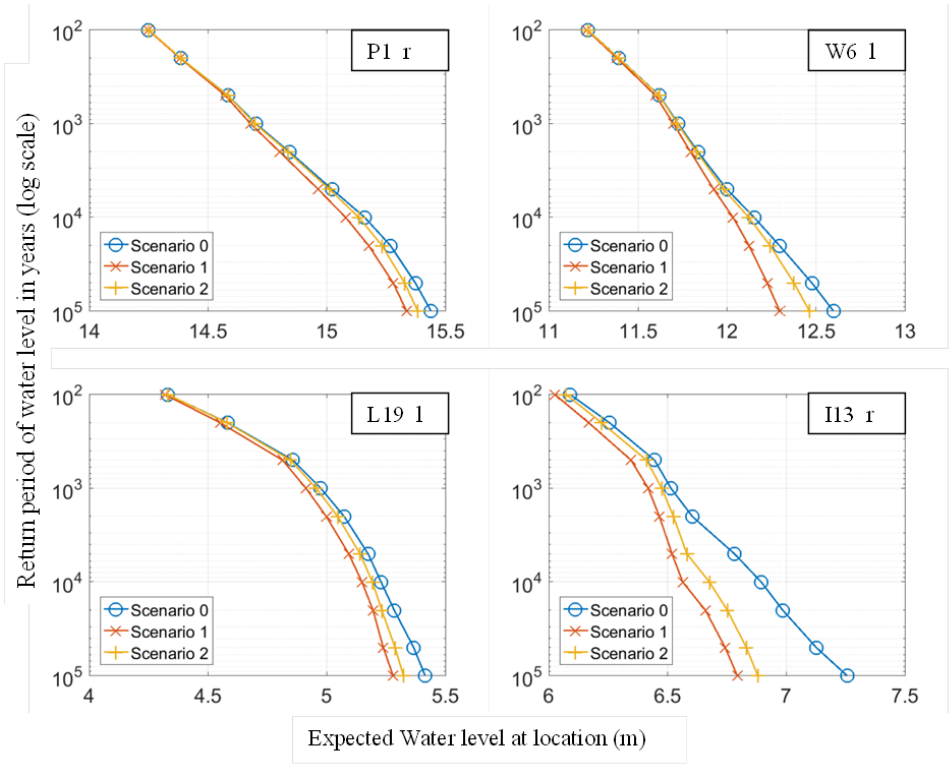

Figure 2.4: Return period water levels for Scenarios 0, 1 and 2, at locations $P1\_r$, $W6\_l$, $L19\_1$ and $I13\_l$. These locations can be seen on a map in Figure 2.2. Note that the x-axis scales are not the same per location. Scenarios 0, 1 and 2 represent no system behaviour, system behaviour dependent on water level and system behaviour dependent on water level and duration respectively.

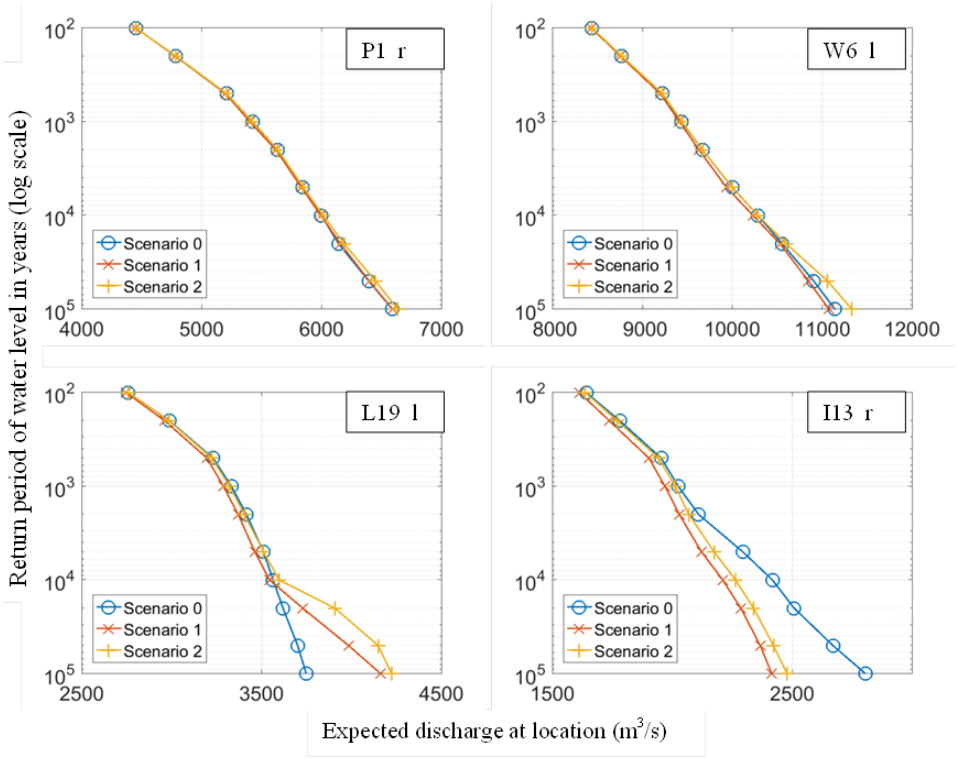

Figure 2.5: Return period discharges for Scenarios 0, 1 and 2, at locations*P*1_*r*, *W*6_*l*, *L*19_1 and *I*13_*l*. These locations can be seen on a map in Figure 2.2. Note that the x-axis scales are not the same per location Scenarios 0, 1 and 2 represent no system behaviour, system behaviour dependent on water level and system behaviour dependent on water level and duration respectively.

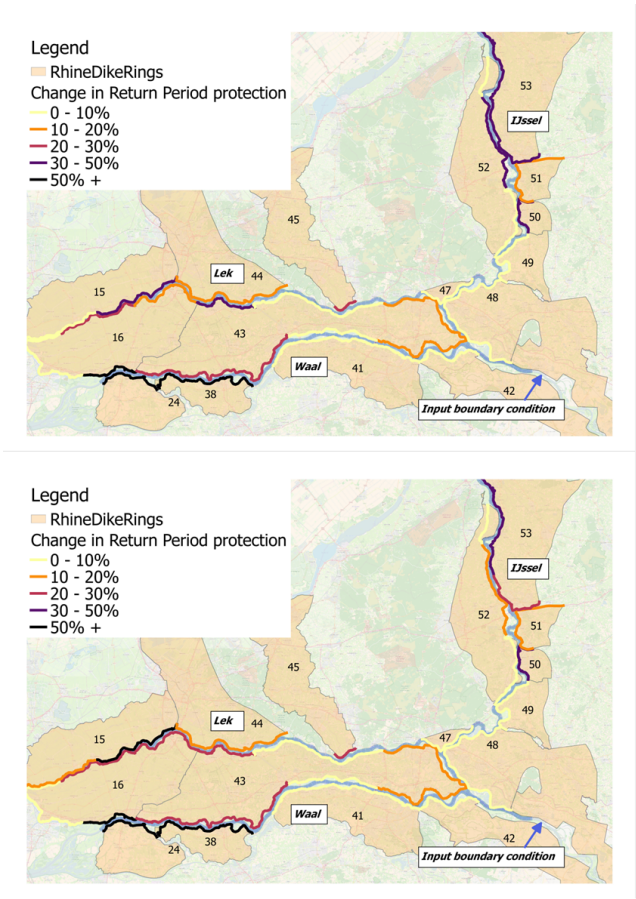

Figure 2.6: Relative change in failure probability of the overall trajectories when system behaviour is implemented, scenarios 1 (top) and 2 (bottom) Scenarios 1 and 2 represent system behaviour dependent on water level and system behaviour dependent on water level and duration respectively.

2.4.2. FAILURE PROBABILITIES

The relative change in trajectory failure probability for scenarios 1 and 2 is given in Figure 2.6, below. As expected, in both scenarios the failure probabilities generally decrease (return period protection increases), with little or no effect at the upstream sections (0-10% change) and the largest effect seen at the downstream ends. However, at the most downstream locations ends of these branches, the boundary conditions dampen the effect of system behaviour, and the effect is reduced. Small differences in failure probability decrease between the scenarios are observed on the IJssel and Lek, but they are not significant enough to draw conclusions. The full set of failure probabilities is given in section 2.A.

Table 2.2: Averaged breaching data for scenarios at selected location. Data relates to the 12000 simulations performed for each scenario.

Attribute	Scenario	Value			
Location	**-**	**P1_r (48_1)**	**W6_l (41_2)**	**L19_1 (16_3)**	**I13_r (53_1)**
Number of breaches	**1**	251	961	388	1014
	2	318	1067	497	1167
Average volume when breached (m3)	**1**	93,500 m^3	335,000 m^3	375,000 m^3	7,230 m^3
	2	72,100 m^3	309,000 m^3	324,000 m^3	4,410 m^3
Average breach width (m)	**1**	200 m	360 m	316 m	59 m
	2	185 m	353 m	310 m	63 m

2.4.3. BREACHING

The statistics relating to the breaches in each scenario at the locations of interest can be seen in Table 2.2. It should be noted that these figures are subject to a large degree of uncertainty as described previously, but do demonstrate trends in the comparison of the two system behaviour scenarios. The frequency of breaching in the 15000 simulations increases at each location in scenario 2 compared to scenario 1, but the average volume of breach flow reduces. This is principally due to the potential for later breaching in scenario 2. In theory, two factors should reduce the breach widths observed in scenario 2. The first is that breaching can occur late in the simulation, (after the flood wave); reducing the time for growth and the second is that the difference in water levels is less severe in scenario 2, due to the dependence on duration. However, the difference in breach widths is small, and the trend is reversed at location $I13\_r$. The reason for this specific trend reversal is related to breaches upstream, local floodplain schematisation, and even downstream breaches, demonstrating the complexity of the system.

The expected number of breaches and total breach volumes in the entire system are given in Figure 2.7, for various return periods. An increase in expected breaches from scenario 1 to 2 is again observed, however this difference is small in comparison to the expected breaches that would occur if system behaviour was not taken into account. Although most locations experience less breach volume in scenario 1 than in scenario 2, the higher number of breaches ensures that the expected overall breach volume is larger for extreme events.

2.5. CONCLUSIONS

This study analyses the effect on flood hazard of two breaching triggering mechanisms in a system behaviour framework for the Dutch Rhine system. Variability in the load and strengths of the system are accounted for using 1D simulations in a Monte Carlo analysis. Potential breaches can occur dependent on water level in scenario 1 and both water level and duration in scenario 2, implemented using fragility curves and surfaces respectively. These fragility functions are adjusted to conform with the new protection standards in the Netherlands, and the results are compared in relation to hydraulic loads and breaching statistics.

As previously concluded by De Bruijn et al. (2016), it is clear that system behaviour

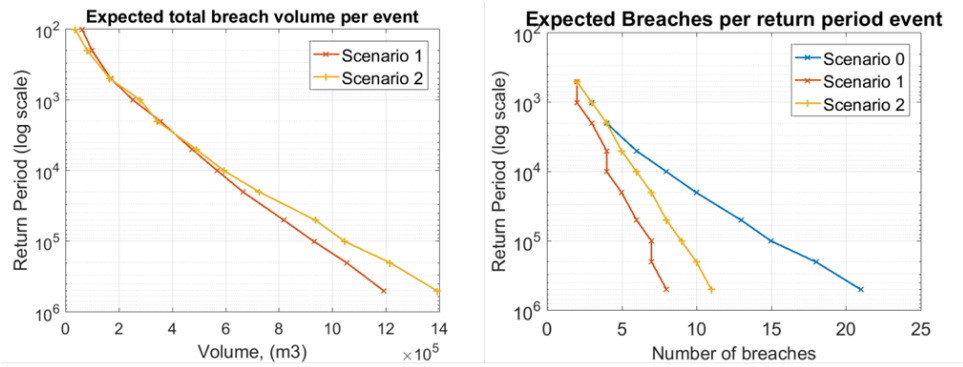

Figure 2.7: Expected breaches and breach volumes per return period event in the system.

has an impact on the downstream loads in the system, and as expected, this impact is generally reduced with the inclusion of duration in the failure mechanism. However, the results suggest that this reduction in impact is small for the modelled system, and even absent in terms of peak discharge (Figure 2.5). As seen in the results, the changes in hydraulic loads will directly affect the probability of failure downstream, and the breach volume experienced when breached. The combination of these effects will have an overall effect on the hazard and thus risk in the system.

The method and results presented have a number of limitations. Firstly, the effect of water level duration on the breach probability is very uncertain. The experts' opinion on this effect differs significantly and the probabilities cannot be validated easily since there is a lack of data. Given that the events of interest are of extremely low probability, this drawback of validation is unlikely to be overcome. Secondly, the hydraulic loads inputs to the system have also been simplified by using generic wave-shapes. In reality the floodwave may have much more variability, such as double peaks, as seen in the load data obtained from GRADE. Finally, the floodplains are represented by simple reservoirs here and do not represent the timing or volume of breach flow accurately. Besides, the water levels in the reservoirs are not directly related to local water depths which mean that this approach cannot be directly linked to flood impact models.

These simplifications mean that although this method is applicable to policy analyses on large scale (for systems understanding etc.), the method is not suitable for design purposes. The results can be considered representative of system behaviour and the effect of including water level duration in the dike breaching component.

An understanding of the likely behaviour in a system during extreme events has intrinsic value for flood risk strategy development, and may have applications in other fields such as emergency response and insurance. Other lowland river areas with a defence system in place, such as the Elbe, Danube, Po and the Vietnamese Red River could also benefit from such an analysis.

Recommendations for improving the method are to better represent the floodplains include the influence of the sea and the Meuse River on the area. Given the large uncertainties in system behaviour and the small effects observed when including duration of

the water level, a more geotechnically accurate breaching mechanism to represent the influence of duration may not add value. However, a more structured expert opinion session may produce a better method of representing this uncertainty.

Finally, it should be noted that the results only count in case the system complies with the new safety standards, which is not the case at the moment. In fact there are almost no embankments in the river that do comply currently. Assessing the system using an estimate of the current protection levels is likely to show a more pronounced effect of system behaviour in general, and may also change the effect of the duration dependency.

APPENDICES

2.A. FAILURE PROBABILITIES, BREACH LOCATIONS AND TRAJECTS

The 62 breach locations used in the model are shown in Figure 2.8, and the associated trajectories and failure probabilities are shown in Table 2.3. The information from the breach locations is combined to generate the overall trajectory failure probabilities. The third column of the table shows the protection standard and the fourth and fifth columns show the calculated failure probabilities of these trajects in scenario 0, for both breach triggering mechanisms. As the fragility curves and surfaces were adjusted to meet the desired probabilities, these values should approximate the third column. The final 2 columns show the new failure probabilities when system behaviour is applied. In all cases, the failure probabilities decrease (return times increase) with respect to than their non-system behaviour equivalents.

2.B. VERHEIJ VAN DER KNAAP PARAMETERS

The breach growth formula is shown in Equation 2.1.The parameters input prior to calculation are given in Table 2.4, H is the difference in water level, and t is the time in hours since the breach occurred.

$$B(t) = B_0 + f_1 \frac{g^{\frac{1}{2}} H^{\frac{3}{2}}}{u_c} \log\left(1 + \frac{f_2 g}{u_c} t\right) \tag{2.1}$$

2.C. ORIGINAL AND ADJUSTED FRAGILITY CURVES

Below are the calculated original fragility curves calculated, represented as mean and standard deviation for each mechanism. For the two scenarios, the standard deviations were maintained, and the mean values were adjusted at each location so that the dike as a whole conformed to the new protection standards. As the change in mean values was the same for each mechanism, it is represented as a single value on the columns on the left.

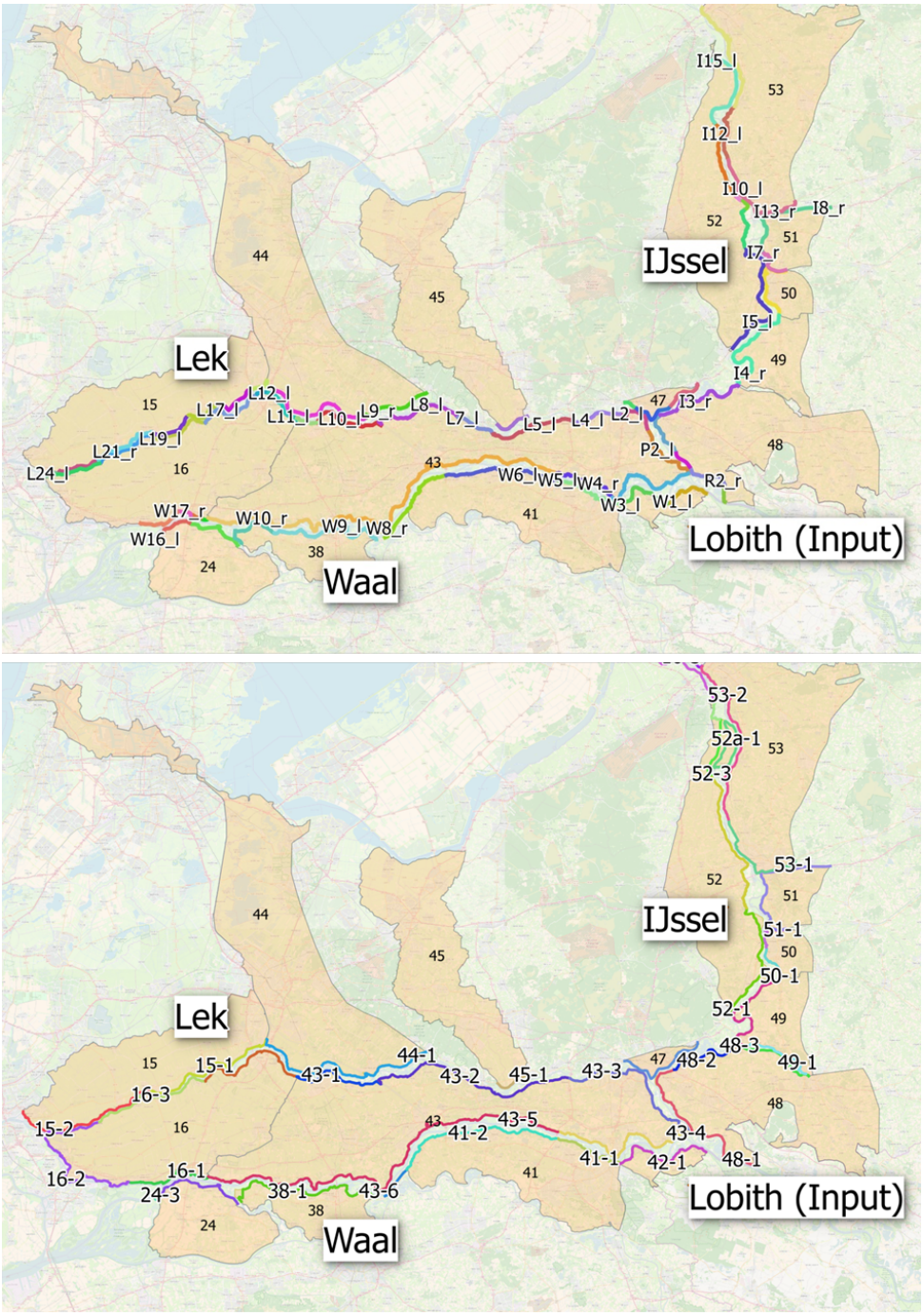

Figure 2.8: Breach locations used in the model and associated dike sections.

Table 2.3: Traject location failure probabilities given in return period years. The protection standard is shown against the failure probabilities calculated with and without system behaviour for each dike breaching scenario. The values are rounded for clarity.

Trajectory location	Associated breach locations	Failure probability in return period years				
		Protection Standard	Sc0 (Water level trigger)	Sc0 (Water level and duration trigger)	Sc1	Sc2
15_1	L16_r, L18_r, L20_r, L14_r, L21_r, L13_r	30000	26500	28200	38100	44800
15_2	L23_r	30000	23200	50100	23200	56500
16_1	W15_r, W17_r, W13_r, W14_r	30000	30900	50500	368000	437000
16_2	L24_l	10000	10000	12000	10000	12000
16_3	L19_l,	10000	9880	8960	12200	11400
16_4	L15_l, L17_l, L12_l	10000	11200	9580	13200	11800
24_3	W12_l, W16_l	10000	10700	17500	29200	37200
38_1	W11_l, W9_l	10000	10200	18700	22300	32800
41_1	W5_l	10000	7960	8290	8380	9030
41_2	W7_l, W6_l	3000	2460	2700	2550	2830
42_1	W1_l, W3_l	3000	3100	2970	3220	3080
43_1	L11_l, L10_l	10000	9730	8430	12700	10600
43_2	L8_l, L7_l, L5_l	3000	2750	2490	2880	2640
43_3a	L4_l, L2_l, P2_l, W2_r	10000	9810	9310	11700	10900
43_4a	W4_r	10000	8280	8330	8680	9020
43_5	W10_r, W8_r	10000	10100	9140	12800	11400
44_1	L9_r	10000	11000	9390	12900	11100
45_1	L6_r	30000	24100	28100	30600	33900
47_1	I2_l, I1_l, L1_r, L3_r	30000	26500	28200	38100	44800
48_1	P3_r, P1_r, R2_r, R1_r	30000	23200	50100	23200	56500
48_2	I3_r	30000	30900	50500	368000	437000
49_2	I4_r	10000	10000	12000	10000	12000
50_1	I6_r	10000	9880	8960	12200	11400
51_1	I8_r, I7_r	10000	11200	9580	13200	11800
52_1	I15_l	10000	10700	17500	29200	37200
52_2	I12_l, I9_l, I10_l, I11_l	10000	10200	18700	22300	32800
52_3	I5_l	10000	7960	8290	8380	9030
53_1	I13_r	3000	2460	2700	2550	2830
53_2	I14_r, I16_r	3000	3100	2970	3220	3080

Table 2.4: Verheij van der Knaap parameters used in the breach growth formulation.

Parameter name	Description	Range	Default value	Unit
f1	Empirical factor for breach width	0.5 – 5	1.3	-
f2	Empirical factor for breach width	0.01 - 1	0.04	-
Uc	Critical flow velocity	0.1 - 10	0.2	m/s
B0	Initial breach width	-	20	m
g	Acceleration due to Gravity	-	9.81	m/s2

Table 2.5: Fragility curves calculated from BOA data, and the adjustments required to the means to conform to the new protection standards, for each scenario. See Figure 2.2 for locations of breaches on a map.

	Sigma values for mechanisms (m)			
Location	**Overtopping**	**Piping**	**Macro - stability**	**Difference between Mu values; Sc2-Sc1**
L9_r	0.16	0.8	1.03	-0.08
L16_r	0.12	3.5	1.21	-1.07
L18_r	0.08	1.12	1.29	-0.15
L23_r	0.12	1.46	1.39	-0.39
L20_r	0.16	1.25	1.29	-0.16
L14_r	0.16	0.99	1.25	-0.11
L21_r	0.07	1.61	1.33	-0.34
L13_r	0.13	0.87	0.97	-0.06
I14_r	0.14	1.48	0.85	-0.36
I16_r	0.1	1.48	0.75	-0.31
I13_r	0.2	0.95	0.72	-0.18
I15_l	0.12	0.68	0.71	-0.13
I12_l	0.1	0.78	0.8	-0.15
I9_l	0.12	0.72	0.85	-0.1
I5_l	0.17	0.65	0.7	-0.14
I8_r	0.17	0.58	0.67	-0.07
I7_r	0.16	0.51	0.68	-0.07
I6_r	0.22	0.62	0.38	-0.04
I4_r	0.13	1.75	0.35	-0.41
I3_r	0.2	0.88	0.84	-0.13
P3_r	0.09	1.08	0.73	-0.08
P1_r	0.18	1.33	0.86	-0.12
R2_r	0.5	1.02	0.73	-0.08
R1_r	0.25	1.28	0.75	-0.15
I2_l	0.13	1.38	1.05	-0.13
I1_l	0.09	1.61	1.24	-0.14
L1_r	0.23	1.29	1.12	-0.08
L3_r	0.17	1.14	1.17	-0.16
L11_l	0.12	1.1	0.49	-0.06
L10_l	0.23	0.55	0.43	-0.02
L8_l	0.17	0.55	1.16	-0.05
L7_l	0.19	0.82	1.33	-0.07
L5_l	0.13	0.59	1.19	-0.02
L4_l	0.12	0.74	0.7	-0.04
L2_l	0.15	0.72	0.79	-0.02
P2_l	0.1	1.01	0.61	-0.08
W10_r	0.15	0.73	0.97	0.01
W8_r	0.24	0.84	1.27	-0.02
W4_r	0.18	0.93	1.94	-0.02
W2_r	0.12	1.09	2.79	-0.04
W1_l	0.17	1.36	0.86	-0.12
W3_l	0.14	1.83	0.87	-0.26
W7_l	0.15	1.41	1.53	-0.19
W6_l	0.17	1	1.49	-0.08
W5_l	0.11	1.28	0.56	-0.12
W11_l	0.25	0.72	1.55	-0.3
W9_l	0.14	0.65	1.41	-0.25
L15_l	0.13	0.8	0.68	-0.06
L24_l	0.1	0.77	1.44	-0.54
W15_r	0.2	0.2	0.2	-0.11
L17_l	0.15	2.02	0.54	-0.31
L6_r	0.18	0.77	1.11	-0.05
W12_l	0.13	0.11	0.11	-0.09
W16_l	0.15	0.14	0.14	-0.21
W17_r	0.14	0.16	0.16	-0.02
W13_r	0.07	0.16	0.16	-0.05
L19_l	0.14	0.88	0.49	-0.04
L22_l	0.15	1.13	0.47	-0.14
L12_l	0.07	1.01	0.57	-0.07
W14_r	0.19	0.2	0.2	-0.03
I10_l	0.11	0.84	1.07	-0.12
I11_l	0.11	0.88	1.26	-0.13

3

SPATIAL INTERDEPENDENCIES OF INUNDATION THROUGH SYSTEM BEHAVIOUR

ABSTRACT

To make informed Flood Risk Management (FRM) decisions in large protected river systems, flood risk and hazard analyses should include the potential for dike breaching. 'Load interdependency' analyses attempt to include the system-wide effects of dike breaching while accounting for the uncertainty of both river loads and dike fragility. The intensive stochastic computation required for these analyses often precludes the use of complex hydraulic models, but simpler models may miss spatial inundation interactions such as flows that 'cascade' between compartmentalised regions and overland flows that 'shortcut' between river branches. The potential for these interactions in the Netherlands has previously been identified, and so a schematisation of the Dutch floodplain and protection system is here developed for use in a load interdependency analysis. The approach allows for the spatial distribution of hazard to be quantified under various scenarios and return periods. The results demonstrate the importance of including spatial inundation interactions on hazard estimation at three specific locations, and for the system in general. The general modelling approach can be used at a local scale to focus flood-risk analysis and management on the relevant causes of inundation, and at a system-wide scale to estimate the overall impact of large-scale measures.

A slightly modified version of this chapter has been published as "Large Scale Flood Hazard Analysis by Including Defence Failures on the Dutch River System" in the special issue "Flood Risk Analysis and Management from a System's Approach" in *Water* (Curran et al., 2019).

3.1. INTRODUCTION

3.1.1. LOAD INTERDEPENDENCIES

In the flood hazard analysis of protected lowland river systems, the spatial and temporal changes in local and system-wide hazard due to dike breaches are often called 'load interdependencies' (Klerk, 2013), 'river system behaviour' (De Bruijn et al., 2014; van Mierlo et al., 2007) or 'system-risk' (Gouldby et al., 2012). Analysis of this behaviour has become more widespread in recent years, thanks in part to a 'systems approach' (Vorogushyn et al., 2017) to Flood Risk Management (FRM) being adopted. Examples of load interdependency analysis in FRM include those by Ciullo et al. (2019)] and Dupuits et al. (2019, 2016), who demonstrated the importance of this behaviour when developing optimal management strategies.

Load interdependency analyses have been used to estimate flood impacts such as; fatalities (De Bruijn et al., 2010), economic losses (Assteerawatt et al., 2016), and both economic losses and fatalities (Dunn et al., 2016). However, much of the research into the field has focused on accurately identifying changes in hazard rather than flood risk (for example, Apel et al., 2009; Kiss et al., 2015). In either case, the occurrence of breaches in space and time usually causes the greatest uncertainty, and therefore a probabilistic Monte Carlo method is almost universally adopted (Diermanse et al., 2014; Gouldby et al., 2012). In the Monte Carlo approach, within any given simulation of the system, the occurrence of a breach is dependent on hydraulic loads and dike strengths sampled from respective distributions.

3.1.2. SPATIAL ASPECTS OF LOAD INTERDEPENDENCIES

In a load interdependency analysis, the location of a potential breach is usually based on a discretisation of the dike system to which distributions of dike strength such as fragility curves or functions (see, for example Curran et al., 2018; Wojciechowska et al., 2015) are applied. This discretisation can be determined by distance, for example on the Po River (1.2km sections - Domeneghetti et al. 2013) and the Elbe River (500 m sections - Vorogushyn et al. 2010), or on similarities in inundation consequences (e.g. Rhine River, Jongejan et al. 2013). The dependency of failure between neighbouring sections can also be considered, for example by Assteerawatt et al. (2016) and in the Dutch Hydra-Ring software (Diermanse et al., 2013).

Once a breach occurs, downstream river flow is reduced. This aspect of system behaviour has been termed 'a positive interdependency' (De Bruijn et al., 2016; Dupuits et al., 2016; Klerk, 2013) due to the reduced hazard and risk downstream. The breach outflow over time must be accurately calculated in order to quantify both the remaining discharge in the river system and the inundation to the connected floodplain. This outflow will be a function of the river discharge and the floodplain topography but is also heavily influenced by the breach growth in time. Empirical methods to estimate breach growth are available (Verheij and der Knaap, 2002), however in many load interdependency analyses simplified growth functions are used.

Various methods exist to model the effect of dike breaches on river flows and floodplain inundation, as discussed by Klerk (2013). Breach simulations often use a fixed grid or mesh where flow is modelled using the two-dimensional (2D) St. Venant equations in

the floodplain domain (Teng et al., 2017). However, such fully hydrodynamic models are not widely used in load interdependency analyses, primarily due to the computational effort required when running Monte Carlo simulations. Nevertheless, load interdependency analysis using a fixed grid in the 2D domain can be performed for relatively small systems or subsystems of embanked rivers (Domeneghetti et al., 2013; Gouldby et al., 2012). Fast 2D models that solve simplified versions of the St. Venant equations (Ahmadisharaf et al., 2013; Bates and De Roo, 2000) have also been used in load interdependency analyses (Falter et al., 2016; Lhomme et al., 2008).

Floodplains can also be schematised in one-dimension (1D) based on expected flow routes (see for example De Bruijn 2005), and can perform as well as 2D simulations for certain topographies (Horritt and Bates, 2002). Examples of 'zero-dimensional' (0D) schematisations, which split up the floodplain into different areas with a certain storage capacity include the RFSM model (Lhomme et al., 2008), used in a load interdependency analysis by Gouldby et al. (2012). In software packages where this modelling type is not explicitly implemented, it can be approximated using connected retention nodes. An example of this is Sobek (Dhondia and Stelling, 2004), which has been used with estimates of polder storage capacities in various load interdependency analyses (Apel et al., 2009; Curran et al., 2018; De Bruijn et al., 2014). In these studies, storage nodes were used at each breach location, but the potential for dynamic interactions between these storage volumes (as modelled by Klerk, 2013) was not implemented. The use of either 0D or 1D floodplain modelling necessitates calibration against 2D simulations, or where possible, against observed inundation extents and depths.

With a sufficiently accurate schematisation of the floodplain domain in a load interdependency analysis 'negative' interdependencies can be modelled. In compartmentalised floodplain regions these interdependencies have the potential to occur when flood volumes move between the regions (cascading) or return to the river system through the compartment (shortcutting). In either case the effect of the breach to hazard in downstream areas has increased, thus causing the 'negative' interdependency between components. While this effect has the potential to occur in any protected river system, the low-lying, branched and compartmentalised river system of the Netherlands is particularly vulnerable, as discussed in section 3.2. Therefore, in the present study a load interdependency analysis for the Netherlands is combined with 'fast' quasi-2D modelling methods to produce hazard estimates under various defence failure scenarios relating to breaches caused by floodplain inundation. The introduction of the fast quasi-2D schematisation not only allows enough simulations to be performed to generate localised and system-wide risk estimates, it also provides the opportunity to assess negative system behaviour effects due to defence failures in the floodplain domain.

3.2. LOAD INTERDEPENDENCIES IN THE NETHERLANDS

Since the 16th century, the compartmentalisation of floodplain areas in the Netherlands has developed primary defences that protect polders from the rivers and sea, and secondary defences that divide the polders into smaller regions (Driessen, 1994). The primary defences consist of multiple dike rings that have been assigned higher and higher protection standards over the years, due to the occurrence of extreme events and increased economic and societal exposure (De Moel et al., 2011). New protection stan-

dards to which the primary defences must conform have recently been imposed under Dutch law (Slomp, 2016), however it is known that most of the defences do not currently adhere to these standards. The most recent estimate of current protection levels are given by the VNK2 project (Jongejan and Beek, 2015), however the calculated failure probabilities are generally considered to be conservative. Within the study, the probability of breaches along defined sections of dike was used to estimate the overall failure probability of 'trajects' or segments of the dike ring defences. The VNK2 project only accounted for load interdependency effects between dike rings 14, 15 and 44 (see Figure 3.1), in effect treating this highly developed area as a single dike ring (Ter Horst, 2012). However, investigations into load interdependencies by Delft Hydraulics (Van Mierlo et al., 2003) suggest that negative effects are likely to be significant in a number of regions not addressed in the study, three of which are highlighted in the present study.

The first location for which spatial aspects of load interdependencies may be relevant is in dike ring 43 (the 'Betuwe', see Figure 3.1, location A). The region is shown to be vulnerable to floods both economically (Wagenaar et al., 2016) and with respect to loss of life (Kolen et al., 2013). Simulations of breach flows into this dike ring demonstrate how secondary defences delay and compartmentalise the flood waters, causing high water depths upstream of these defences. Studies suggest this effect reduces overall economic risk and further 'compartmentalisation' of the region would likely further reduce risk (Klijn et al., 2010). Flood water can overflow back into the river system downstream in the dike ring, however failure of this system would likely result in a cascading or domino effect of flows into dike ring 16 ('Alblasserwaard') (Van der Most and Klijn, 2013).

Another potential floodplain shortcut highlighted by Van Mierlo et al. (2003) is dike ring 41, or 'Land van Maas en Waal' (Figure 3.1, location B). As the name suggests, this region sits between the Waal and Meuse rivers, which converge to within 1 km of each other at the Western end of the dike ring. The dikes on the Meuse are generally lower than those of the Waal in the regions of dike rings 41 and 40 (see Figure 3.1). This, together with the Meuse's smaller capacity means that large breach flows originating from the Waal could increase flood risk downstream on the Meuse. A probabilistic computational framework for system behaviour analysis of this area was described by Courage et al. (2013). The authors concluded that load interdependencies are highly significant in the area, and that a framework encompassing the entire system was required for further analysis.

The potential for cascading and shortcutting of breach flows originating on the right bank of the German Rhine and propagating down the IJssel (through dike rings 48-53, see Figure 3.1, location C) has been addressed in studies by Klerk (2013) and Bomers et al. (2019). In both studies, a large redistribution of risk was observed. During high flows on the Rhine, bifurcation control structures convey only 1/9 of the Rhine flow towards the IJssel, due to the limited capacity of this branch. However, breaches on the right bank of the Rhine, upstream of the bifurcations, have the potential to increase this flow beyond the capacity of the river, should the flows rejoin the system.

This paper analyses load interdependencies in the Dutch river system that include the potential for spatial inundation effects such as cascading and shortcutting. Scenarios are evaluated to model the effects of polder-side and regional defence failures, and the results from the three locations described above (dike ring 41, dike ring 43 and the

IJssel valley) are analysed in detail. While load interdependency analysis that include the potential for negative interdependencies have been applied to isolated areas in the Netherlands, it was not previously possible to quantify the effect on overall hazard in the system. Furthermore, by developing scenarios that allow for polder-side and regional defence failures, the effects of a non-static floodplain domain can be assessed.

3.3. METHODOLOGY

3.3.1. CASE STUDY

The case study is based on the lower Rhine and Meuse Rivers in the Netherlands.The floodplains of this region have been compartmentalised into a system of dike rings in which roughly 67% of the population of the Netherlands (17 million people) live. The area has been schematised in a calibrated Sobek 3 model (Dhondia and Stelling, 2004) (see Figure 3.1). Downstream, stage-discharge boundary conditions are used on the Meuse, and on the three Rhine branches of the Waal, Lek and IJssel. These locations are considered to be upstream of where tidal influences are dominant in the system. The upstream boundary conditions use available hydraulic load distribution data from the 'GRADE' (Generator of Rainfall and Discharge Extremes) project (Hegnauer et al., 2014) for both the Meuse and Rhine rivers. Smaller tributaries are ignored or modelled as steady state contributions.

As the risk of pluvial flooding is small relative to fluvial, floodplain inundation is only possible from the rivers. Potential breach locations and the dike ring sections they represent are defined as per the VNK2 study, with the addition of 12 locations in Germany, where dike rings 42 and 48 extend across the Dutch-German border. These latter breach locations are defined as per inter-agency reports on the dike rings (Duits-Nederlandse Werkgroep Hoogwater, 2009). Other potential breaches further upstream on the Rhine are likely to be smaller and contained within the floodplain valley, however the effect of these breaches on the incoming floodwave is a limitation of the study.

Historical breaching events such as floods in 1805 and 1926 have been suggested as precedents for cascading and shortcutting flows (Hesselink et al., 2003; Ververs and Klijn, 2004), however too much has changed in the river and floodplains to consider these events for validation of 2D schema. Instead, the present schematisation was validated using coupled 1D-2D breach simulations from available models and a repository of existing 1D-2D simulations (Rijkswaterstaat).

In the Sobek model, once a breach occurs it enters the floodplain domain, which is delineated by the dike rings (Figure 3.1). To reduce the computation time required, the flow is schematised as either 1D or 0D in the floodplains, and the available 1D-2D breach simulations are used to delineate, schematise and calibrate the floodplain domain.

An example of this process for dike ring 43 can be seen in Figure 3.2, showing the inundation calculated over time by a particular breach simulation, as well as the final schematisation used in the present study. Here, the breach flow is considered to behave like a series of connected reservoirs (i.e. 0D) rather than a floodplain flow route (1D). Areas where the floodplain flow builds up before overflowing into a new region are in this case delineated by major roads and secondary defences. Breaches from the river fill a shared reservoir representing the retention capacity of the region in relation to the

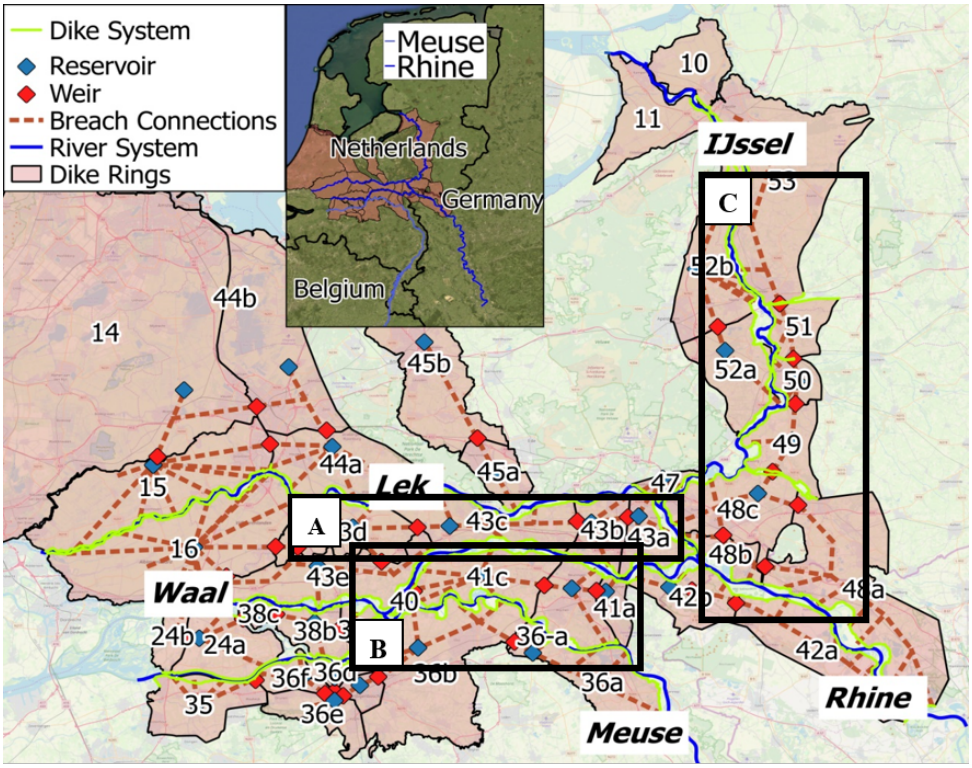

Figure 3.1: Schematised river and dike system for the Netherlands, as well as quasi-2d floodplain schematisation. The numbers refer to the dike ring IDs used in the model. Inset: Relative location of case-study. Three specific locations discussed in the results are highlighted in black (A-C).

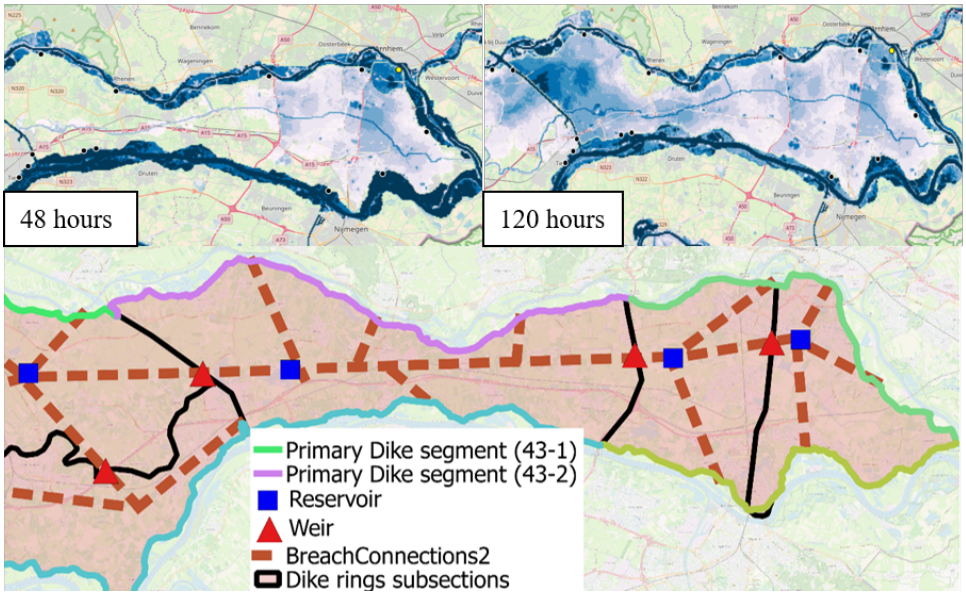

Figure 3.2: Top panels: Flooding from the Lek to dike ring 43 over time. Bottom panel: resulting delineation and schematisation of dike ring 43 based on flood simulations.

water depth, which is calculated through a GIS analysis of that area. The location of overflows which connect the compartments are schematised with weirs that can be adjusted dynamically. The locations of these reservoirs and weirs are shown in Figure 3.1. The 0D schematisation was applied almost unilaterally to the compartments delineated in this analysis, apart from upstream regions in which the steeper topography was better schematised by 1D flow route.

The 2D simulations were also used to benchmark the quasi-2D model. At a given location, breach outflow discharge hydrographs from the 2D model are reproduced in the quasi-2D model by imposing the same floodwave and breach growth conditions. Then the water level time-series from particular 2D cells at downstream locations in the compartments are compared to the water-level time-series from the reservoirs used in the quasi-2D model. These comparisons showed the level and timing of inundation to be sufficiently approximated by the quasi-2D model to represent flows and interactions in the system. The use of the quasi-2D model reduces computation time from about 4 h to 8 min on an Intel Core i5 laptop with 8 Gb of RAM.

The maximum inundation volume stored in the compartments in any simulation is here used as the metric to indicate hazard. Even though the quasi-2D model was validated with respect to timing and inundation depths, maximum volume was used due as it is more consistently accurate and demonstrates interactions relatively clearly. In general, the use of a quasi-2D model prevents other important hazard variables (such as velocity, Dang et al., 2011; Kreibich et al., 2009) from being obtained. This is a significant limitation of the study that could only be overcome with the use of a more complex 2D model.

3.3.2. COMPUTATIONAL FRAMEWORK AND SCENARIOS

The computational framework used to assess the spatial risk is adapted from Wojciechowska et al. (2015). A Monte Carlo analysis is performed in which multiple event parameters are sampled from distributions of load (discharge peak and wave shape) and dike strengths (fragility functions). The hydraulic load distributions are obtained from the GRADE database (Hegnauer et al., 2014), which produces 50,000 yrs of flow data using a weather generator. Both distributions are tabular or relative frequency distributions; however, the wave shape parameter relates to a complete hydrograph that is then scaled according to the sampled peak. This allows for the variability in the duration of flood waves to be included in the simulations. Correlation between sampled events on the river was introduced using a correlation factor of 0.9, which is taken from a report on the dependence of the Meuse and Rhine Rivers by Diermanse (2002). The dike strengths are sampled from fragility functions that are discussed below.

The events are then simulated in the hydrodynamic model to assess the resulting water levels, discharges, breaches and inundation volumes. Importance sampling is used to generate 16,000 simulations for each scenario (see Table 3.1), which was sufficient to ensure convergence of the failure probabilities at each dike section. The outcomes of all simulated events are combined to derive hazard characteristics such as failure probabilities, discharge and water level distributions at various locations and floodplain inundation statistics.

Four implemented scenarios of this framework are assessed to evaluate the effects of inter-riverine flow (caused by polder-side breaching) and inter-regional flows (caused by breaches between dike rings). In all scenarios flow can occur over defences (Table Table 3.1).

Table 3.1: Scenarios used in analysis, indicating which failure mechanisms are used in each scenario.

Scenario Name	River Breach	Regional Breach	Polder-Side Breach
NoSys	✗	✗	✗
RivBr	✓	✗	✗
RegBr	✓	✓	✗
PolBr	✓	✓	✓

In the 'NoSys' scenario, no system behaviour occurs as water does not leave the 1D domain, however the breaches that would have occurred are recorded for the purposes of comparison. In the 'RivBr' scenario, breaches can alos occur from the river but do not occur between dike rings and regions, or from the polder back into the river. In the 'RegBr' scenario breaches can also occur between regions and dike rings, and in the final scenario ('PolBr'), breaches can also occur from polders back into the river. In all scenarios overflow can occur between domains, even if a defence has not been breached.

For river breaches, predetermined breach locations are used to represent a section of dike with a given failure probability. These failure probabilities are based on the VNK2 assessment for each dike 'traject' or segment. At each breach location, previously developed fragility surfaces (Curran et al., 2018), are used to represent the failure probabilities as well as their associated uncertainty in terms of water level and duration of exceedance

of that water level. These surfaces are generated combining the three main failure mechanisms of overtopping, piping and macrostability. The water level uncertainty is based on the amalgamation of fragility curves (Levelt et al., 2017), while the duration component is elicited from expert opinion (Curran et al., 2018). Breach triggering thresholds for each Monte Carlo simulation are sampled from the fragility surfaces, which allow for stochastic breaches before and after the peak of the floodwave. The growth of the breaches is defined using the formula of Verheij and der Knaap (2002), using the default parameters for initial breach width (10 m) and critical flow velocity (0.2 m/s).

In the available 2D breach simulations, the topography of the floodplain is considered static (apart from the initial dike breach). In low-lying and compartmentalised regions, however, barriers to flow may succumb to the water pressure and overtopping volumes from the inundated floodplain. Therefore, the possibility of their breaching is included in 'RegBr'. Due to a lack of research into this type of breaching, this is assumed to be at the moment of initial overtopping, when the formula of Verheij and der Knaap is again used to estimate breach growth.

In the 2D simulations large pressures and overtopping volumes are also observed from the polder side of the dike rings to the rivers, which may cause breaching in this direction. The 'PolBr' scenario therefore also accounts for this failure type. In this scenario, polder-side breaching can (in theory) occur at any location where a river breach is possible, but only practically occurs at locations where flood volumes accumulate and exert pressure on the polder-side slope (i.e., at the downstream end of a dike ring). The method to account for these failure types has been adapted from Klerk (2013), and conversations with dike stability experts. Polder side breaches are assumed to occur due to overtopping and macrostability only, while piping is ignored due to the likely presence of high water pressures on both sides of the dike. As no fragility curves are available for this side of the dike, deterministic breach thresholds are used in the simulations. Overtopping failures occur when the floodplain levels surpass dike height for 3 hrs, whereas macrostability failures occur when the floodplain levels are 3 m higher than the river levels for a period of 12 hrs or more. The results from all scenarios are shown and discussed in the following section, for the entire system and for three specific locations of interest.

3.4. RESULTS AND DISCUSSION

3.4.1. OVERALL SYSTEM

The clearest impact of load interdependencies is observed when assessing extreme events that have the potential to cause more than one breach in the system. On the left side of Figure 3.3, the expected number of breaches (from the primary defences) in an event of a given return period are shown for each scenario (note that in the 'NoSys' scenario, locations that would have breached are recorded, but no flow leaves the river system). The number of breaches is seen to be higher in the 'NoSys' scenario for return periods >500 years. The right side of Figure 3.3 shows the net flow of volume out of all breach locations. This net volume is slightly reduced when flow can breach from the polder-side in the 'PolBr' scenario. The 'NoSys' scenario does have some inundation due to overtopping at extreme events, but this is several orders of magnitude smaller than the other scenarios.

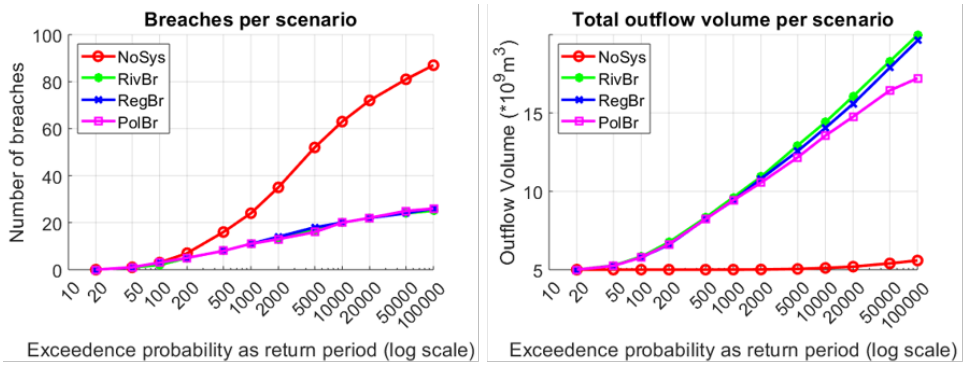

Figure 3.3: Exceedance probabilities in the entire system for number of breaches (**left**) and total breach outflow (**right**).

These results are similar to those observed in the studies of Bruijn et al. (2016) and Curran et al. (2018), in which the lower downstream discharges and failure probabilities due to load interdependencies are also highlighted. However, the 1D models used in those studies make it difficult to ascertain local system behaviour effects caused by floodplain flow. These effects can be examined by comparing the three system behaviour scenarios but are not apparent in the overall values given in Figure 3.3. Three localised system behaviour interactions are therefore examined in detail below. The locations are as discussed earlier, i.e. dike ring 43, dike ring 41 and dike rings 48-53 (The IJssel valley - Figure 3.1).

3.4.2. A: DIKE RING 43

Dike ring 43 is enclosed on the west by a regional defence to dike ring 16 (Figure 3.4). In the quasi-2D model, overflow is possible from subsections 43d and 43e into dike ring 16, and in the 'PolBr' and 'RegBr' scenarios this regional defence can be breached. The expected inundation volumes for various return periods in these regions are shown in Figure 3.4. From these graphs it can be seen that regional failures increase the expected inundation in dike ring 16, while lowering inundation volumes in 43d and 43e. While the volume changes are relatively small, these regional failures cause inundation in dike ring 16 for events with a shorter return period. As most impact models show a steep increase in damage with initial inundation, the larger inundation area caused by regional breaches will likely outweigh any reduction in damage caused by smaller volumes in the upstream compartments.

3.4.3. B: DIKE RING 41

'Shortcutting' (i.e. breach flows that re-join a river system through the polder) has the potential to occur at dike ring 41, which lies between the Waal and Meuse rivers (Figure 3.5). Of the simulations in which the dike ring is inundated, breaching of dike segment 41-2 on the Waal is most often the cause. The resulting inundation volumes are usually high, as the Waal takes a large portion (~2/3) of the discharge from the Rhine.

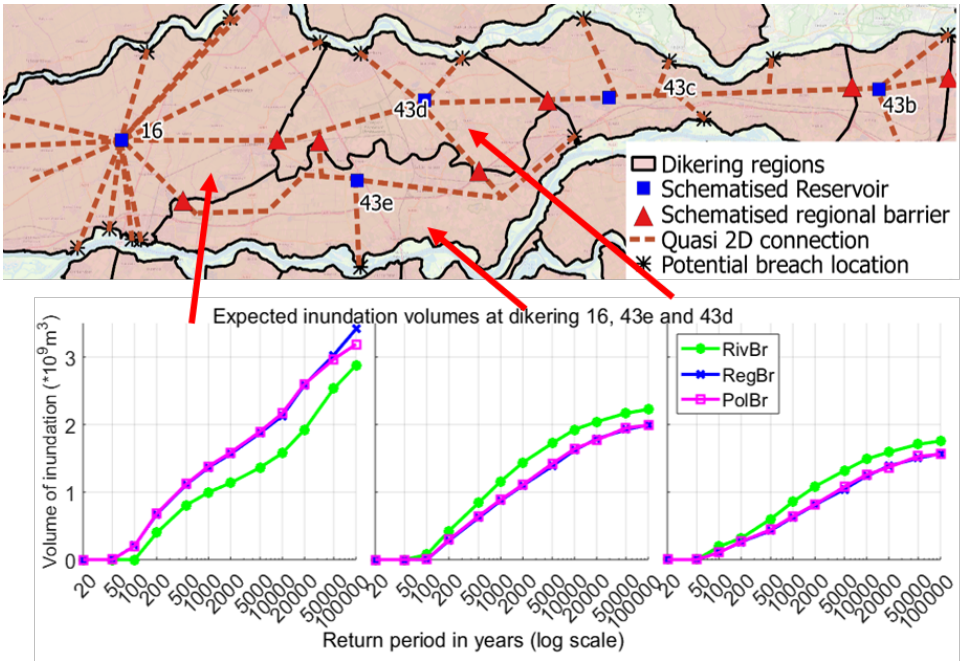

Figure 3.4: Expanded version of location dike ring 43 (Area A) from Figure 3.1. (**Top**): Close up of dike ring 43. (**Bottom**): expected inundation volumes at compartments 16,43e and 43d.

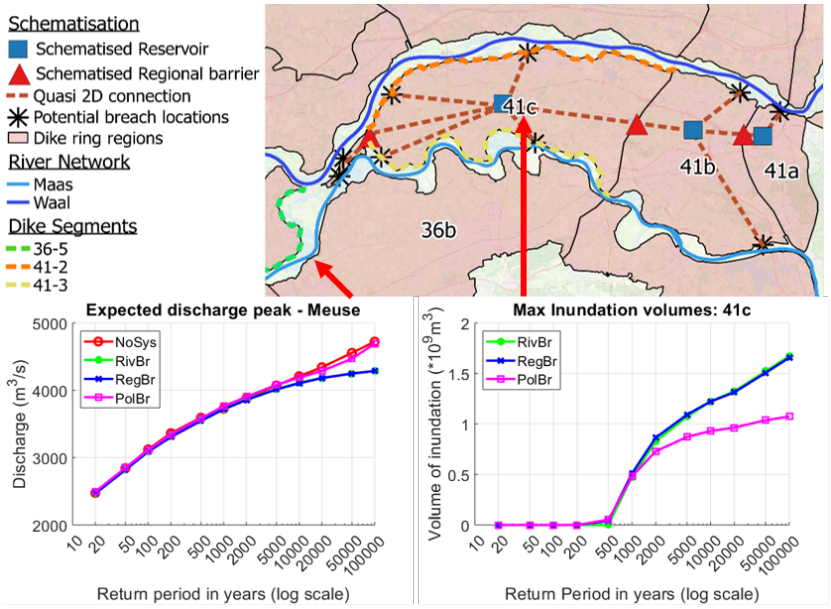

Figure 3.5: Example of shortcutting from Waal to Meuse. (**Top**) Expanded version of location B from Figure 3.1. Inundation volumes are seen to reduce in compartment 41c for scenario 'PolBr' (**Borrom right**). This increases the expected discharge downstream in the Meuse (**Borrom left**).

The expected inundation volumes for compartment 41c are given in Figure 3.5, and the scenario with the potential for polder-side breaching (PolBr) is seen to have lower expected volumes during extreme events than scenarios without polder-side breaching. A consequence of the polder-side breaching into the Meuse is that the expected discharges downstream are affected in this river. For the PolBr scenario, extreme discharges downstream in the Meuse are comparable to the scenario in which no breaching occurs anywhere (NoSys).

3.4.4. IJSSEL VALLEY

Analysis of 2D breaching simulations show that flood flows from breaches that occur on the right bank of the German Rhine generally flow toward the IJssel. In Figure 3.6, compartment 48c is seen to have higher expected inundation volumes for extreme events in the scenario in which failure of regional defences is not possible (RivBr). In the other scenarios, failure of the regional defence from 48c to 49 occurs, reducing the expected volume. In the simulations flows cascade down the IJssel valley through dike rings 50 and 51. However, large pressures build up in these compartments, and in the scenario in which polder-side failures can occur (PolBr), the expected volumes are reduced in compartments downstream (such as dike ring 51), due to polder-side breaching.

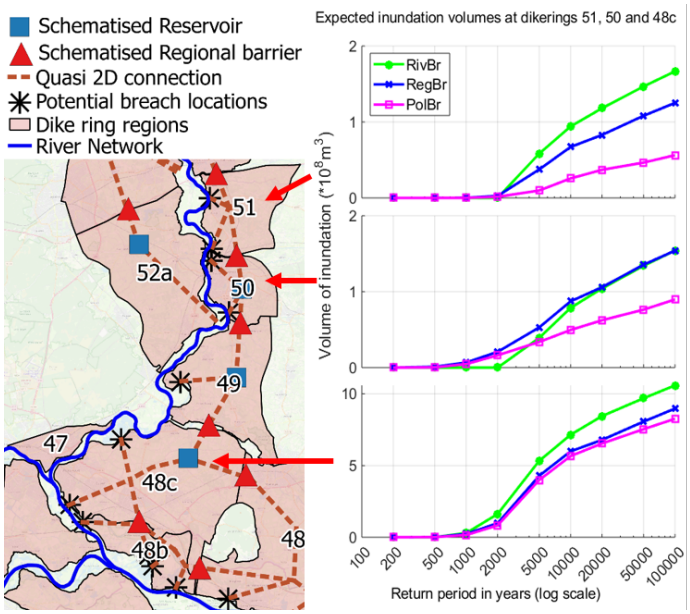

Figure 3.6: (**Left**) Expanded version of location C from Figure 3.1. (**Right**) Expected inundation volumes in dike ring compartments 48c, 50 and 51 for all scenarios. N.B. Y-axis scale changes in bottom graph.

3.5. CONCLUSIONS

For many protected river systems, the overall and local flood risks computed from large-scale analyses have been shown to be dependent on the 'load interdependency' effects that are observed when dike breaching is accounted for. The probabilistic computation required for such studies can preclude the use of sophisticated 2D models, often resulting in certain river-dike-floodplain interactions to be overlooked in the analysis. Even with 2D models, static topographies do not allow for floodplain interactions such as regional and polder-side breaching. As the floodplains of many large protected lowland river systems are compartmentalised, fast quasi-2D hydrodynamic models are often a reasonable alternative to estimate breach flow inundations. Furthermore, these models can include breaching of secondary defences that delineate the compartments. This paper conducted a load interdependency analysis of the Dutch river system using a fast quasi-2D model that allowed for system-wide and localised risk estimates to be generated and 'negative load interdependencies' to be demonstrated. The 2D domain is calibrated on existing breach simulations, and four scenarios were investigated to evaluate the effects of river-side, regional and polder-side breaching.

The case-study results showed that load interdependencies can have a significant impact on hydraulic load distributions and thus failure probabilities in the system, which is in agreement with results from Klerk (2013); Curran et al. (2018) and Bruijn et al. (2016). The addition of a fast quasi-2D model to the 1D domain allowed for useful statistics (such as expected inundation volumes) to be estimated at each region, and highlighted areas in which inundation would cause significant pressures on secondary/regional defences

or on the polder-side of primary defences. Failure of these defences are explored in two scenarios, and in many regions these failures have a large impact on the volume, level and timing of flood hazards. Specifically, the model highlighted the possibility of; 'short-cutting' and 'cascading' of flows in the regions of; the German Rhine to the IJssel, dike ring 41 and dike ring 43.

The study is limited in a number of areas. While fast, the quasi-2D approach does not allow for certain hazard variables to be calculated that may contribute to risk, such as flow velocities. The coincidence of river discharges and storm surges and tidal influences is also not currently included. Various assumptions were required for the analysis, such as the simplified thresholds for failure of regional and polder-side defences. The failure probability of the dike sections assumed in the paper (from the VNK2 study, Jongejan and Beek 2015) are considered to be too high, and many of these sections are currently being reassessed in light of the new safety standards.

These new standards are optimised based on (among other variables) expected economic damage from breaching, but do not include many of the interactions explored in this study. Therefore, calculating the expected economic damage and loss of life resulting from a system behaviour analysis under the new safety standards could be a worthwhile future research for the case study. In general, the approach developed can be used to evaluate risk and develop scenarios for many protected floodplain systems such as the Elbe, Po, Mekong and Mississippi. The results could be of use for decision-making in many large-scale flood risk management applications; for example, when evaluating compartmentalisation or detention area mitigation strategies.

4

System behaviour and spatiotemporal dependencies on the Po River

Abstract

Reliable hazard analysis is crucial in the flood risk management of river basins. For the floodplains of large, developed rivers, flood hazard analysis often needs to account for the complex hydrology of multiple tributaries and the potential failure of dikes. Estimating this hazard using deterministic methods ignores two major aspects of large-scale risk analysis; the spatial-temporal variability of extreme events caused by tributaries, and the uncertainty of dike breach development. Innovative stochastic methods are here developed to account for these uncertainties and are applied to the Po River in Italy. The effects of using these stochastic methods are compared against deterministic equivalents, and the methods are combined to demonstrate applications for an overall stochastic hazard analysis. The results show these uncertainties can impact extreme event water levels by more than 2 m at certain channel locations, and also affect inundation and breaching patterns. The combined hazard analysis allows for probability distributions of flood hazard and dike failure to be developed, which can be used to assess future flood risk management measures.

A slightly modified version of this chapter has been published as *Large-scale stochastic flood hazard analysis applied to the Po River* in *Natural Hazards* (Curran et al., 2020)

4.1. INTRODUCTION

4.1.1. FLOOD RISK ANALYSIS AND RESEARCH OBJECTIVE

Each year flooding causes the most damage of any natural disaster (Jongman et al., 2012) and, as such, many Flood Risk Management (FRM) strategies employ a risk-based approach (Voortman et al., 2009), where risk is the combination of exposure and hazard (with its associated probability). In analysing the hazard of large river systems, potential interactions between sub-catchments, dikes and other connected components becomes more relevant (Vorogushyn et al., 2017), and often requires system wide models simulated using stochastic approaches.

Hydraulic models used to analyse flood hazard and other hydraulic aspects of protected river systems have been developed for the Elbe (Merz et al., 2016), the Rhine (Hegnauer et al., 2014), the Mississippi (Remo et al., 2012), and the Po River in Italy (Castellarin et al., 2011), amongst others. Such models are often used to calculate the location-specific hydraulic load associated with a given probability or return period (Vogel and Castellarin, 2017). Hydrological boundary conditions provide the characteristics of the extreme event being modelled (e.g. a 1/200 yr event), while the schematisation of the model dictates how that event is routed in the area of interest.

However, deterministic estimates of these two components are unlikely to provide sufficient information for a reliable hazard analysis to be performed. Extreme events may originate from multiple tributary catchments, and can cause defence failures at various locations. Therefore, the present study proposes methods to include these sources of uncertainty (catchment hydrology and dike breaching) in large-scale flood hazard (and thus risk) analyses. The effect of including each of these components is also analysed individually, by comparing it to its deterministic equivalent. The concepts behind these methods are given below, along with a general framework for their application and analysis. In the following sections they are applied to the Po River case-study, and the results discussed.

4.1.2. HYDROLOGICAL EXTREMES

The concept of a return period discharge at a given location is much used in flood risk analysis (FRA). Extreme value theory can generate these discharge values, provided gauged locations with sufficiently long timeseries are available (Towler et al., 2010). To see the effect of an extreme discharge on a complete river system, a 'design hydrograph' (Mediero et al., 2010) can be applied as a boundary condition to a model. This hydrograph will generally have an associated probability represented either by the hydrograph itself or the resulting hydrographs at specific locations. The use of one or more design hydrographs to represent extreme events was formerly standard practice on the Dutch Rhine and Meuse systems (Van der Most, 2015) and is currently applied to the Po River system in Italy (Castellarin et al., 2011).

Applying a single design hydrograph to a river channel will not represent the variability in the shape of the floodwave. Recent studies have addressed this by developing multi-variate distributions from which hydrographs can be sampled. As well as the peak discharge, these distributions can include other hydrological characteristic variables such as 30-day volume (Domeneghetti et al., 2013), 3-day volume (Liu et al., 2009),

or the duration above a baseflow (Gräler et al., 2013).

The tool most commonly used to account for the dependence between multiple hydraulic variables, such as those listed above, are copulas, (Favre et al., 2004; Salvadori and De Michele, 2010, amongst others). A more detailed explanation of copulas is given by Renard and Lang (2007), but its principal function is to model the dependence between variables while maintaining their marginal distributions. As well as the dependence between characteristics of a single hydrograph, copulas can also be used to model streamflow characteristics from multiple sites (Hao and Singh, 2013), which may be correlated due to rainfall patterns. Weather generators can be applied to produce hydrographs that are spatially and temporally coherent (Dunn et al., 2016; Merz et al., 2016), but are not always readily available for many regions. In such situations, copulas can be used to model the dependence between multiple tributaries, for example in the Brisbane River catchment (Charalambous et al., 2013).

In the present study, a copula is developed to model both the dependencies of floodwave characteristics to each other and to characteristics at other tributary boundaries. The results from the use of the copula are compared with a model using deterministic hydrological boundary conditions.

4.1.3. DIKE BREACHING

As well as the catchment hydrology, river routing also introduces uncertainties when generating the hydraulic loads associated with return periods. Parameters such as roughness are part of this uncertainty (Pappenberger et al., 2005), however when routing extreme events in a protected river system, the breaching of defences may cause the greatest change in expected loads. Possible breaching mechanisms include overtopping, piping and macrostability (Steenbergen et al., 2004), and the conditions required to trigger breaching are often highly complex and subject to uncertainty.

The influence of breaches on downstream flows is often called 'system behaviour' and has been shown to be highly influential in determining local and system-wide hazards. System behaviour analyses that account for the uncertainty related to breaching include those by Apel et al. (2009), De Bruijn et al. (2016), Assteerawatt et al. (2016), Gouldby et al. (2012), Vorogushyn et al. (2010), and Curran et al. (2018). As downstream loads are dependent on upstream breaches, the above methods all utilise large models that try to represent the entire system. These models are run in Monte-Carlo simulations, in which both the hydraulic loads and dike strengths are varied per simulation.

In system behaviour analyses, the strength of the dike in resisting different breaching mechanisms is often approximated using fragility curves (Wojciechowska et al., 2015), which define the failure probability as a function of the hydraulic load for a discretised section of dike. Breaching uncertainty for that section can then be quantified by sampling the strengths defined in these fragility curves as a stochastic threshold for breaching in Monte Carlo simulations (Bruijn et al., 2016). Generally the fragility curves define failure probability as a function of water level (Bachmann et al., 2013; Mazzoleni et al., 2014a), however advanced methods to include both water level and duration of exceedance for that water level have been applied by Vorogushyn et al. (2009) and Curran et al. (2018).

Once a breach is triggered in a hydraulic simulation, the breach growth is determined

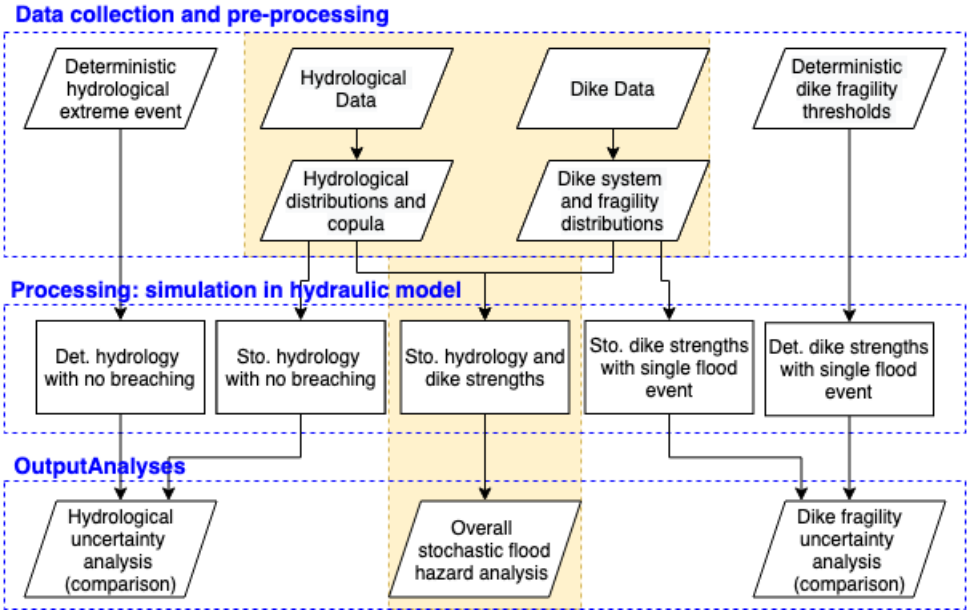

Figure 4.1: Yellow shaded area: Proposed approach for stochastic analysis of large-scale protected river systems with multiple tributaries. Unshaded areas show complementary analyses used to gauge the individual effects of including hydrological and dike breaching

by several variables which are also subject to uncertainty. Empirical models have been developed to estimate this growth (Verheij and Van der Knaap, 2003), but most studies use a distribution based on historical data, (Domeneghetti et al., 2013; Mazzoleni et al., 2014a; Vorogushyn et al., 2010). In the present study, both the dike breach triggering and growth functions are developed and applied to multiple potential breach locations in a system behaviour analysis. This stochastic analysis is compared with the use of deterministic breach fragility estimates.

4.2. GENERAL APPROACH

The general approach proposed to account for the effects of the sources of uncertainty described above is given in the yellow-shaded section of Figure 4.1. For each tributary in the system of interest, hydrological timeseries data are analysed, and distributions of relevant variables are fit and used as inputs to a copula. Similarly, dike data are collected and analysed to 1) discretise and schematise the protection system into a hydraulic model, and 2) generate distributions of dike strength for each discretised section. Both the hydrological event copula and the sets of dike strength distributions are sampled as inputs for simulations of a hydraulic model in a stochastic analysis. This allows for a complete stochastic flood hazard analysis to be generated.

As well as this overall analysis, it is also interesting to see the individual effects on the system when including these uncertainties. These analyses are shown in the unshaded sections of Figure 4.1. For the hydrology, a single extreme hydrological event is compared

against the events aggregated from sampling the hydrological copula. In these comparisons dike breaching is not included. For the dike breaching uncertainty analysis, a single extreme hydrological event is repeatedly simulated in the system with variable dike strength thresholds sampled from the developed distributions, and the aggregation of these simulations is compared against a simulation using deterministic thresholds.

The application of this approach to the Po river is described in the following section, with more specific detail about the models and methods used (e.g. the data used, the relevant hydrological variables etc.). The results of each of the analyses proposed are then given and discussed, and concluding remarks are given in the final section.

4.3. CASE STUDY AND APPLICATION

4.3.1. STUDY AREA AND AVAILABLE DATA

The case study is the Po River basin in Italy, which has a catchment area of ~75,000 km^2, and is fed by tributaries from the Alps in the North and West, and the Apennines in the South, Figure 4.2. The region is considered highly vulnerable to flooding, both economically and with respect to loss-of-life (Domeneghetti et al., 2015), and thus the floodplain is compartmentalised using a dike protection system. 'C-Buffer' compartments are protected from the river by embankments with a safety standard of 1/200 yrs and may be situated directly beside the main channel of the river or to smaller 'B-Buffer' compartments that lie inside the main embankments (see inset of Figure 4.2). The C-Buffer boundaries relate to the maximum inundation extents of catastrophic floods (Parte, 2016), and at certain downstream locations extend beyond the catchment boundaries, Figure 4.2 (see Castellarin et al., 2011, for more detail). The present study utilises four main data sources for the case study; dike profile data, a 30 year daily discharge dataset of the tributaries, a hydraulic model of the main channel, and boundary conditions for that hydraulic model that represent a 1/500 yr flood event. These data sources are discussed below and in the following sections.

The 1D HEC-Ras hydraulic model, representing a 370 km stretch of the main channel and selected tributaries, was schematised by Castellarin et al. (2011), and includes a quasi-2D schematisation of the multiple protected compartments in the floodplain. The model was calibrated on water level stages from the October 2000 flood event (Castellarin et al., 2011), which is estimated to have a 1 in 50 year return period.

The deterministic boundary conditions used in this study are based on an empirical method to estimate synthetic design hydrographs (SDHs) for ungauged locations on the Po river by Maione et al. (2003). The method was used to develop a set of 1/500 year SDHs for the major tributaries in a study by Italcopo (2002) and were adapted for use in the HEC-Ras model. This set of SDHs is hereafter called Tr500. The SDHs are generated ensuring peak discharges and volumes at multiple locations along the main channel conform to the return period loads estimated by flood frequency analysis of historical data. SDHs have also been developed relating to a 1/200 year event (Tr200 - Colucci et al., 2003), but these were calibrated using an earlier version of the hydraulic model, and thus ignored in the present study.

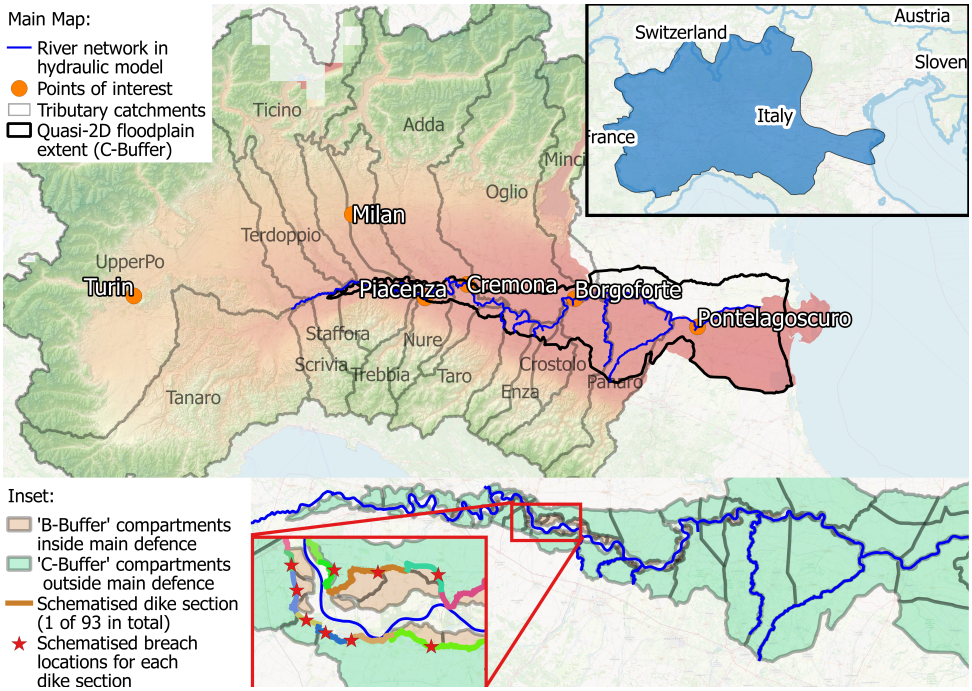

Figure 4.2: Top: Po River catchment (inset) and subcatchments (main). Below: River schematisation in HEC-Ras and connected quasi-2d compartments. Green compartments are 'C-Buffer' and orange compartments are 'B-Buffer'. Bottom inset shows a section of the river with selected breach locations and associated dike sections.

4.3.2. HYDROLOGY UNCERTAINTY ESTIMATION

Despite Tr200 and Tr500 having been used in many studies (Castellarin et al., 2011), they contravene the spatial and temporal variability of actual events present in the region. This can be seen in the study of Maione et al. (2003), where historical events are compared against the return period Flow-Duration Frequency (FDF) curves that were used to develop Tr500. The Maione et al. study demonstrates that historical floodwave events are not characterised by the same return period at all locations. For example, the October 2000 event appears to be a ~1/35 year event at Pontelagoscuro and a ~1/60 year event at Borgoforte (see locations in Figure 4.2). Therefore, the assumption of homogeneous return period loads all along the main channel is unrealistic. This is also the conclusion of Bianchi (2018), who highlights the role the various tributaries play in the inhomogeneity of return periods of hydraulic loads along the main river. The spatial and temporal hydrological uncertainty in load estimation caused by the tributaries to the Po River is addressed in the present study by simulating multiple events sampled from a copula.

The proposed hydrological method generates a long timeseries of annual maximum (AMAX) floodwaves in the main channel of the Po by routing multiple 'yearly' events, each of which is represented by a set of SDHs. Each SDH within an event is applied as a boundary condition for a tributary and has certain characteristics which come from sampling a Gaussian copula. This copula is chosen due to its simplicity, as more complex versions might not be suitable for the short (30 year) timeseries available. A resulting limitation is that the copula cannot include more complicated dependence structures than correlation coefficients (Zhang and Singh, 2019), such as tail dependency. The Gaussian copula takes as input an $n * n$ correlation matrix, where n is the number of correlated variables, i.e. the total number of characteristics for all SDHs. The sample taken for each event is then an $n * 1$ vector of correlated standard uniformly distributed random variables. These represent probabilities of non-exceedance for each of the characteristics and can be easily transformed into 'real-world' values using probability distributions. Three floodwave characteristics were used to build SDHs on 16 tributaries, and therefore 48 probability distributions and a $48 * 48$ correlation matrix are required.

As the goal of the sampling technique is to produce AMAX floodwaves in the main channel of the Po, using AMAX distributions for each tributary would likely over-estimate these events. Instead, timeseries of SDH characteristics are derived based on the tributary floodwaves that 'contributed' to events on the main channel, i.e. that occurred within a certain time window of the AMAX floodwave on the main channel. Therefore, timeseries of concurrent discharges for the main channel and all tributaries are required. Historical timeseries of discharge data are available for many stations along the main channel and tributaries, however some locations are missing and some data are incomplete. Instead, a 30 year daily discharge dataset from the SMHI (Swedish Meteorological and Hydrological Institute) is used, based on historical weather data and the HYPE hydrological model (Lindström et al., 2010). As this is hindcast data, it includes recent major events in the regions such as in October 2000.

Discharge data are obtained from the SMHI dataset for the outlets of the 16 tributaries whose sub-catchments shown in Figure 4.1, as well as the discharge on the main channel at Pontelagoscuro. It is possible that using this single reference location would

cause extreme events at that location alone but, in reality, the variability introduced by the copula prevents this. Five other tributaries are considered too small to develop SDHs and are therefore modelled as steady-state contributions. The annual maximum (AMAX) floodwaves at this reference are identified, and the peak discharge on each of the tributaries within a period from 20 days before to 10 days after this downstream peak are noted. These heuristic bounds simplify the hydrological and hydraulic processes involved, and may need to be addressed in future studies.

As well as peak discharge, two more floodwave characteristics are obtained from each the contributing floodwaves; duration above baseflow, and time lag with respect to the AMAX floodwave (Figure 4.3). The latter is simply the time between main channel AMAX peak and contributing peak, which can also be 'negative', i.e. the tributary peak occurs after the AMAX downstream peak. For the 'duration above baseflow' characteristic, the baseflow for each tributary is estimated using a filtering algorithm (Arnold and Allen, 1999), so that periods of direct runoff for each peak can be calculated. For a single AMAX event, the red and blue lines in Figure 4.3 show how the three characteristics are obtained for an example tributary floodwave. For the main channel floodwave (blue), the contributing tributary (red) has a peak flow of (5,500 m^3/s) which occurs two days previously, and is above its baseflow for 10 days. The 30 year timeseries' of these three floodwave characteristics for all 16 tributaries provide the information used in the Gaussian copula (both the marginal distributions and correlation matrix).

Once the time-series of characteristics are obtained, the $48*48$ correlation matrix can be generated. This matrix represents correlations between the three floodwave characteristics of each tributary. Distributions are fit to each timeseries, however due to their short (30 year) time span, the selection of a best distribution fit to the data is in many cases trivial. For simplicity, the characteristics of each tributary use the same distributions, but different parameters. The distributions used are; log-normal (peak discharge), normal (time lag) and log-normal (duration above baseflow), and the parameters for each are given in section 4.A.

With the correlation matrix and distributions defined, events sampled from the copula be used to produce the set of SDH boundary conditions for the hydraulic model. An example of an SDH generated from the three characteristics of the tributary in Figure 3 are shown by the black triangular floodwave. When generating the SDHs, the rising and recessing limbs above the baseflow were considered to be 1/3 and 2/3 of the sampled duration time respectively.

With sufficient samples, the water levels associated with specific return periods can then be estimated at any location. However, assumptions such as the contributing time period, the rising and recessing limbs ratios, and the reference main channel location simplify hydrology of the region. One example effect is that floodwaves from tributaries that do not 'contribute' to an AMAX event at the reference location on the main channel are missed. As a validation for the method, the deterministic Tr500 boundary condition is used to directly compare water levels along the main channel. Despite a positive validation (see section 4.4.1), these simplifications should be addressed in future studies.

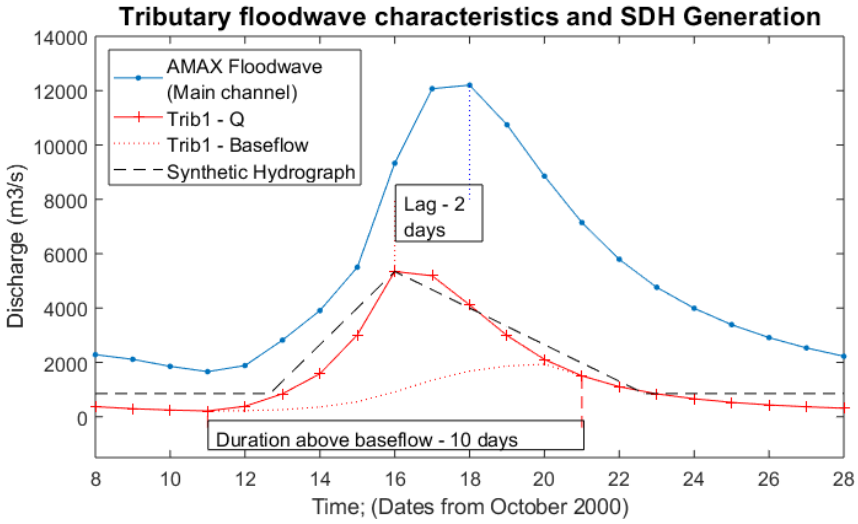

Figure 4.3: Example of identifying floodwave characteristics (peak, duration and lag) of a tributary (red) contributing to downstream flow (blue) for a single event of the 30 yr timeseries. An SDH generated from these characteristics is shown in black.

4.3.3. DIKE BREACHING UNCERTAINTY ESTIMATION

Research addressing the large-scale impact of uncertainty in dike breaching for the region (like the hydrological uncertainty) limited. Although studies on stochastic breaching for subsections of the Po River have been performed by Mazzoleni et al. (2014a) and Domeneghetti et al. (2013), only the study of Castellarin et al. (2011) considers the entire river stretch linked to the C-Buffer, and thus the effect of breaches on the entire system. However, that study used deterministic breaching thresholds for overtopping based on dike heights. Mazzoleni et al. (2014a) include piping threshold uncertainty by developing fragility curves, but these were only built for a 100 km stretch of the Po. Breach growth data are available from Govi and Turitto (2000), who fit a lognormal distribution to 200 years of historical breach data in the region. The formation times of these breaches were considered deterministic at 0.1 hrs by Mazzoleni et al. (2014b), but sampled from a normal distribution with a mean of 2 hrs by Domeneghetti et al. (2013). In the present study, the uncertainties in breach triggering (due to overtopping and piping) and growth are estimated by sampling probability distributions developed for discretised sections of the entire 370 km main channel.

As a first step in this process, dike sections are discretised to ensure each dike section is connected to at most one C-Buffer compartment on the floodplain side, and either the river or a B-Buffer compartment on the river side (see inset at bottom of Figure 4.2). For each section, the starting point of a potential breach (red stars in Figure 4.2) is identified at the location considered to be most vulnerable to overtopping. This is selected by comparing the model dike heights with the water levels observed in a steady-state flow. The schematised breaches have a pre-defined bottom elevation equal to the connected compartment, while the width is a function of time (see Table 4.1 below). The breaches

corresponding to the 93 discretised sections are detailed in section 4.C.

The next step is to develop dike strength distributions to apply to these sections and the breach starting points. This allows a set of sampled values from these dike strength distributions to be used as failure thresholds in each simulation for the potential breach locations. For overtopping, Castellarin et al. (2011) assumed a deterministic condition that if the water level exceeded the dike height at a breach location for 3 hours, failure would occur. However, in most cases these dike heights are based on interpolations between cross sections, which are themselves based on surveyed or LIDAR data. While the underlying LIDAR data are reasonably accurate, the linear interpolation between sections introduces error. In the present study, the linearly interpolated values are compared with ~6km of dike for which the actual heights are known, and a normal distribution of the error was found to have a standard deviation of ~0.5m. This was therefore applied as an uncertainty distribution to all locations.

While these distributions may over-estimate the uncertainty in some places, it is maintained at all sections to account for other uncertainties such as errors in the water levels calculated by the model, and errors in the LIDAR data. It should be noted that this method does not take account of the length effect in each section (i.e. the longer a section is, the higher the probability of overtopping at some location), however this limitation is mitigated by the selection of vulnerable breach locations within each dike section. The duration of water level exceedance required for overtopping is also made variable in the simulations, using a uniform distribution between 2 and 4 hours, based on previous research (Domeneghetti et al., 2015).

For piping, fragility curves have been developed for each breach location using cross section data from the Po river basin authority and the limit state formulation of Mazzoleni et al. (2014a), in which failure is determined by:

$$Z = 0.237\frac{1-n}{n} - \frac{\Delta H}{L} \tag{4.1}$$

where n is the porosity, ΔH is the water level and L is the critical length through which the pipe must form. The curves are developed by varying the n and L values according to a triangular and uniform distribution respectively. As with overtopping, the method does not take account of the length effect in each section. Hence, in the present study the curves are generated using the available cross section data immediately upstream and downstream of the potential breach location. The curves also do not include the duration required to induce piping failure. Given these limitations, the analysis of the effect of piping is kept separate in the present study, see Table 4.2.

In relation to breach growth, the final breach width and the time required to reach it are here considered fully dependent. Therefore, in each Monte Carlo simulation, a single sampled exceedance probability is applied to distributions for both these variables. The final breach width is sampled from the truncated lognormal distribution developed by Govi and Turitto (2000) while the distribution of breach development time is taken from the truncated normal distribution suggested by Domeneghetti et al. (2013). The growth is assumed to be linear in time towards this final width.

As a comparison for the breach triggering and growth uncertainties, deterministic events are also simulated. These simulations use the values of maximum likelihood from

Table 4.1: Deterministic and variable breach parameters

	Variable	Distribution	Parameter for deterministic simulations	Data for variable simulations
Triggering	Piping Level	Fragility curve	Value of maximum likelihood from curve	Full fragility curve
	Overtopping	Normal	Dike height at breach location	Mu = Dike height at breach Sd = 0.5m
	Overtopping duration	Uniform	3 hours	Min = 2 hours Max = 4 hours
Growth	Overtopping	Lognormal	91 m	Mu = 91m, sd = 21.7m (truncated)
	Duration	Normal	2 hours	Mu = 2hrs, sd = 1.5hrs (truncated)

Table 4.2: Analyses in the study

Analysis Name	Overall Simulation name	No. of simulations	Boundary Conditions	Hydraulic Model configuration	Failure Thresholds
Hyd	Det_Hyd500	1	Tr500	NOBREACH	None
	Var_Hyd	20000	Copula sampling	NOBREACH	None
Dike	Det_DikeO500	1	Tr500	BREACHBL	Overtopping (Det)
	Det_DikeOP500	1	Tr500	BREACHBL	Overtopping and piping (Det)
	Var_DikeO500	6000	Tr500	BREACHBL	Overtopping (Var)
	Var_DikeOP500	6000	Tr500	BREACHBL	Overtopping and piping (Var)
All	Var_AllO	30000	Copula sampling	BREACHBL	Overtopping (Var)
	Var_AllOP	30000	Copula sampling	BREACHBL	Overtopping and piping (Var)

each distribution, and in the case of overtopping duration, the midpoint of the uniform distribution used, Table 4.1.

4.3.4. ANALYSIS STRUCTURE

Three analyses are conducted for this case study which reflect the general analysis structure given in Figure 4.1. The effects of the hydrological and breaching uncertainty are quantified separately in the 'Hyd' and 'Dike' analyses described in sections 4.3.2 and 4.3.3, and the 'All' analysis evaluates hazard distributions generated by including the uncertainties of both components. The simulations compared within each analysis are also given a descriptive name (Table 4.2). These simulations use either the breachable (BREACHBL) or unbreachable (NOBREACH) implementations of the HEC-Ras model, and in both cases flow over the dike (here called 'overflow' to distinguish it from the breaching mechanism 'overtopping') is implemented using the weir equation.

The 'Hyd' analysis evaluates the effect of the hydrological uncertainty by comparing deterministic and variable boundary conditions. 20,000 simulations are performed for Var_Hyd, which is a long enough timeseries to estimate extreme events. As discussed, in the 'Dike' analysis the influence of the simplified piping failure estimates is kept separate

to the overtopping method. In both cases, 6,000 simulations are performed for sampling the individual distributions in the 'Var_Dike' analyses,. The 'All' analysis also separates the piping failure estimates, simulating 30,000 events for each. This is enough to get convergence of dike sections failure probabilities, accounting for the multiple sources of uncertainty. For future studies, efficiency in the number of simulations could be improved using methods such as importance sampling (Diermanse et al., 2014).

4.4. RESULTS AND DISCUSSION

4.4.1. HYDROLOGICAL ANALYSIS - 'HYD'

The purpose of this analysis is to compare hydraulic loads under deterministic hydrological boundary conditions (Tr500) to those observed from the stochastic boundary conditions developed using the Gaussian copula and the SMHI data.

RETURN PERIOD WATER LEVELS

For each breach location along the main channel, the maximum water levels from the 20,000 Var_Hyd simulations at that location are ranked, allowing the expected levels for various return periods to be estimated. Combining these return period levels for each location along the main channel makes a 'profile' of return period water levels. It should be noted that this profile does not represent any single simulation from Var_Hyd. As the SDHs in the Tr500 boundary condition are developed in such a way to reproduce the 500 year return period event at every point along the main channel, the water levels from the Det_Hyd500 simulation can be directly compared to the 500 year return period water profiles from Var_Hyd. Figure 4.4 shows the locations and elevations of the return period profiles and the river chainage of the main tributary confluences. To see the results more clearly, the levels of these return period profiles relative to the elevations in the Det_Hyd500 simulation are also plotted.

The 500 year profile from Var_Hyd slightly under-estimates the levels given by Det_Hyd500 by a maximum of 30 cm at a chainage of 340 km upstream. Further downstream, the levels match much more closely, however this is in large part due to overflow that often occurs during extreme events (see Figure 4.5).

RETURN PERIOD INUNDATION

Although breaches do not occur in the Var_Hyd analysis, the compartments experience inundation due to overflow. The total maximum flood volume for each compartment from the 20,000 Var_Hyd simulations are ranked so that the expected volumes for various return periods can be estimated. Again, it should be noted that the Var_Hyd results do not represent any single simulation, but the combined results from each storage area. Figure 4.5 shows how these volumes compare to those observed in the deterministic simulation.

For extreme events, many B-Buffer compartments are completely filled, and therefore show little change in volume between the simulations. However, a number of C-Buffer compartments are seen to experience a change in volume of over 0.1 Mm^3, just from overflow. The comparison highlights the error in assuming the Det_Hyd500 boundary conditions will cause 1/500 year inundation levels due to overflow. These results are further discussed below.

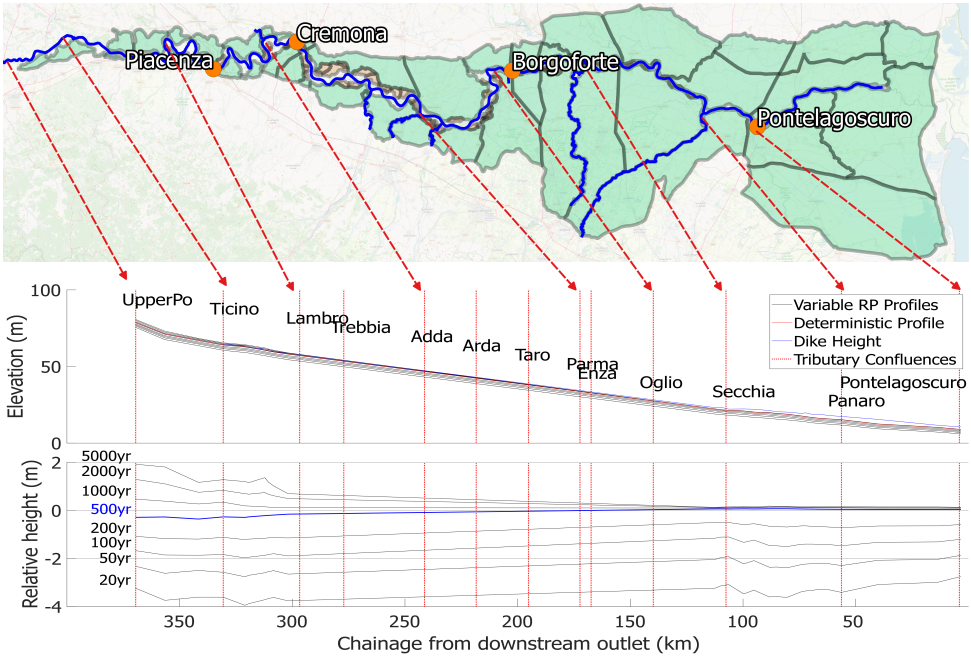

Figure 4.4: Return period peak water level profiles from Var_Hyd and corresponding mapped locations. Top graph; absolute elevations above sea level. Bottom graph; elevations relative to Det_Hyd500 (i.e. RP elevation profile from Var_Hyd elevation profile from Det_Hyd500)

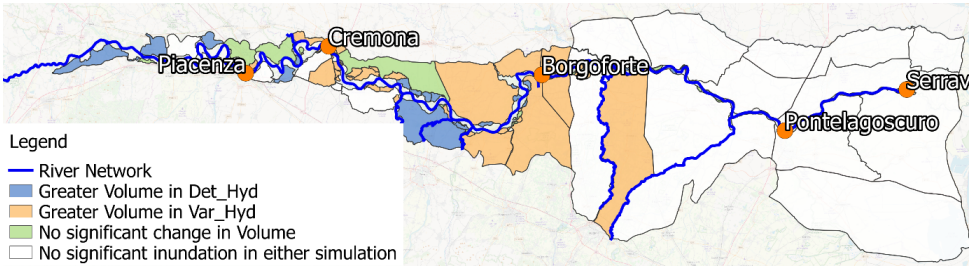

Figure 4.5: Comparison of maximum inundation volumes (due to overflow) for DetHyd_500 and the 500yr expected volumes for Var_Hyd. Areas with volumes <0.1 Mm^3 are shown in white. A 'significant' change in volume is considered to 0.1 Mm^3

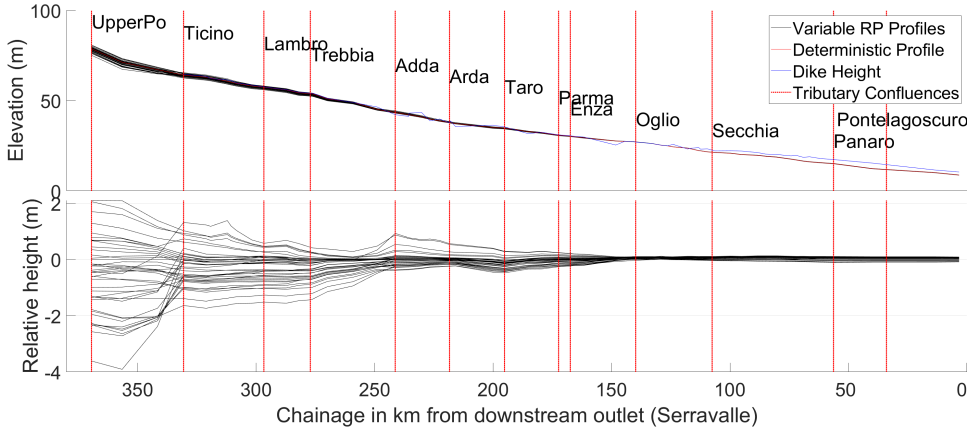

Figure 4.6: Individual simulation profiles from Var_Hyd that 'match' (±10 cm) the elevation of Det_Hyd500 at Pontelagoscuro. The bottom graph shows the relative profiles (simulation profile from Var_Hyd elevation profile from Det_Hyd500)

EVENT UNCERTAINTY

While the aggregation of the Var_Hyd simulations can show the expected return period values at various locations, the individual simulations represent realistic events and do not necessarily conform to a single return period load at every location. Figure 4.6 compares 46 individual simulations from Var_Hyd with Det_Hyd500. The 46 Var_Hyd simulations are selected due to having an observed maximum water level at Pontelagoscuro that is within 10 cm of the level simulated in Det_Hyd500 at the same location. For this reason, the Var_Hyd simulations appear to converge at this downstream point, while the upstream levels in these simulations can differ largely to the deterministic simulation. For clarity, in the bottom part of the figure the Var_Hyd profiles are shown relative to Det_Hyd500 profile.

Most of the deviation of these events occurs upstream, prior to the confluence of the Adda tributary, after which the contributions from tributaries are relatively small. Another reason the events are more similar downstream is that a large degree of overflow occurs in the region of the Oglio tributary (near Borgoforte), as can be seen in Figure 4.5.

4.4.2. DIKE BREACHING ANALYSIS - 'DIKE'.

The purpose of this analysis is to compare the effects of deterministic and stochastic breaching simulations on the Po. As shown in Table 4.2, separate 'overtopping' and 'overtopping and piping' analyses have been performed due to the simplified methods used for piping. The boundary conditions used are in all cases the Tr500 event. In the stochastic simulations, the thresholds are sampled from the uncertainty estimates described in section 4.3.2. In the deterministic simulations the values of maximum likelihood are used as the thresholds.

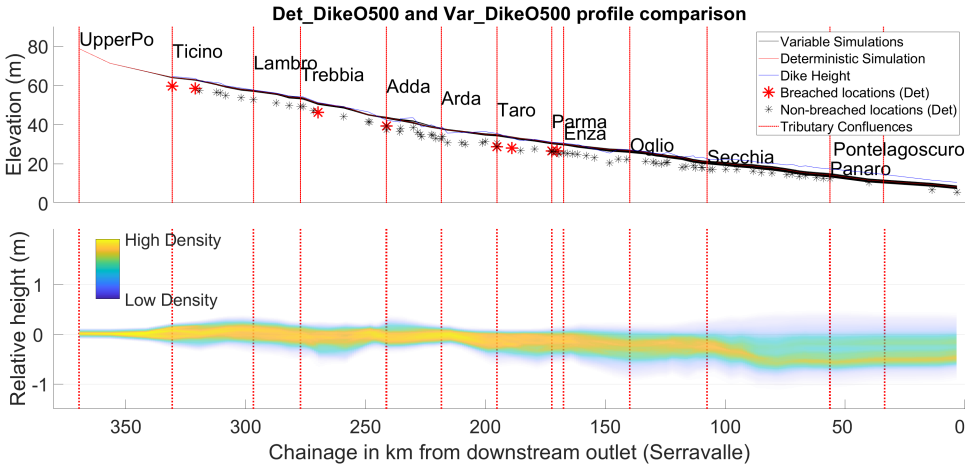

Figure 4.7: Profile comparison for Det_DikeO500 and Var_DikeO500. Top: elevations (masl) of profiles including location of breaches from Det_DikeO500. Bottom: elevations of Var_DikeO500 relative to Det_DikeO500, shown in terms of 'density'.

WATER PROFILE UNCERTAINTY

The water level profiles of the deterministic and variable simulations in which breaching occurs due to overtopping are shown in Figure 4.7. The locations of breaches that occurred in Det_DikeO500 are highlighted in the top plot. For clarity, in the bottom plot variable profiles are shown relative to the deterministic one, and as 'denser' in locations where the 6000 profiles converge. As the boundary conditions are all the same, no deviation is seen before the first potential breach location at around 360 km upstream. In contrast to the hydrological analysis, the water level uncertainty due to dike breaching is more pronounced downstream.

The same comparison can be made when the breaching occurs due to both overtopping and piping. The difference in the range of uncertainty surrounding the water level profile when piping is included is negligible, and the corresponding graph is therefore provided in section 4.D.

BREACH AND INUNDATION UNCERTAINTY

The inundation volumes and breach locations resulting from Det_DikeO500 are shown at the top of Figure 4.8. As a comparison, the averaged compartment inundation volumes and the percentage of breaches that occurred over the 6000 simulations of Var_DikeO500 are shown at the bottom of the figure.

As can be expected, breached sections of Det_DikeO500 have high corresponding breaching percentages in Var_DikeO500, and the compartments connected to those sections are also subject to a large degree of inundation. However, a number of other dike sections also appear to be vulnerable in the stochastic analysis, causing other compartments to experience significant inundation. Again, the results are similar when the thresholds for the piping mechanism are included, are therefore presented in section 4.D.

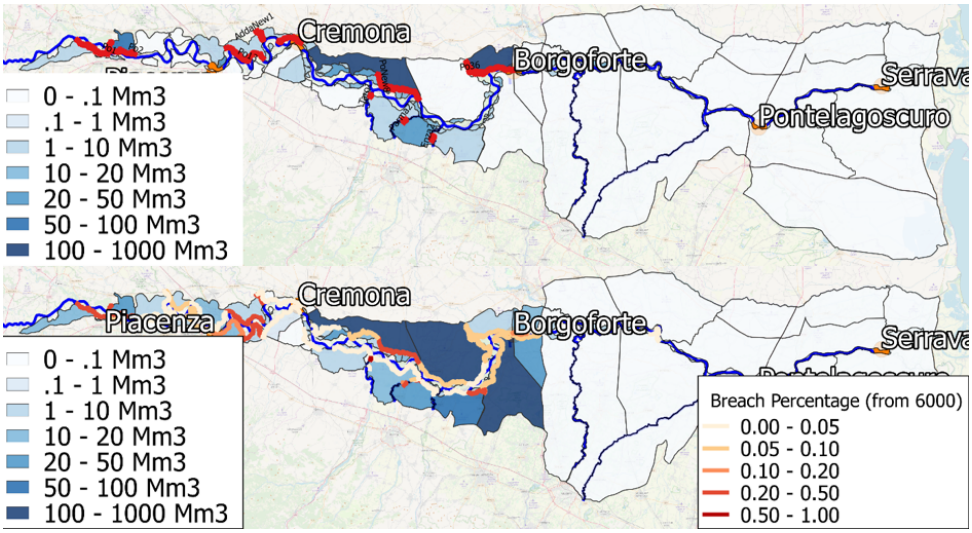

Figure 4.8: Breaches and inundation caused by Det_DikeO500. (Bottom) Breach percentages and average inundation caused by Var_DikeO500.

4.4.3. Overall Analysis – 'All'

This section shows two of the potential applications of using both sources of uncertainty in flood hazard analyses; dike failure probabilities and expected hazard distributions. From Figures 4.5 and 4.8 it can be seen that the floodplain compartments upstream of Borgoforte are the most vulnerable to flooding and breach failures, and thus only this region is considered in this analysis (Figure 4.9). As the Var_AllO and Var_AllOP simulations include both hydrological and dike breaching uncertainty, failure probabilities can be calculated from these scenarios. However, the differences between these two scenarios are minor, and therefore only Var_AllO is plotted in Figure 4.9. A complete list of calculated failure probabilities is given in Appendix 4.C. It can be seen that the calculated failure probabilities for most sections conform to or surpass the protection standard for the region (1/200 year).

For the three stochastic simulations that sample annual hydrological boundary condition from a copula (Var_Hyd, Var_AllO, and Var_AllOP), the expected maximum inundation volumes for various return periods can be calculated for each compartment. Two of these C-Buffer compartments (**A** and **B**) of these are shown in Figure 4.10, and the others (**D** – **F**) are given in section 4.D.

In most cases, the return period inundation volumes expected in the compartments are lower for Var_Hyd as overflow is included, but dike failures are not. For the two compartments shown, dike breaching causes inundation to be seen in events as small as 1/50 yrs. Some upstream compartments (such as **A**) have a smaller maximum capacity when a breach occurs (as flow can return to the river through the breach). This means that, for extreme events, these compartments can show higher inundation levels if breaching is not included.

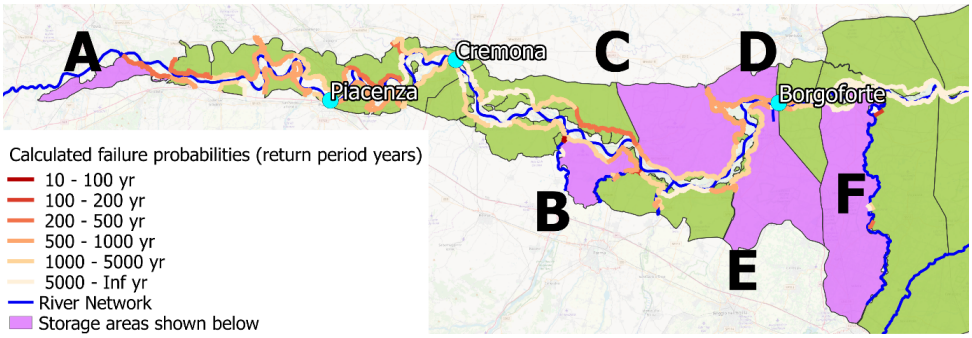

Figure 4.9: Dike failure probabilities for the upstream region of the Po, for Var_AllO. Storage areas for which statistics are shown in Figure 4.10 and Figure 4.13 (section 4.D) below are also highlighted in violet.

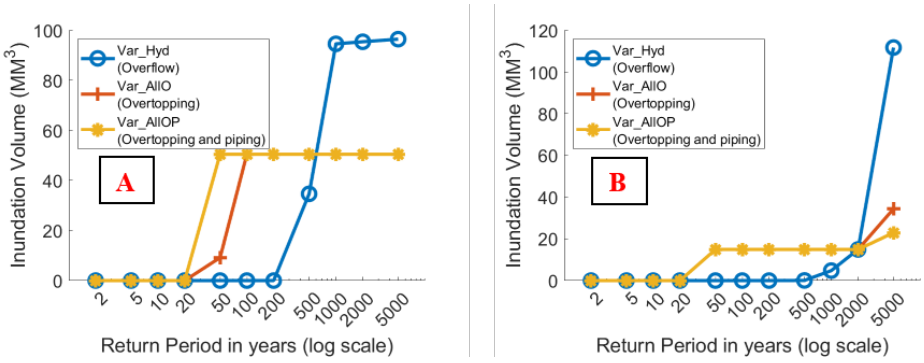

Figure 4.10: Expected inundation volumes at different return periods (log-scale) for C-Buffer storage areas A and B. The plots show the result for overflow (Var_Hyd - Overflow), overtopping (Var_AllO - Overtopping) and overtopping and piping (Var_AllOP - Overtopping and Piping). See Figure 4.9 for locations

4.4.4. DISCUSSION

As a validation for the method of uncertainty estimation used in the Hyd analysis, the return period water levels calculated from Var_Hyd are compared against those from Det_Hyd500 (Figure 4.4). It should be noted that neither method provide the 'true' water levels but do allow for a benchmark of the variable analysis. The 500 year levels from the variable method agree closely with those from the deterministic boundary conditions, despite no historical water levels being utilised in their calculation. The levels are under-estimated upstream by about 20-30 cm, which is considered acceptable given the simplified methods through which the SDHs are created.

The Tr500 boundary conditions elicit the 500 year hydraulic load at every location along the main channel, based on flood-frequency analysis of historic data. However, they cannot be used to estimate 1/500 year inundation levels in the compartments, as seen in Figure 4.5. The reason for this is the variability in water level profiles (±2 m at their most extreme) observed in Figure 4.6, which suggests that it is unlikely that an event matches the 1/500 year water levels at every location along the main channel, especially upstream. This is in agreement with the results of Maione et al. (2003), who demonstrated the same result for the October 2000 event. Both the deterministic and stochastic methods depend on the principle of hydrological stationarity, which may not be applicable in the catchment (Milly et al., 2005).

The methods through which dike breaching is analysed are simplified, and validation of the fragility of the current dike system based on real-world data is not feasible. However, the fact that most calculated failure probabilities conform to the standard of protection in the region (1/200 year) helps to validate the method. The vulnerable areas also conform to those predicted by Mazzoleni et al. (2014a). The results of the 'Dike' analysis indicate that downstream water levels may vary by as much as 1 m for an extreme event due to the possibility of breaches (Figure 4.7and Figure 4.11). Furthermore, many sections of dike and connected storage areas are shown to be vulnerable to breaching when stochastic simulations are used instead of deterministic ones (Figures 4.8 and 4.9).

Finally, including both sets of uncertainty in the 'All' analysis demonstrates some of the applications of stochastic analyses in the region, as well as insights that can be gained. Failure probabilities of most sections are estimated to conform to the standard of protection in the region (1/200 year), but the analysis highlights many sections that may need further investigation (Figure 4.9). Although the differences between the two breaching scenarios ('Overtopping' and 'Overtopping and Piping') appear minimal, the separation was necessary due to the simplified approach used to estimate piping.

Including both sets of uncertainty also allows expected hydraulic loads in the storage areas to be calculated for different return periods. Ideally, damage models could be applied directly to water depths to estimate values such as Expected Annual Damage (EAD). However, the quasi-2D structure used in the model means the depths calculated are not always representative of actual flood events. Instead the maximum inundation volume experienced in each compartment is here shown (Figure 4.10), which could also potentially be used in damage estimates (Prettenthaler et al., 2010; van Berchum et al., 2019).

4.5. CONCLUSIONS

Flood risk analysis in large protected river systems is highly dependent on uncertainties in the tributary hydrology and dike fragility. If the distributions and dependencies of these variables can be estimated, Monte Carlo (MC) simulations of events sampled from the distributions can be used to estimate hazard and thus risk. In comparison with deterministic events, the aggregated MC results may provide valuable information in terms of uncertainty and probability. The presented research investigates the effect of hydrological and dike fragility uncertainty on flood hazard in the Po River region of Italy, compared against existing deterministic hazard analysis methods. Applications of combining these stochastic analyses for complete hazard analyses are also demonstrated.

Hydrological uncertainty is estimated using multiple Synthetic Discharge Hydrographs (SDHs) for each tributary, which are built by sampling floodwave characteristics from a copula dependence model. Dike breaching uncertainty is based on distributions representing dike fragility and breach growth rate. The validation of the hydrological results show close agreement with those from a prior flood frequency analysis (< 30 cm). Validation of the uncertainty in dike breaching is more difficult but, for most dike sections, failure probabilities calculated from the method achieve or surpass the 1/200 year standard of protection in the region. Comparing deterministic methods against these uncertainty estimations demonstrates the inhomogeneity of return period flows along the river, due to tributary inflows (±2 m upstream) and breach outflows (±.5 m downstream).

Combining these uncertainty estimation methods in a complete hazard analysis allows probability distributions of hydraulic loads in the compartments and river to be computed, as well as dike failure probabilities. From these results, the potential dynamics of the river-dike-floodplain system during extreme events can be observed, such as the possibility of reduced storage capacities upstream when breaches allow inundated compartments to flow back into the river. However, the simplifications and assumptions used in generating these results should be taken into account in future studies. For the hydrology, these include the probability distributions, the copula and the short (30 year) timeseries used to generate them both, while for the dike strengths they include the piping formulation and growth functions. Finally, the quasi-2D simulation method also limits the inundation hazard information that can be obtained from the analyses.

Nevertheless, the proposed approach provides useful hazard information in the system, which (in combination with a damage model) could be used in the assessments of expected annual damage or proposed measures. The availability of such information, together with the uncertainty estimations, are certain to be of benefit to flood management decision makers. The overall approach is likely to be applicable to various large-scale protected river systems worldwide, including the Elbe and Rhine (Germany), Mississippi (USA) and the Yellow River (China).

APPENDICES

4.A. PARAMETERS FOR FLOODWAVE CHARACTERISTICS OF SDHS

The parameters for the distributions used in the Hyd analysis are shown in Table 4.3 below. As mentioned, for the 16 tributaries the same distribution is used for each floodwave characteristic; log-normal (peak discharge), normal (time lag) and log-normal (surface runoff duration). The Nash-Sutcliffe efficiency resulting from the fitted distributions of the discharge peak are also shown. As well as the baseflow applied to each tributary. The original timeseries are available at http://hypeweb.smhi.se/europehype/time-series/, accessed on 19/10/2018.

Table 4.3: Fitted distribution data of floodwaves contributing to AMAX peaks on Po

Tributary	Baseflow Q (m3/s)	Peak - Scale Parameter (m3/s)	Peak - Shape Parameter (m3/s)	Peak Fit (NSE)	SR Duration - Scale Parameter (hrs)	SR Duration - Shape Parameter (hrs)	Lag - Scale Parameter (hrs)	Lag - Shape Parameter (hrs)
Adda	334.9	684.4	360.6	0.74	56.3	10.8	-72.7	155.8
Enza	12.1	38.9	42.8	0.36	51.3	7.0	32.8	57.2
Lambro	20.3	190.9	127.4	0.69	34.2	10.5	41.6	27.4
Mincio	52.9	67.4	40.8	0.69	20.3	23.6	-233.6	148.9
Oglio	126.9	389.6	210.7	0.79	46.4	11.6	14.4	57.3
Olona	8.5	89.6	75.5	0.73	37.1	9.3	56.8	49.4
Panaro	24.7	45.1	73.6	0.41	37.9	13.1	-0.8	130.2
Parma	17.3	45.2	47.4	0.24	46.6	10.0	15.2	105.2
Scrivia	50.3	203.3	148.0	0.65	48.6	6.5	2.4	19.3
Secchia	35.2	70.2	128.1	0.32	31.0	16.3	-1.6	133.8
Tanaro	185.1	890.9	938.5	0.71	48.6	7.3	45.6	43.8
Taro	32.9	116.2	131.3	0.50	51.5	7.1	28.0	56.4
Terdoppio	6.2	76.3	81.8	0.71	31.5	11.6	48.8	69.5
Ticino	501.9	1062.4	819.0	0.87	53.5	11.7	-86.4	120.2
Trebbia	29.6	108.2	97.8	0.54	47.6	8.2	27.8	24.2
UpperPo	397.2	1598.2	1236.6	0.83	63.9	2.5	34.4	62.4
Arda	1.9	-	-	-	-	-	-	-
Crostolo	0.5	-	-	-	-	-	-	-
Nure	1.0	-	-	-	-	-	-	-
Staffora	5.8	-	-	-	-	-	-	-
TidoneVersa	1.7	-	-	-	-	-	-	-

4.B. CORRELATION MATRIX FOR CONTRIBUTING PEAKS ON ALL TRIBUTARIES

A $48 * 48$ correlation matrix is used in to model the dependencies between the 3 characteristics of the floodwaves for the 16 tributaries. Table 4.4 shows the correlation matrix obtained for the peak values.

Table 4.4: Correlation Matrix for contributing peaks on all tributaries.

	Adda	Enza	Lambro	Mincio	Oglio	Olona	Panaro	Parma	Scrivia	Secchia	Tanaro	Taro	Terdoppio	Ticino	Trebbia	UpperPo
Adda	1	0.15	0.72	0.74	0.84	0.65	0.25	0.18	0.45	0.29	0.40	0.13	0.47	0.87	0.34	0.46
Enza	0.15	1	0.21	0.36	0.42	0.16	0.53	1.00	0.42	0.58	0.21	0.97	0.11	0.01	0.68	0.02
Lambro	0.72	0.21	1	0.74	0.69	0.92	0.40	0.23	0.72	0.42	0.63	0.20	0.67	0.57	0.58	0.46
Mincio	0.74	0.36	0.74	1	0.86	0.62	0.51	0.39	0.52	0.55	0.45	0.31	0.36	0.63	0.49	0.40
Oglio	0.84	0.42	0.69	0.86	1	0.56	0.55	0.44	0.50	0.61	0.40	0.37	0.35	0.69	0.48	0.41
Olona	0.65	0.16	0.92	0.62	0.56	1	0.27	0.19	0.82	0.28	0.78	0.20	0.90	0.62	0.60	0.62
Panaro	0.25	0.53	0.40	0.51	0.55	0.27	1	0.54	0.52	0.99	0.43	0.49	0.11	0.11	0.60	0.24
Parma	0.18	1.00	0.23	0.39	0.44	0.19	0.54	1	0.45	0.59	0.23	0.97	0.14	0.04	0.70	0.04
Scrivia	0.45	0.42	0.72	0.52	0.50	0.82	0.52	0.45	1	0.52	0.92	0.50	0.81	0.42	0.88	0.61
Secchia	0.29	0.58	0.42	0.55	0.61	0.28	0.99	0.59	0.52	1	0.41	0.52	0.10	0.14	0.60	0.22
Tanaro	0.40	0.21	0.63	0.45	0.40	0.78	0.43	0.23	0.92	0.41	1	0.30	0.81	0.49	0.70	0.75
Taro	0.13	0.97	0.20	0.31	0.37	0.20	0.49	0.97	0.50	0.52	0.30	1	0.20	0.00	0.76	0.09
Terdoppio	0.47	0.11	0.67	0.36	0.35	0.90	0.11	0.14	0.81	0.10	0.81	0.20	1	0.56	0.52	0.73
Ticino	0.87	0.01	0.57	0.63	0.69	0.62	0.11	0.04	0.42	0.14	0.49	0.00	0.56	1	0.20	0.66
Trebbia	0.34	0.68	0.58	0.49	0.48	0.60	0.60	0.70	0.88	0.60	0.70	0.76	0.52	0.20	1	0.29
UpperPo	0.46	0.02	0.46	0.40	0.41	0.62	0.24	0.04	0.61	0.22	0.77	0.09	0.73	0.66	0.29	1

4.C. DETAILS OF DIKE SECTIONS

Details of the breach sections discretised in the model are given in Table 4.5, including the ID, the length, of the section, the C-Buffer compartment to which it is connected, the bank-side of the main channel (looking downstream) and whether the connection is via a B-Buffer or directly from the river. The bottom elevation of the breach and the dike height at the breach location are also given. The failure probabilities calculated from the VarAllO and VarAllOP analyses are given in the final columns as return periods.

Table 4.5: Details of dike sections.

Breach ID	Length	Connected C-Buffer compartment	River or B-Buffer connection	Bank side of river	Bottom Elevation of breach	Dike height at breach location	Failure Probability (return period) - VarAllO	Failure Probability (return period) - VarAllOP
Po1	10682	staf_vers	Riv	Right	59.6	63.1	428	109
Po10	12490	tido_treb	Riv	Right	53.1	54.7	691	741
Po11	3097	treb_nure	Riv	Right	49.2	54.2	1057	1053
Po12	15887	treb_nure	Riv	Right	50.7	53.6	998	1053
Po13	13607	lamb_addaC	Riv	Left	46.6	50.2	449	426
Po14	11831	nure_chia	Riv	Right	43.4	49	599	541
Po15	5478	chia_ardaA	Riv	Right	43.2	46.4	4490	5000
Po16	4771	adda_ogliA	Riv	Left	42.6	44.6	1996	2222
Po17	3304	chia_ardaA	Riv	Right	40.2	43	1382	1429
Po18	4858	chia_ardaA	Riv	Right	40.9	43	1057	124
Po19	7529	adda_ogliA	Riv	Left	39.2	43.1	1382	34
Po2	10601	rogg_lambA	Riv	Left	60.3	62.4	461	488
Po20	2563	chia_ardaA	Riv	Right	37.6	41.8	1633	1429
Po21	3948	adda_ogliB	Riv	Left	37.6	40.5	inf	inf
Po22	2996	adda_ogliB	Riv	Left	36.9	39.4	1382	45
Po23	2188	arda_ongiB	Riv	Right	36.3	38.7	1497	1176
Po24	2875	ongi_taro	Riv	Right	35.9	38.8	2566	2857
Po25	4389	ongi_taro	Riv	Right	36.3	38.7	17961	inf
Po26	4342	ongi_taro	Riv	Right	30.8	36.3	4490	5000
Po27	10370	taro_parm	Riv	Right	32.5	35.5	4490	4000

Continued on next page

Table 4.5 – *Continued from previous page*

Breach ID	Length	Connected C-Buffer compartment	River or B-Buffer connection	Bank side of river	Bottom Elevation of breach	Dike height at breach location	Failure Probability (return period) - VarAllO	Failure Probability (return period) - VarAllOP
Po28	10555	tar0_parm	Riv	Right	30.1	33.4	898	909
Po29	4356	adda_ogliC	Riv	Left	28.5	32.5	945	1053
Po3	5659	vers_po	Riv	Right	57.2	62.5	665	156
Po30	3209	adda_ogliC	Riv	Left	23.3	30.5	2566	2222
Po31	6857	enza_cros	Riv	Right	25.9	30.8	8981	6667
Po32	10310	adda_ogliC	Riv	Left	24.3	29.9	4490	4000
Po33	10894	cros_seccA	Riv	Right	25	27.8	1283	1538
Po34	17088	adda_ogliC	Riv	Left	25.6	27.4	748	800
Po35	4934	cros_seccA	Riv	Right	20.4	27.2	781	1333
Po36	16680	ogli_mincA	Riv	Left	25	27.2	998	50
Po37	3968	ogli_mincB	Riv	Left	22.4	26.2	619	741
Po38	1226	cros_seccA	Riv	Right	21.8	26.2	inf	inf
Po39	5128	cros_seccB	Riv	Right	23.9	25.3	1633	2857
Po4	5145	rogg_lambB	Riv	Left	58.2	61.6	1123	1111
Po40	4460	ogli_mincB	Riv	Left	22.3	25.7	5987	6667
Po41	2410	cros_seccC	Riv	Right	20.9	24.9	inf	inf
Po42	3779	ogli_mincC	Riv	Left	21.5	25.6	inf	inf
Po43	2944	cros_seccC	Riv	Right	22.8	24	8981	10000
Po44	5711	ogli_miincC	Riv	Left	20.6	24.6	inf	inf
Po45	1824	cros_seccC	Riv	Right	21.2	23.8	inf	20000
Po46	3557	ogli_mincC	Riv	Left	23.5	24.9	inf	inf
Po47	4952	cros_seccC	Riv	Right	18.9	23.2	inf	inf
Po48	5414	adig_poA	Riv	Left	21.4	23.4	17961	20000
Po49	9282	secc_panaA	Riv	Right	18.8	22.2	17961	20000
Po5	7388	po_tido	Riv	Right	58.8	60.7	1633	1111
Po50	6231	adig_poA	Riv	Left	21.7	22.3	inf	inf
Po51	9753	secc_panaB	Riv	Right	20.5	21.4	inf	inf
Po52	8410	adig_poB	Riv	Left	18.4	21	inf	inf
Po53	6756	secc_panaB	Riv	Right	17.9	19.8	17961	20000
Po54	2592	adig_poB	Riv	Left	18.4	20.4	inf	inf
Po55	7404	aid_poB	Riv	Left	18.3	21.2	inf	inf
Po56	6149	secc_panaB	Riv	Right	14.8	19.4	inf	inf
Po57	5098	adig_poB	Riv	Left	16.3	19.1	inf	inf
Po58	8290	secc_panaB	Riv	Right	16.7	19.1	inf	inf
Po59	4959	adig_poC	Riv	Left	15.9	18.4	inf	inf
Po6	7388	po_tido	Riv	Right	55.9	60.1	inf	inf
Po60	5865	secc_panaB	Riv	Right	15.7	17.9	inf	inf
Po61	14214	Pana_poA	Riv	Right	12.7	17.8	inf	20000
Po62	13591	adig_poC	Riv	Left	13.7	17.3	inf	20000
Po63	31689	pana_poB	Riv	Right	8	14.9	inf	3333
Po64	28985	adig_poE	Riv	Left	12.7	14.9	inf	5000
Po65	17698	adig_poE	Riv	Left	7.3	12.2	17961	2000
Po66	10660	pana_poC	Riv	Right	5.9	11.6	17961	2000

Continued on next page

Table 4.5 – *Continued from previous page*

Breach ID	Length	Connected C-Buffer compartment	River or B-Buffer connection	Bank side of river	Bottom Elevation of breach	Dike height at breach location	Failure Probability (return period) - VarAllO	Failure Probability (return period) - VarAllOP
Po67	6110	pana_poC	Riv	Riight	6.3	10.3	17961	2000
Po68	3838	adda_ogliC	Riv	Left	28.5	31	1283	1250
Po7	10355	tido_treb	Riv	Right	55.4	58.3	718	741
Po8	11796	lamb_addaA	Riv	Left	54.1	57.3	748	714
Po9	13628	lamb_addaB	Riv	Left	52.6	56.3	1283	1176
PoNew1	12950	rogg_lambB	Riv	Left	51	58.6	748	741
PoNew10	4094	enza_cros	BBuff	Right	25	30.2	inf	inf
PoNew11	4887	adda_ogliC	BBuff	Left	23.2	30	1123	1429
PoNew12	5648	enza_cros	BBuff	Right	21.5	28.8	561	606
PoNew13	10417	cros_seccA	BBuff	Right	21.8	28.5	1123	1250
PoNew14	3341	cros_seccB	BBuff	Right	18.4	25.5	816	1111
PoNew15	6855	cros_seccC	BBuff	Right	16.8	24.5	17961	20000
PoNew16	4242	secc_panaA	BBuff	Right	13.3	22.1	inf	inf
PoNew17	7212	adig_poA	BBuff	Left	14.3	22.7	inf	inf
PoNew18	4905	adig_poC	Riv	Left	13	18	inf	inf
PoNew2	6077	lamb_addaB	BBuff	Left	46.4	52	855	741
PoNew3	6387	lamb_addaC	BBuff	Left	41	46.7	8981	10000
PoNew4	3873	chia_ardaB	BBuff	Right	35.1	39.3	1057	1176
PoNew5	9000	adda_ogliB	BBuff	Left	34.5	38.5	17961	20000
PoNew6	10094	ongi_taro	BBuff	Right	31.1	36.8	1633	1667
PoNew7	10990	adda_ogliB	BBuff	Left	30	35.7	1633	1667
PoNew8	15848	adda_ogliB	BBuff	Left	27.5	33.4	449	513
PoNew9	6992	parm_enza	BBuff	Right	25.5	31.3	1497	1667
PoSA1	4813	adda_ogliB	BBuff	Left	35	36.6	inf	inf
PoSA2	2367	chia_ardaB	BBuff	Right	37	38.6	inf	inf
PoSA3	2466	chia_ardaA	BBuff	Right	38.5	39.8	inf	inf
PoSA4	2990	adda_ogliA	BBuff	Left	38.5	40.3	inf	inf

4.D. EXTRA RESULTS

The following figures show details of results not provided in the main text, including water level variability when piping is included, dike failure probabilities when piping is included and expected inundation for downstream compartments. Although the impacts of breaching on downstream risk are not discussed in the text above, the effects can be seen in compartment D in **??**. In this compartment, the risk in the Var_AllO scenario is higher for certain extreme events when breaching is not included. This is because upstream breaches reduce the amount of flow in the river and thus the downstream risk. More precise details on changes in risk and failure probabilities could be determined from the dataset in future studies.

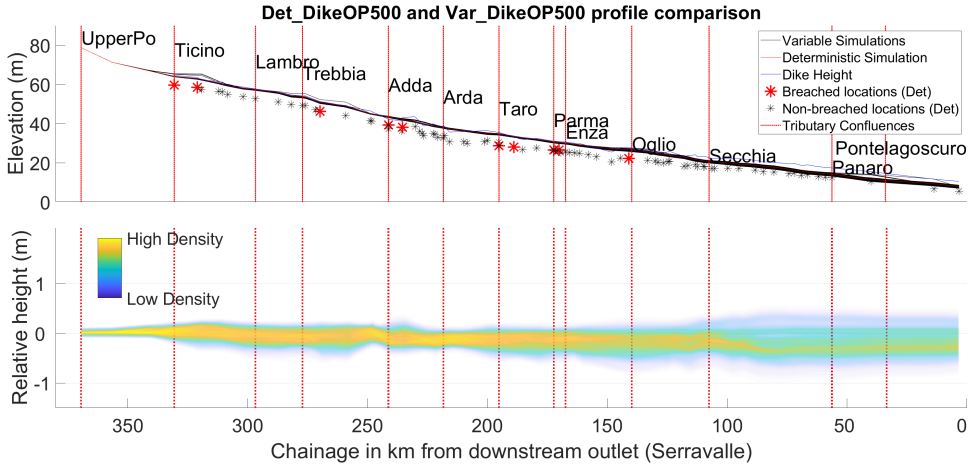

Figure 4.11: Profile comparison for Det_DikeOP500 and Var_DikeOP500. Top: elevations of profiles including location of breaches from Det_DikeOP500. Bottom: elevations of Var_DikeOP500 relative to Det_DikeOP500, shown in terms of 'density'.

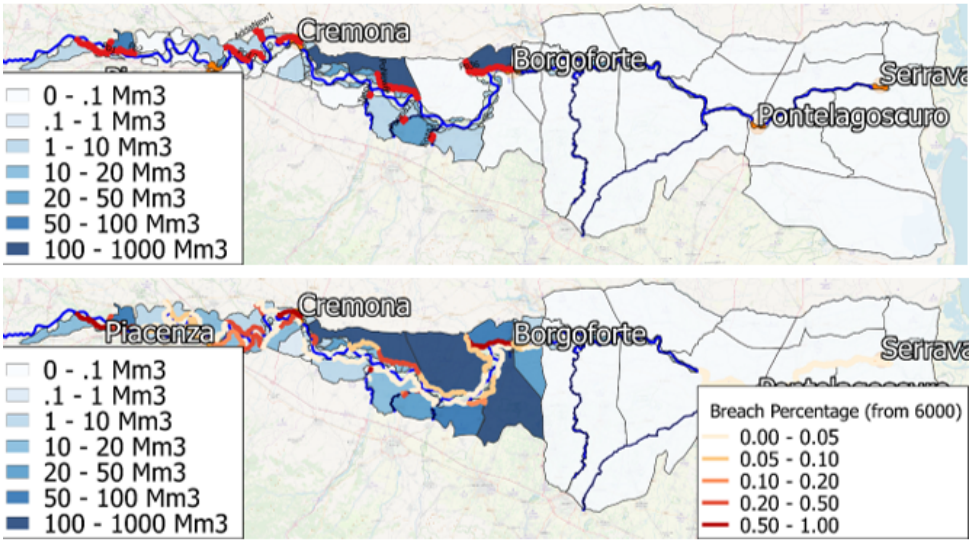

Figure 4.12: (Top) Breaches and inundation caused by deterministic thresholds of overtopping and piping during the Tr500 event (Bottom) Breaches and inundation caused by stochastic thresholds of overtopping and piping during the Tr500 event

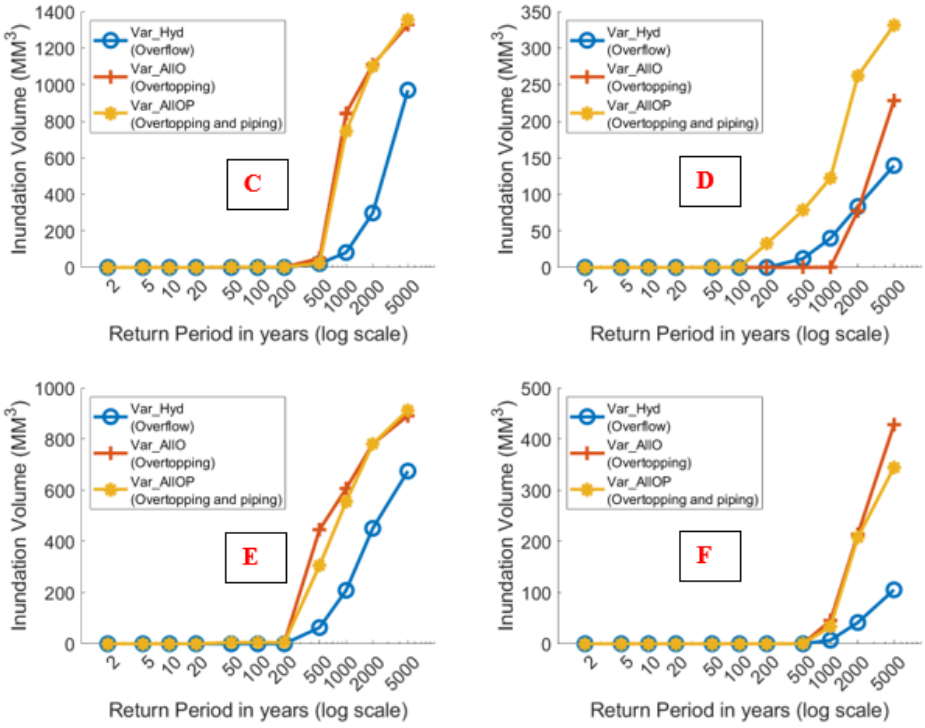

Figure 4.13: Expected inundation volumes at different return periods (log-scale) for C-Buffer storage areas C - F. The plots show the result for overflow (Var_Hyd - Overflow), overtopping (Var_AllO - Overtopping) and overtopping and piping (Var_AllOP - Overtopping and Piping). See Figure 4.9 for locations

5

A FRAMEWORK FOR SENSITIVITY AND SCENARIO ANALYSES IN SYSTEM BEHAVIOUR

ABSTRACT

Flood-risk analyses of embanked lowland river systems often need to include 'system behaviour' interactions, i.e. changes in hazard and risk in the system due to breaches and overtopping. Accounting for this behaviour has been shown to be crucial in many systems. However, the complexity of system-behaviour analyses and the numerous simplifications and assumptions required to implement them hampers their uptake as a decision-support tool in Flood Risk Management (FRM). This study, therefore, develops a framework for the steps involved in assessing both; the uncertainty of outputs (due to their sensitivity to various inputs), and the results of possible future scenarios in the system. As a case study, the framework is applied to estimate the expected annual damage (EAD) of riverine flood risk for the Netherlands and its uncertainty due to various dike fragility, hydraulic loading and impact calculation parameters. The model uncertainty of using a systems analysis instead of aggregating risk from multiple regions is also assessed, showing a €20 million (~25%) reduction in EAD, a difference which is eclipsed by other uncertainties. In general, the results demonstrate the importance of a systems approach to flood risk analysis and the usefulness of a framework to structure analyses of that system.

A modified version of this chapter has been submitted to *Risk Analysis* under the title *Evaluating flood risk with a systems approach: a framework for scenario and sensitivity testing applied to the Netherlands.*

5.1. INTRODUCTION

Lowland river floodplains and deltas are often home to highly developed areas in terms of population and economic assets. When embankments are used to protect these areas from the rivers, assessing the likelihood of defence failures is crucial in the estimation of flood risk. Localised failure probabilities at dike sections, and risk to the corresponding protected floodplain regions, can both be calculated using established flood-risk analysis and structural reliability methods. However, combining regionalised estimates to evaluate overall risk ignores potential interactions between these regions, a phenomenon often called 'system behaviour' (De Bruijn et al., 2016). For example, outflow from upstream breaches will reduce risk downstream (termed a positive interdependency) and may subsequently re-join another river branch and so increase the risk of breaching elsewhere (a negative interdependency) (Klerk, 2013).

This behaviour has been shown to be important when calculating risk metrics such as expected economic damage (Assteerawatt et al., 2016) and flood fatality (De Bruijn et al., 2014). Evaluating these metrics at a system-wide scale can be used in the development and implementation of large-scale flood-risk management (FRM) measures. For example, the concept of the 'societal risk' of floods (risk of a large number of fatalities from a single event) has been used in the development of flood protection standards in the Netherlands (De Bruijn et al., 2010). For accurate assessments of these societal risks, integrated system-wide analyses are required (Maaskant et al., 2010). Then, FRM measures that are optimal in terms of metrics like cost-benefit ratio and equity can be determined whilst accounting for system behaviour, as shown by Dupuits et al. (2016) and Ciullo et al. (2019).

Risk analyses that include system behaviour have been developed for many river protected systems worldwide, such as the Po river in Italy (e.g. Domeneghetti et al. 2015), the Elbe in Germany (Vorogushyn et al., 2010), Japan (Assteerawatt et al., 2016), the Mississippi in the USA (Dunn et al., 2016), and Nepal (Oliver et al., 2018) The overall output uncertainty caused by hydraulic load and dike strength distributions are generally included in such studies, but it is often useful to assess the sensitivity of the output distributions to upper and lower of specific inputs. System behaviour analyses may also include 'scenarios', which are for this study defined as a possible future state of the system. Using this definition, scenarios could be used to assess the impact of a proposed FRM measure, or future possible changes in the climate or population. Sensitivity and scenario analyses can be very useful in FRM decision-making, as the former provides confidence in the values generated by the analyses, while the latter can allow for cost-benefit comparisons or 'what-if' analyses.

In many system behaviour studies, flowcharts are used to illustrate how the sensitivities or scenarios being assessed relate to the model-chain and processing steps. However, such flowcharts are generally case-specific and do not elaborate on methods to test other aspects of the system. In the following section, a framework is presented providing a generalised approach to perform both uncertainty and scenario analyses when accounting for system behaviour in flood risk. The framework takes the form of a flowchart relating the components of a system behaviour analysis, combined with a description of each component. These descriptions provide information on the possible scenarios or sensitivities that could be assessed by changing that component. In section 5.3, to

demonstrate the application of the framework on a case study, uncertainty analyses are performed on the EAD for the Dutch river system, based on upper and lower estimates of various inputs to a system behaviour analysis. These upper and lower values are subjective, but the motivation behind their choice is given for each input parameter. As well as this parametric uncertainty, model uncertainty (see Loucks and van Beek 2016) is also assessed by comparing a system behaviour analysis to the aggregation of multiple regionalised risk estimates. The results of these uncertainties are discussed, and conclusions are drawn about the specific case study and the application of the framework in general.

5.2. GENERAL FRAMEWORK

5.2.1. DESCRIPTION OF FRAMEWORK AND COMPONENTS

The general framework below is a combination of a flowchart showing the components of a system behaviour analysis (Figure 5.1) and an itemised description of those components. Scenario or sensitivity analyses that could be conducted on each component are proposed in these descriptions, as well as their relevance in FRM decision making. Flowcharts explaining the various processes in system behaviour analyses can be seen in studies of Dunn et al. (2016), Oliver et al. (2018), Vorogushyn et al. (2010) and Apel et al. (2009) amongst others. Although these flowcharts are specific to the analyses performed, they are commonly divided into three parts; inputs and pre-processing, processing, and outputs, and this division is used for the general framework flowchart below. It should be noted that the framework relates to snapshot assessment in time, and the long-term dynamic that are therefore not included are discussed at the end of this section.

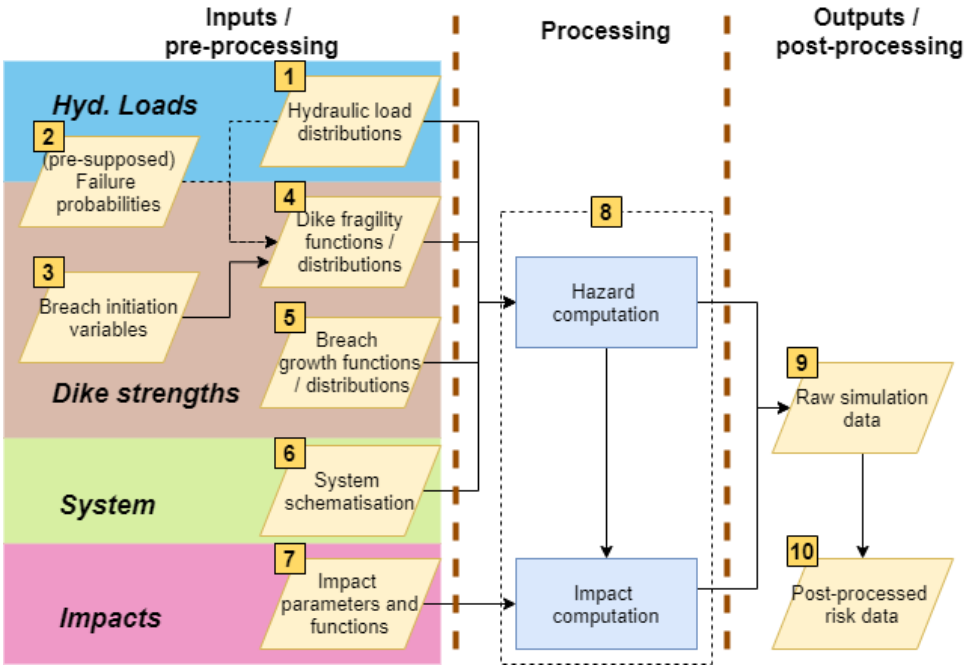

Figure 5.1: Generalised flowchart for system behaviour FRA, as part of the overall framework to assess scenarios and sensitivities in system behaviour analysis.

1. Hydraulic load distributions

Uncertainty in the hydraulic loads that the system can expect is accounted for using stochastic simulations in which extreme events are sampled from probability distributions. If multiple flood sources (or boundary conditions) are present, the simulations should also be spatially and temporally coherent, representing the likely dynamics of meteorological events for the region. A sensible method of ensuring this coherency is to use a weather generator and routing model to generate continuous boundary conditions to a system over a long period (e.g. Falter 2016). Specific hydraulics events from this time series can then be simulated in the system based on yearly maximums or events surpassing a threshold.

In the absence of such a tool, the hydraulic loads can be sampled from extreme-value distributions. The use of more than one distribution may require the introduction of a method to account for dependent variables (such as a copula - Renard and Lang 2007). Examples of boundary conditions that could be dependent are; river flows and storm surges, river flows in adjacent tributaries and the characteristics of a floodwave (e.g. peak discharge and duration). Scenario analyses implemented at this stage might use different parameters for the weather generator (e.g. for a certain climate change scenario) or a different extreme value distribution (e.g. because of a proposed change in the river system upstream, like a detention area).

2. (Pre-supposed) Failure probabilities

An estimation of failure probabilities may be a desired output of a system behaviour analysis. In that case, pre-defined failure probabilities are not required, and therefore the arrows relating to this component in Figure 5.1 are shown as dashed. However, the failure probabilities of the dikes may sometimes need to be defined in advance. One reason for this would be to assess a proposed scenario in which dike failure probability standards are changed. Another reason could be that the failure probabilities calculated using available dike fragility data contrast with expert judgement or historical observations.

If the dike system failure probabilities are defined in advance, the fragility functions of each dike section must be adjusted to conform to the pre-defined failure probability, using a distribution of hydraulic loading at that location. The probability distributions of hydraulic loading, together with the fragility of the dike at that location, allow for the failure probabilities to be estimated using reliability methods (FORM, Monte Carlo etc.). The fragility then can be adjusted to ensure the correct overall failure probability is achieved (see, for example, Diermanse et al. 2014).

3. Breach initiation variables

In system behaviour analyses, the conditions that cause breaches are often simplified, and as shown by Curran et al. (2018) this can have a considerable impact on the outputs. The most important factors in defining the variables that initiate or 'trigger' a breach are; the known breaching mechanisms and the available dike data. For breaching mechanisms, if overtopping is known to be dominant, the water level reached in a simulation may provide enough information to initiate failure. However, mechanisms such as piping and macrostability may require other dependent variables to be included such as the duration of those water levels (see Chapter 2).

The availability of data is another practical consideration in the selection of triggering variables. For example, dike fragility data is often summarised in fragility curves that relate water level to failure probability (Wojciechowska et al., 2015). Such curves can be directly used as a Monte-Carlo input to a system behaviour analysis, but this means that failure within each simulation is based on water level alone. A consequence of this is that breaching after the peak of the floodwave cannot occur, which is known to happen in reality for mechanisms such as piping and macrostability. Uncertainty analyses can often show the results are highly sensitive to the use of different breach initiation variables.

4. Fragility functions

Fragility functions can be developed once the variables that contribute to breach triggering are defined. The functions relate to a discretisation of the dike system that can be implemented in the hydraulic model, and therefore should be considered in conjunction with the system schematisation. This implies the functions also consider the length effect, i.e. the increase in probability of a breach over longer sections of dike. The discretisation is usually based on distance (e.g. Domeneghetti et al. 2013) but can also be related to the inundation patterns resulting from breaches (e.g Jongejan et al. 2013). Closely linked to the discretisation is the issue of correlation, as a dependence structure may need to be introduced for dike sections that are close in proximity or similar in composition.

Even with a sufficient discretisation, dependence structure and set of triggering variables, the complexity of dike breaching means that the fragility functions will inevitably be subject to uncertainty, even for known hydraulic loads. Estimating this uncertainty is generally achieved using geotechnical failure simulations in which stochastic parameters are varied to output a distribution relating hydraulic variables to failure probabilities, i.e. a fragility function. If the probabilities are related to water level alone, they are generally called fragility curves. When the fragility curve or function is combined with the distribution of loads at that location, the overall failure probability of a section can be determined. Like the hydraulic loads, the uncertainty of these functions means that failure thresholds are generally sampled from them in Monte Carlo simulations.

5. Breach growth functions

Breach growth functions can be just as complex as breach triggering functions, and naturally have a significant effect on the inundation and channel hydraulics of the system. The breach growth and outflow are mutually dependent and should ideally be calculated together rather than in sequence. In practice, hydraulic models that include breach growth functions calculate the breach hydraulics and geotechnics separately, but using sufficiently small timesteps between calculations mitigates this problem. Parameter uncertainty in the growth models may need to be addressed, for example in the growth rate functions developed by Verheij and Van der Knaap (2003) and in the hydraulic software HEC-Ras.

However, considering the uncertainty of these functions, system behaviour implementations often include breach growth functions as another stochastic variable (as well as the load and dike fragility distributions) in the Monte Carlo simulations. This could either be achieved by sampling the parameters used in a breach growth model, or directly

sampling the 'final' characteristics of breaches such as width and development time (e.g. Castellarin et al. 2011).

6. System schematisation

The system must be schematised to sufficiently represent the flooding mechanisms being evaluated and all possible river-dike-floodplain interactions in the system. Rivers are usually modelled in 1D for computational speed, using boundary conditions sampled from the hydraulic load distributions. Dikes are generally schematised as controllable structures positioned to represent the discretisation used in the fragility functions. The 2D domain connected to these breaches will often be the 'bottleneck' in terms of computational speed, and thus efficient modelling techniques may be required, such as quasi-2D modelling, GPU modelling or using a database of existing simulations.

Possible future scenarios in the form of mitigation measures (e.g. flood control structures) can be assessed by making changes to the system schematisation. The model uncertainty of whether a systems approach to assessing risk is necessary can also be assessed at this stage. Comparing a systems approach to the accumulation of multiple regionalised risk estimates can be achieved running simulations in which breaches occur but have no impact on the river hydrodynamics. Comparing failure probabilities and hydraulic load distributions to a 'normal' system behaviour analysis will show the impact of including this behaviour.

7. Estimating impact

Evaluating mitigation measures (e.g. evacuation methods) and analysing the sensitivity of outputs to impact parameters (e.g. flood damage curves) can be useful for FRM decision-making. They can also be performed relatively quickly, as they don't require the set of hydraulic events generated for the system to be rerun. Of course, mitigation measures that impact the hydraulics of the system (e.g. sandbags or opening gates) will require re-running the hydraulic simulations. The method through which impact is assessed should be decided upon prior to the analysis, as it will determine the hazard outputs required.

8. Computation

The uncertainty surrounding the dike fragility functions and hydraulic loads (and perhaps also breach growth functions) means that a probabilistic approach is required to calculate hazard, such as Monte Carlo simulations. Practically, the process of simulating and processing multiple sampled events needs to be automated, and the implementation of breach triggering and growth functions for the dikes will also need to be pre-programmed. Many hydraulic modelling packages either support programming languages to control the software itself or can be manipulated from an external environment. Even with automated simulations, the large amount of processing at this stage may necessitate statistical methods to be used, such as importance sampling. To ensure enough simulations have been performed, convergence plots and statistics should also

be generated.

9. Output data

Retaining all hazard data from the simulations will likely be intractable, especially if fully 2D schematisations are used, so consideration must be taken when deciding what data to record. For hazard, the failure of dike sections is obviously important, but information about the river flow, breach flow and breach growth might also be relevant. Outputting the hydraulic loading experienced at various locations in the river will help evaluate localised risk, even if a breach does not occur at that location. For the calculation of impact, economic damage, fatalities and people affected are the metrics most often used to define the risk. It is also worth noting that the database of simulations (prior to post-processing) is a useful result in itself, and could be used for data mining of other aspects of the system.

If a fully 2D model is used, the maximum extents and depths of floodplain inundation are the most important datasets to record. However, other information such as time of first arrival, flow velocities and rise rate of inundation will also influence flood fatality and economic risk. Fast schematisations (e.g. quasi-2D) will improve computation time and reduce data-handling issues, but provide less detailed information, and are not always as easily translated to risk.

10. Post-processing data

Post-processing the data is a crucial aspect of such analyses and should be done in conjunction with end-users. The large database of simulations and spatial information allows for a lot of potential applications of the data, but too much information can be overwhelming. One of the simplest metrics is the single-value expected annual damage (EAD) of the system that has been studied, which can be easily calculated after a damage analysis. Net-present values (NPV) of measures can then be estimated using their expected life-cycle for the purpose of cost-benefit analyses.

Risk curves relating an impact (e.g. 10 deaths, 100 people affected, €1 million damage) or a hazard (e.g. water levels, inundation volumes) to an exceedance probability are an effective way to represent the output data. They can be generated for the entire system but are also useful when separated by location. For issues such as risk-transfer and equity in FRM, such location-based data is crucial in FRM, and Geographical Information Systems (GIS) can therefore be used to better visualise the data.

5.2.2. LONG-TERM DYNAMICS NOT INCLUDED IN FRAMEWORK

It should be noted that the flowchart and descriptions above are related to a method to provide hazard and risk estimates related to a snapshot in time and do not include long-term dynamic processes. Long-term processes can sometimes be included through scenarios (e.g. a future climate change scenario), but often the processes alter the system itself, and thus the complete evolution over time is required. The main dynamic processes that should be accounted for in risk estimates for long time periods are;

- River morphology. Erosion and deposition will change the river dynamics over time and could be included in the hydraulic schematisation.

- Structural degradation. The condition of flood defences degrades over time, and this could be accounted for in the fragility functions. Similarly, maintenance cycles may also need to be accounted for, as well as the methods employed to fix breaches when they occur

- Exposure changes. Expected future changes in population density or building and infrastructure exposure should be included for long-term impact assessments.

- Non-stationary hydrology. The probability distribution of flood events is likely to change over long periods of time, for example due to climate change or human influences in the catchment or upstream system.

Methods to include them can include continuous assessment, (see, for example, Oliver et al. 2018) or the use of multiple 'snapshot' assessments over time. These processes could, of course, also be the subject of scenario or sensitivity analyses, however their inclusion complicates the framework and component descriptions, and may make actual large-scale computation unfeasible.

5.3. CASE STUDY AND IMPLEMENTATION

The case study application of the framework assesses the output distributions of Dutch riverine flood risk due to both input (parametric) and model uncertainties. For this, a quasi-2D model (Figure 5.2) developed by Curran et al. (2018) is used.

The components described in the framework are applied to a 'base case' analysis of the case study using the information given below. Analyses conducted that alter this base case (to analyse a sensitivity) are given in the description and also summarised in Table 5.1. No long-term dynamic processes are included in the analyses, and therefore the risk estimates for each analysis (expected annual damage, expected annual fatalities) are 'snapshots' where the system state properties (economic exposure, flow distribution etc.) are assumed fixed in time.

1. Hydraulic loads

For the upstream boundary conditions, the peak discharge and waveshape parameter distributions of extreme events on the Rhine and Meuse are obtained from GRADE (Hegnauer et al., 2014). The expected distributions from the year 2050 are chosen as they align with the timeline for implementation of the protection standards used in the base case (also 2050). In the Monte Carlo approach, the floodwave characteristic are sampled from distributions, and simplified hydrographs are then generated for the simulations using standard design flood waves. The dependence between the peak discharge on the rivers is modelled using a correlation coefficient of 0.9, which, although high, is a standard assumption for the system.

The impact of using the standardised floodwaves to define the hydraulic load is assessed by comparing the base case breaching statistics with those from analysis $L1$ (Table 5.1). In the $L1$ analysis, 'realistic' hydrographs from a weather generator that match the sampled peak values are used instead of standardised floodwaves. To assess whether

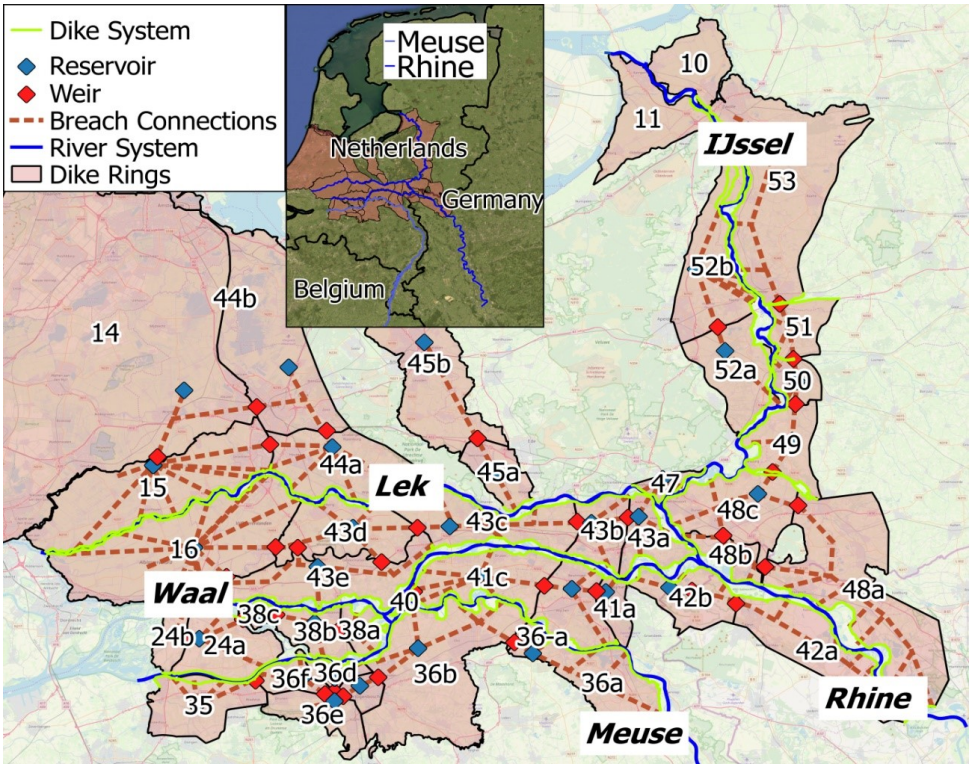

Figure 5.2: Case study area pf the Dutch River system. Compartmentalised dikering areas are schematised by storage reservoirs and connections between the compartments are schematised as weirs.

the estimated correlation between the rivers has a significant impact on flooding, the *L*2 analysis uses a coefficient of 0.5, which is suggested as more likely by Diermanse (2002).

2. (Pre-supposed) Failure probabilities

Dike failure probabilities for the base case are pre-supposed based on the the newly imposed protection standards (Slomp, 2016), specifically the 'ondergrens' (lower threshold) values. This is the lower limit of protection to which the dikes can deteriorate before they need to be upgraded. Although these probabilities don't represent a 'base case' in the normal sense, the protection standards have been written into law with the provision that they are implemented by 2050 (Van der Most, 2015).

'Current' failure probabilities resulting from available fragility curves (OKADER - Levelt et al. 2017) and a recent study (VNK2 - Jongejan et al. 2011) are much higher than what is expected based on experiences of past events. For this reason, the probabilities given by the new standards were chosen for the base case. To highlight the inaccuracy of using the 'current' estimates in a large-scale analysis, and to compare against the future standards, the VNK2 and OKADER datasets are used in analyses *S*2 and *S*3 (Table 5.1).

3. Breach initiation

In the base case, breaches are initiated or triggered using water level and duration of exceedance of that water level. This is necessary due to the known potential for piping and macrostability failures in the dike system. These failure mechanisms are duration dependent (Sellmeijer et al., 2011; Van et al., 2005)and therefore may occur after the peak of the floodwave. Triggering breaches due to water level alone will not capture this behaviour, and so the duration component is introduced in the form of fragility surfaces (Curran et al., 2018).

However, the duration variable was included in the fragility functions by means of expert judgement, with little agreement in terms of its effect. While the factors derived from expert judgement could be tested, it is more useful to investigate if this variable is required at all. If so, it would suggest a more comprehensive approach (or a more rigorous expert judgement approach) is required in the development of fragility functions in the Netherlands in general. Therefore, in analysis *S*1, breaches are triggered due to water level alone (Table 5.1) and compared against the base case.

4. Fragility functions

As mentioned, the failure probabilities in the system are pre-determined. However to include the uncertainty around these failure probabilities, the fragility functions use the uncertainty estimates derived from the available OKADER fragility curves (Levelt et al., 2017). These curves are developed for sections of dike of about 1 km, and are combined (assuming independence) to match the discretisation of dike sections defined in the new national standards (between 3 km and 14 km). The duration of exceedance of the water level is then included as a dependent variable to create 'fragility surfaces'. Finally, the surfaces are shifted in the variable space so that they conform to the desired failure probability.

The assumption of independence between the OKADER curves is due to a lack of available research on this topic, but it may have a significant effect on both the fragility

functions and calculation of overall risk. This assumption is therefore tested by comparing analysis *S*4 (Table 5.1) to the base case. In *S*4, the OKADER curves are combined using a correlation coefficient equal to 0.9 (highly dependent). The correlation coefficient in *S*4 is chosen heuristically, and the analysis is used to demonstrate a known deficiency in input data.

5. Breach growth function

The breach growth is modelled using the formula of Verheij and der Knaap (2002), which separates the vertical and (subsequent) horizontal breach formation. The vertical formation is relatively quick and initially applied to a small dike section. It is therefore considered less relevant to large-scale analysis than the horizontal growth. The horizontal growth for any timestep is based on the difference in water level between the river and floodplain, which is calculated by the hydraulic model. The growth must be calibrated to the correct soil type using the critical velocity (u_c) parameter, for which the resulting breach widths can be highly sensitive. In the base case, the default value of 0.2m/s provided by Verheij and der Knaap is used at every potential breach location.

Localised u_c values are a known data deficiency of the analysis, and so analyses *S*5 and *S*6 try to estimate the impact of using the default value. The *S*5 and *S*6 analyses use high (0.6 m/s) and low (0.16 m/s) estimates of the u_c parameter, which are suggested by Verheij and der Knaap for clayey and sandy dikes respectively.

6. System schematisation

The system is schematised in a calibrated Sobek (hydraulic) model, as shown in Figure 5.2. Output uncertainty of the system due to breaching of secondary defences has previously been demonstrated by Curran et al. (2018), and is therefore not included in the present study. In the 2D domain, a database of pre-existing breach simulations is used to determine the maximum inundation extents and depths in each dikering. If more than one breach occurs on a dikering, the inundation maps are overlaid with the highest depth used in each cell.

As discussed in the general framework, the evaluation of flood risk mitigation measures (such as dike strengthening, retention areas and diversions) could also be possible at this stage, but are not assessed for this case study.

7. Impacts

The base case uses the SSM2017 damage model to estimate economic losses with the 'no evacuation' scenario to quantify flood fatalities. Higher and lower estimates of fatalities are considered in analyses I1 and I2. An estimate of damage sensitivity is given by changing the damage curves used in analyses *I*3 and *I*4. These new curves were made in consultation with a flood damage modelling expert, and an example is given in Figure 5.3.

8. Computation

The computation is performed using software to automatically wrap the simulations, in which importance sampling is used to decrease the number of simulations required.

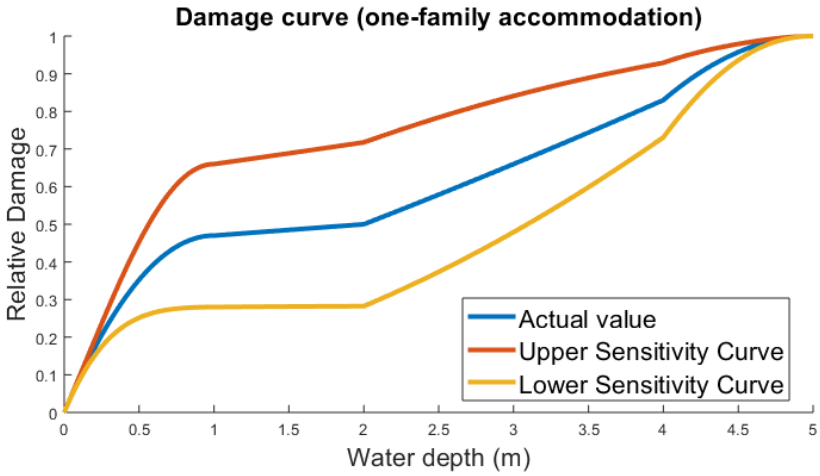

Figure 5.3: Damage curve for a particular feature class in the case study (one family accommodation buildings), along with upper and lower estimates.

Despite the use of importance sampling and an optimised quasi-2D model, each analysis required about ~100hrs of calculation time, which was spread out over multiple cores and virtual machines. To ensure convergence, plots of failure probability from all dike sections were generated.

9. Output data and (10.) Post-processing

A large degree of hazard information is recorded such as breaching, inundation etc. However, for clarity, only the expected annual impacts (damage or fatalities) are given for each analysis. As well as the overall value for these impacts, a disaggregation of the value over return period events is provided to show how events of varying severity contribute to the overall risk.

The list of analyses conducted is given in Table 5.1, along with the comparisons made.

Table 5.1: The analyses conducted for comparisons in this study.

Uncertainty Analysis Type	Sub - analysis	Input in Base case	Inputs altered in comparative analysis	Name
Model	**Analysis method**	Risk calculation with system behaviour	Risk calculation without system behaviour	**NoSys**
Parametric - Strengths	**Breach triggering**	Water level and duration triggers breach	Water level alone triggers breach	**S1**
	Failure probabilities	New standards	VNK2	**S2**
			OKADER	**S3**
	Fragility Functions	Fragility functions combined with no correlation (r = 0)	Fragility functions combined with high correlation (r = 0.9)	**S4**
	Breach growth	Default u_c parameter	High u_c parameter - (clayey dikes)	**S5**
			Low u_c parameter - (sandy dikes)	**S6**
Parametric - Loads	**Floodwave type**	'Realistic' flood-waves	Standard design floodwave	**L1**
	RHine and Meuse dependence	Rivers highly correlated (r = 0.9)	Rivers correlated with r = 0.5	**L2**
Parametric - Impacts	**Flood fatality model**	Standard fatality model (SSM2017)	High fatalities	**I1**
			Low fatalities	**I2**
	Economic damage curves	Standard damage curves (SSM2017)	Low damage curves	**I3**
			High damage curves	**I4**

5.4. RESULTS AND DISCUSSION

For each of the analyses made in Table 5.1, comparisons are made in terms of Expected Annual Damage (EAD). However, representing the EAD as a single value means that information on the severity of events that cause that damage is lost. In the graphs provided, EAD is disaggregated over the range of extreme events, showing the contribution of different ranges of probability to the total EAD.

5.4.1. MODEL UNCERTAINTY

To compare against the base case, a risk analysis is carried out where no system behaviour is accounted for ('NoSys' in Table 5.1), i.e.upstream breaching does not reduce flow and thus risk downstream. Comparing this analysis against the base case in Figure 5.4 shows a ~€20 million annual risk reduction for the whole country due to system behaviour. In the graph, this annual expected damage (AED) is disaggregated over the range of extreme events. For example, both analyses show no risk at high probability events due to the high standards of protection, and less risk at extreme events due to the

low probabilities associated with them. On the right side of Figure 5.4, a localised AED estimate (at dike-ring 50) shows a more significant relative difference, highlighting the fact that the change in risk is not distributed equally, as it mainly benefits downstream areas.

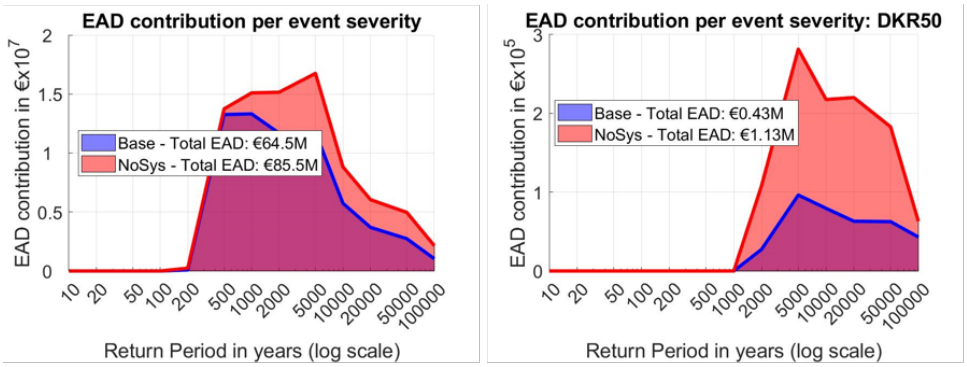

Figure 5.4: Expected annual damage disaggregated over return period events, for the whole of the Netherlands (left) and dike ring 50 (right)

5

5.4.2. PARAMETRIC UNCERTAINTY – DIKE STRENGTHS

BREACH TRIGGERING

Breaches were triggered in the base case due to the combination of water level and the duration of exceedance of that water level. In analysis S1, the pre-determined failure probabilities were the same as the base case, but the triggering was based solely on the water level. This means that breaches only occur before (or at) the peak of the floodwave, and are therefore likely to have a greater total inundation volume. This is seen on the left side of Figure 5.5, which shows a greater impact (~€30 million) on the base case than the method of analysis (left side of Figure 5.5)).

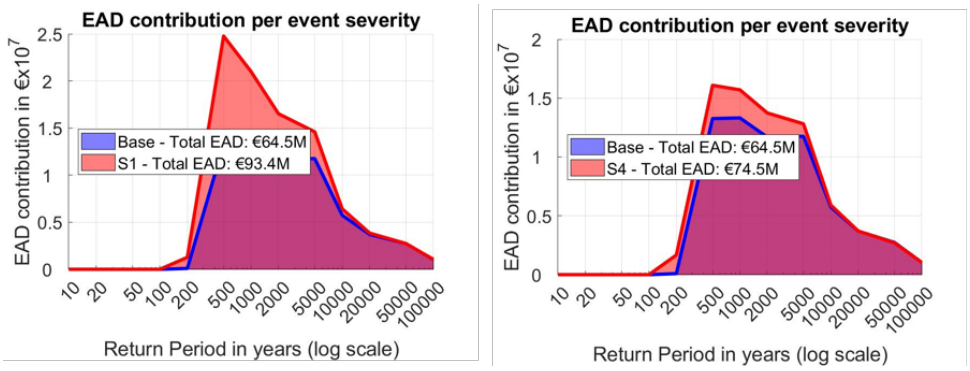

Figure 5.5: EAD in Base and S1 analyses (left). EAD in Base and S4 analyses (right).

DIKE FRAGILITY FUNCTIONS

The significance of the assumption of independence between dike sections is shown on the right side of Figure 5.5, by comparing scenarios *S*4 with the base scenario. In analysis *S*4, the fragility curves were combined assuming a high degree of dependence, which causes a greater uncertainty in the overall fragility function. This then causes a greater overall risk, as seen in the figure.

(PRE-SUPPOSED) FAILURE PROBABILITIES

As discussed in section 5.3, 'current' estimates of failure probabilities resulting from the VNK2 and OKADER studies are likely conservative. Analysis *S*3 (using OKADER probabilities) suggests that numerous breaches would be expected during events as frequent as 1/20 years (Figure 5.6), which does not agree with past experience of the system. Therefore, the EAD is only given for the base and *S*2 analyses on the right side of Figure 5.6. Even then, the expected damage is over 20 times more than the base case, and shows damages occurring at events as frequent as 1/20 years.

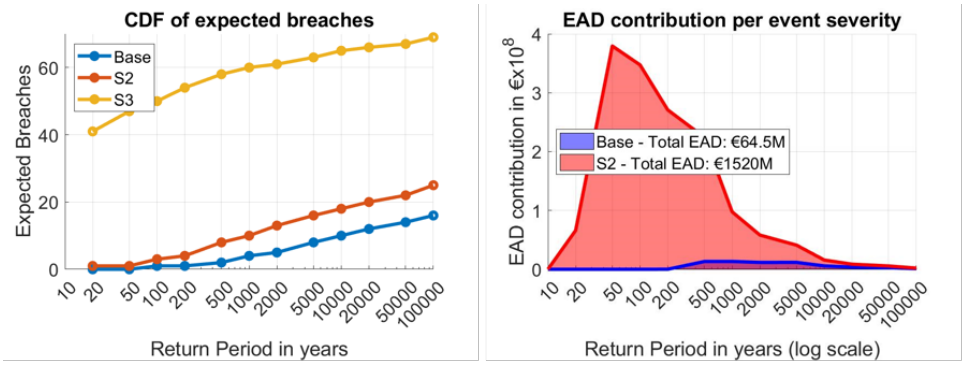

Figure 5.6: EAD in Base and S2, and S3 analyses

BREACH GROWTH FUNCTION

Analyses *S*5 and *S*6 vary the u_c parameter in relation the base scenario. The base scenario uses a default parameter of 0.2 m/s, whereas *S*5 and *S*6 use 0.16 m/s (sandy soils) and 0.6 m/s (clayey soils) respectively (see Table 5.1). From the left side of Figure 5.7, the expected damage is similar in the base and *S*5 cases, which suggests that the default value provided in the breach growth formula is closer to the 'sandy' value. The reason for this may have been to present a 'conservative' default value, but in the overall system, the opposite occurs, as the greatest damage in seen in *S*6 (clayey soils). This result is counter intuitive, but can be understood when considering the amount of breaches (right side of Figure 5.7). The small breaches volumes caused by the clayey soils increases the possibility of breaching downstream, and an increase of volume at one location is generally less impactful than that same volume increase being applied to a completely new region.

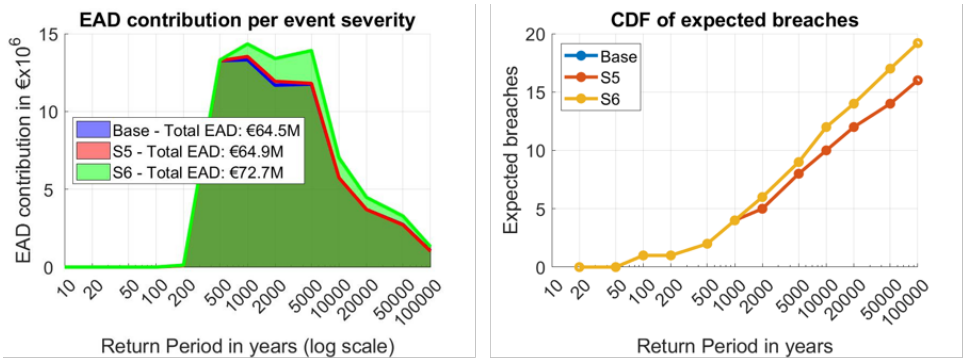

Figure 5.7: Left: EAD in Base, S5, and S6 analyses. Right: CDF of expected breaches (note that the blue 'Base' line is covered by the red 'S5' line)

5.4.3. PARAMETRIC UNCERTAINTY – LOADS

Analyses *L*1 and *L*2 assess the uncertainty caused by two aspects of the hydraulic loads that are used in the model chain. *L*1 uses 'realistic' floodwaves that come from the GRADE database, while *L*2 uses a les strongly correlated flow between the rivers. Neither of these changes has a large impact on the overall damage as shown in Figure 5.8.

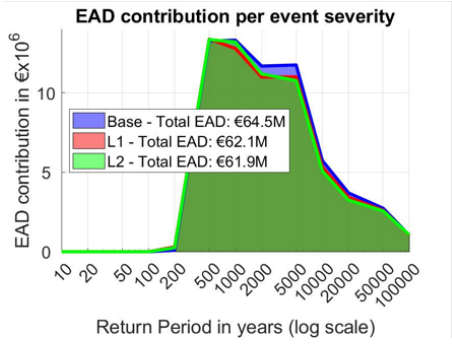

Figure 5.8: EAD in Base, L1, and L2 analyses

5.4.4. PARAMETRIC UNCERTAINTY – IMPACTS

Uncertainties caused by impact parameters tested are given in Figure 5.9, in terms of in expected annual damage (EAD) and expected annual fatalities (EAF). It can be seen that the fatality calculation is much more sensitive to the parameters tested than the damage calculation.

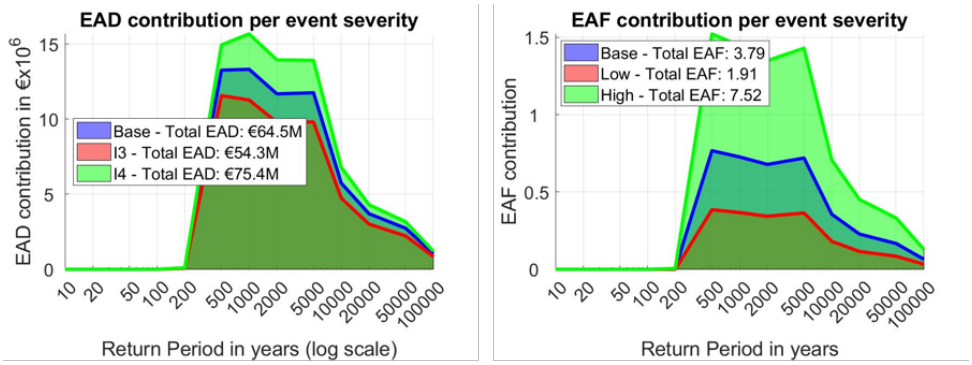

Figure 5.9: Expected damage and fatality uncertainties

5.5. CONCLUSION

5

To estimate flood risk in protected river systems, the effects of breaching should be accounted for. This is required both at the location of the breach and in the rest of the system, which will be subject to so-called system behaviour. Such risk assessments are important for decision-making, but are (as yet) uncommon in FRM. This study, therefore, develops a framework to relate the various components of a system behaviour analysis and define how to assess scenarios and uncertainties in such analyses.

The framework is then applied to the Netherlands case study, evaluating the uncertainty of Expected Annual Damage (EAD) to various input parameter of the hydraulic loads, dike strengths and impact functions. The EAD is disaggregated over extreme events in each comparison, indicating their contribution to the total EAD value. The EADs resulting from analyses with and without system behaviour (model uncertainty) are also calculated, and the former gives a yearly decrease in expected risk of about ~€20 million (or 25%). Such differences are likely to impact cost-benefit ratios of proposed measures, which may have life cycles of 50 years or more.

The case study analysis suggests that the uncertainty in the EAD is not highly sensitive to the waveshape of the loads nor the dependence between the two rivers in the system (Rhine and Meuse). However, the uncertainty in the scale of future loads is unknown and not tested here. The damage appears highly sensitive to the dike strength inputs tested. It is clear that new estimates of failure probabilities should be developed, and that fragility functions should incorporate the duration of exceedance of water levels as one of the failure criteria. The EAD is less sensitive to the damage curves used, but damage calculations are limited by the quasi-2D approach and the use of depth as the only variable contributing to damage. The fatality functions tested show a much larger degree of uncertainty, which would be amplified if uncertainties over early warning and evacuation were included.

The framework could be used as a tool to help risk modellers and decision-makers define how an analysis should be conducted and what outputs are required. Doing so will provide valuable risk analysis data, similar to that shown for the Netherlands case study.

6

DISCUSSION, LIMITATIONS AND RECOMMENDATIONS

INTRODUCTION

As can be expected, there are numerous limitations in the flood risk analysis methods developed to account for system behaviour in the previous chapters. Many of these limitations are discussed at the end of each respective chapter, but are summarised again here, considering the overall systems approach itself and its various components. Implications of these limitations and suggestions to overcome them are also provided. These suggestions are distinct from the recommendations for 'further research' given in the final chapter, which focus more on new research and applications of the work.

As the analysis method in this thesis can be categorised as 'risk-based', the advantages and limitations of this approach are first discussed, as well as the systems approach implemented. The chapter then considers the various components of the overall method, with specific reference to the previous chapters. To provide context as to what component of the method is being discussed, Figure 6.1 is repeated from the introduction. The analysis method was applied to the Po River and Dutch delta, and has helped to identify / highlight a number of issues related to FRA in these case studies. These are discussed in section 6.6 and section 6.7, along with how they could be addressed in future systems approaches to risk analyses.

This work is previously unpublished, but the ideas in section 6.6 have been presented at the 56th Hydraulic Engineering Colloquium at the Civil Engineering department at TU Delft on January 8th 2018

6.1. RISK BASED METHOD AND SYSTEMS APPROACH

Flood assessments are designed to provide information for decision-makers, and a risk-based assessment method (Buijs et al., 2009) achieves this by transforming uncertainties into estimates of current or future risk. This allows the decision-makers to rationalise various options through cost-benefit analysis or similar methods. Four possible limitations of risk based methods here considered relate to; inequity, input uncertainty, lack of subjectivity, and information output.

Inequity

In flood risk analyses, aspects of inequity, where the overall or relative impact of floods is greater for one person (or group) than another, are not easily incorporated and often ignored. However, methods to evaluate risk accounting for social-welfare have been developed by Kind et al. (2017), while a method to evaluate and reduce regional inequities in risk is developed in a study by Ciullo et al. (2019). In the latter study, a large-scale systems approach is used to account for risk transfers caused by mitigation measures.

Input uncertainty

For the uncertain inputs of a quantitative risk assessment, probability distributions are generally required, even if they have to be roughly estimated. Research by Kwakkel et al. (2016) suggests that the overall complexity of flood assessment for management policies may be better approached with simple models that allow for Decision Making under Deep Uncertainty (DMDU). Similar to most risk based methods, DMDU methods utilise multiple simulations. However, the probability distributions of inputs in DMDU are generally considered to be uniform, and focus is placed on the decisions that provide the best (or worst) simulated outcomes, irrespective of probability. Two advantages of risk-based over DMDU methods are 1) the relative likelihood of any simulation can be calculated (and thus overall risk estimates as well) and 2) the use of more accurate models can provide better understanding of the system, and even allow for the discovery of new features, such as the extreme 'drawdown' effect encountered in Chapter 2 that counteracts (and surpasses) positive system behaviour effects.

Subjectivity

Quantitative flood risk assessments are often accused of ignoring the subjective nature of stakeholders' risk perception (Kellens et al., 2013). Scholvinck (2019) argues against their use due to the presence of various 'ontologies' (descriptions or models of a system particular to one person or group) for understanding flood risk, as a given risk metric will not have the same meaning for all stakeholders affected by it. This relates to the argument for more 'qualitative approaches', using subjective assessments of impacts. However, impacts that are difficult to quantify economically, such as fatalities or eco-system services can also be included into risk metrics by evaluating them in terms of money, or assigning them a weight in the case of a multi-criteria analysis.

Information Output

Closely related to the problem of subjectivity and risk perception is the output information provided by a risk analysis. By definition, risk is a single value (e.g. expected annual fatalities or economic damage), providing little information for decision-makers.

However, societies are generally more averse to risk from a large single event than the equivalent combined risk from multiple smaller events. For fatalities, methods to account for this so-called 'societal' risk have been developed in the Netherlands as limit lines for calculated flood fatality curves (Maaskant et al., 2010). In the case of economic damage, the current work provides decision-makers with information about the breakdown of expected annual risk (economic damage) geographically and into bands of probability (Chapter 5).

Despite these problems and alternative approaches, the risk-based method is still a very commonly used approach for flood management decision making. As well as the two case studies discussed in this research, risk based approaches exist in countries such as the UK (Risk Assessment for Strategic Planning, RASP, Sayers et al. 2008) and the USA (Risk Based Decision Making, RBDM, Tung 2005).

6.1.1. SYSTEMS APPROACH

A systems approach to modelling risk is utilised in the present study. Some of the problems of the systems approach to modelling, when compared to reductionist modelling (where parts are modelled separately), are given by Leonard and Beer (1994). These problems include the fact that; modellers may require an understanding of many fields, systems models may take significant time to develop, and both modellers and end-users can get lost in the data. While the advantages for flood risk estimation and understanding may outweigh these problems, they limit the number and complexity of components that can be included. Two such components not included in the present analysis include pro-active measures, and long-term dynamics.

In the protected riverine regions where system behaviour is most relevant, early-warning systems and pro-active protection measures (extra protection measures put in place prior to forecasted flood) are likely to be in place. Pro-active measures including sandbags, support berms, increasing polder water level and other interventions are known to be effective in preventing breaches (Lendering et al., 2013), and are implicit in the 'deep uncertainty' of DMDU approaches, but are omitted from most risk assessments due to the complexity of including them. Similar proactive dynamic processes are also applicable in impact modelling, where householders may move items upstairs, or find ways to evacuate. As methods of addressing these measures are more developed for impact modelling, they have been included in the uncertainty analysis in Chapter 5, but the pro-active defence measures are not. The chapter shows that for the Netherlands case study, the change in Expected Annual damage is ~15%, but reaches almost 50% for Expected Annual Fatalities.

Chapter 5 highlights some of the long-term dynamic uncertainties of a system that are not included in the specific risk analysis methods presented in this research, such as river morphology (Oliver et al., 2018), structural degradation (Klerk et al., 2019), exposure changes (Jongman et al., 2012) and hydrological change (Milly et al., 2005). One option to include these long-term changes in the current analysis method would be to run simulations that span the lifecycle of a measure, say 50 years. This would be achieved by running sets of 50 consecutive yearly maximum events, in which the long-term dynamic processes would be built in to these cycles as functions that alter exposure, hydraulic loads and dike strengths each year. Other long-term developments may be harder to

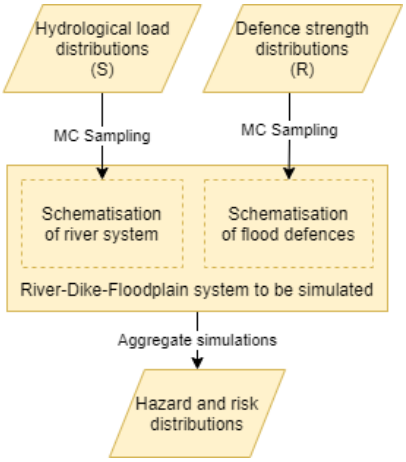

Figure 6.1: Basic analysis method as discussed in introduction

predict, for example new technologies that could make breaches less relevant.

For the primary uncertain components that are included in the systems approach developed in this study (loads and strengths), a Monte Carlo analysis is utilised (Figure 6.1). As discussed in the introduction, Diermanse et al. (2014) suggested Monte Carlo as one of the best options of doing so for the Rhine case study, using advanced sampling techniques to improve efficiency. Such sampling techniques work well in the Rhine-Meuse case study where the number of hydraulic inputs to the system are small, but proved too complicated when applied to the Po river with its many tributaries and dependencies. In the end 'crude Monte Carlo' analysis was used for the Po River, and this may be a limitation in other studies where computational resources might be more prohibitive.

The following sections consider the four specific components of the analysis method used in this study (Figure 6.1); Hydraulic loads, defence strengths, system model and outputs and discuss limitations in those.

6.2. HYDRAULIC LOAD DISTRIBUTIONS (*S*)

In the introduction chapter, three methods of generating hydraulic loads for the boundaries of a system are suggested, namely; a full model chain including weather generator and hydrological model, the results of another system behaviour analysis, or extreme value analysis. Advantages for each method are discussed in that chapter, and the specific limitations for the approaches used in the case studies are given below.

By using the results of the GRADE project (which includes elements of system behaviour), the Rhine-Meuse case study falls into second category. The system behaviour aspect of GRADE is, however, simplified, as breaches are deterministically triggered if the water level is above the crest level of the flood defence. Some of the sensitivities of the expected discharge distribution at the downstream end of the model (Lobith) can be seen in Figure 6.2 (Hegnauer et al., 2014). The sensitivity values used are considered to

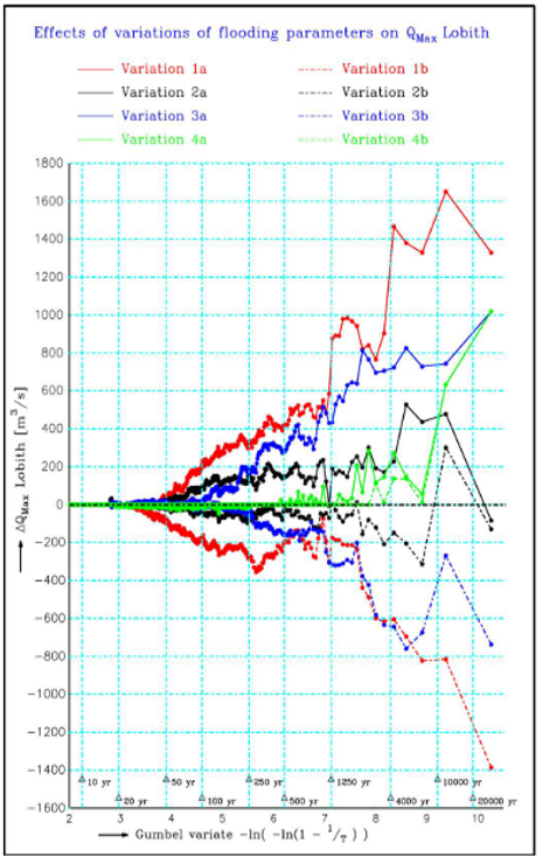

Sensitivity tests conducted in GRADE on discharge distribution at Lobith;

Variation 1: The level of the top of the dike			
1a:	*-0.5m*	*1b:*	*+0.5m*
Variation 2: The width of the breach in the dike			
2a:	*-25%*	*2b:*	*+50%*
Variation 3: The volume of the retention area behind the dike			
3a:	*-50%*	*3b:*	*+50%*
Variation 4: The initial water level behind the dike			
4a:	*-1.0m*	*4b:*	*+1.0m*

Figure 6.2: The results of various sensitivity tests related to out of bank flooding in GRADE. For more detail see Hegnauer and Becker (2013). The largest sensitivity in red is caused by changing the dike crest heights by ±0.5m, which is believed to over estimate this uncertainty.

over-estimate the uncertainty, yet would cause a maximum 10% change in the discharge. While such a change would of course change risk estimates, it is unlikely to change conclusions drawn from the approach.

Another drawback of this dataset is the lack of information on the dependence between the Rhine and Meuse. The GRADE project simulates 50,000 years of events on both the Rhine and Meuse rivers, but unfortunately these two time periods are not synchronous, and no dependence can be inferred. For this reason simple correlation coefficients were used in the present study, based on a memo by Diermanse (2002), and standard practice for FRA in the Netherlands. This was shown in Chapter 5 to have a limited effect on expected annual damage.

The hydraulic boundary conditions for the Po River analysis were based on Extreme Value theory (Gumbel and Lieblein, 1954), and the tributary system required a complex

dependence model to be developed. Due to time, data, and software limitations, a Gaussian copula was used. However, the use of this copula to model the dependence of discharge extreme copula is known to have issues in the tails of distributions, where the extreme events of most interest are found. Specifically, the dependence between distributions weakens for extreme events (Renard and Lang, 2007). Despite this, the Gaussian copula used here validated well for its required function (generating extreme events on the main channel of the Po), but closer scrutiny of closely correlated flows may identify weaknesses. To improve this, Archimedean (Dung et al., 2015), Gumbel or Student-T (Poulin et al., 2007) copulas could be investigated.

Another problem with the use of extreme value theory on the Po River is that the effects of lakes and controlled reservoirs are not easily accounted for. Specific rules could be developed for the distributions of tributaries connected to lakes to account for this, but for a more complete solution, a hydrological model as part of a model chain would be required, with pre-defined operating functions at control structures like the Miorina dam on Lake Maggiore. Similarly, downstream on the IJssel branch of the Rhine, the IJsselmeer lake levels are also controlled, which are not accounted for in the boundary conditions of this study. Adding the operating functions to Lakes on the Po would be an important step in calculating risk on the Po, but the small fluctuations on the IJssel lake would have little effect on the risk in the Netherlands.

On the downstream ends of the other Rhine branches (the Lek and the Waal), the system becomes more branched, but is closed off from major sea storm surges by the Maeslantkering defence near the port of Rotterdam and the Haringvliet barrier further south. Failure of the Maeslant barrier is considered in a system behaviour analysis of compound events (storm surge and river discharges) by De Bruijn et al. (2014) and Diermanse et al. (2014). Compound interactions have been shown to be relevant by Khanal et al. (2018) and Kew et al. (2013) if the sea barriers were to fail. However, in the case study in this project storm surge was not accounted for. This limitation means the risk calculated here may be slightly underestimated especially for the most downstream locations where storm surges in combination with river discharges do significantly contribute to flood risks. Although the Po river delta has no such sea barriers, the steeper terrain and smaller tidal range means that the sea is not as influential far upstream in the system (Maicu et al., 2018).

6.3. DEFENCE STRENGTH DISTRIBUTIONS (R)

Many of the limitations of the dike strength distributions are discussed in the preceding chapters, while specific issues relating to the Dutch dike fragility data (that is used as input in this research) are given in section 6.6. While that section relates to the limitations of the existing fragility data used in the present research, there are also limitations in how the fragility data was adapted for use. In Chapter 5 a method was developed to account for both water levels, and the duration of time those levels were exceeded in fragility curves. This was deemed necessary as the Dutch defences are known to be susceptible to time dependent breach mechanisms like piping and macrostability. The impact of including this duration was shown to be potentially significant, using expert judgement to create fragility surfaces expressing the relationship. However, the experts showed a high degree of variability among themselves on this relationship, and this is a significant

limitation of the work.

The process began with asking the experts to consider the duration of time the fragility curves were most applicable to. For example, would the failure probabilities described in a macrostability curve be applicable if the corresponding water levels were applied to the dike for 1 hour, 1 day, 1 week etc.? Using this as the basis of their thinking, they were then asked to provide ratios to scale the fragility curves for longer and shorter periods. If the suggested duration of a water level that the curves were most applicable to was 5 days, then shorter periods received ratios less than 1, and longer periods received ratios above 1. The experts could not be interviewed together in a structure session, so various issues arise due to this process, such as; knowledge of the development of curves, understanding of the term failure, and what the scaling meant for the curves. These limitations apply to the results of the expert judgement (not the concept of fragility surfaces), and the effect on the case study results themselves are mitigated by the adjustment of the surfaces to defined failure probabilities.

In the Rhine analysis these fragility functions are then adjusted to conform to pre-supposed failure probabilities that would be correct if no system behaviour effects were present (see Chapter 2). However, these input failure probabilities are another major unknown. In this study, both the failure probabilities for the new legal standards and the VNK2 recent estimates (Jongejan et al., 2011) are used. From discussions with experts, however, the actual strengths may lie in between these datasets. One of the most comprehensive dike fragility assessments in the Netherlands (OKADER - Levelt et al. 2017) shows even less credible overall failure probabilities when the dataset is used for large scale risk assessment and compared against load distributions. For this reason, the failure probabilities of OKADER were ignored in favour of pre-supposed failure probabilities.

Whether or not failure probabilities are pre-supposed as a defence strength input, resulting failure probabilities that include system behaviour can be estimated from the output. This was done on the Po River case study. Here, input dike fragility curves were developed based on the work of Mazzoleni et al. (2014b), and the output failure probabilities were shown to be within the same order of magnitude as the safety standard for the region. To generate dike fragility curves in the Netherlands that conform to expected failure probabilities, more knowledge and perhaps a structured session with dike fragility experts is required. In general, validation of such failure probabilities is difficult due to the rarity of breaching, but methods such as Bayesian updating (Roscoe and Hanea, 2015) or expert judgement Cooke and Goossens (2004)may give reliable estimates.

6.4. SYSTEM MODEL

As well as the inputs, scrutiny must be applied to the schematisation of the river-dike-floodplain system itself (Figure 6.1), which should model all the dynamics that occur during a flood event. The hydrodynamics are considered to be the most important of these, and thus numerical hydrodynamic solvers form the base of the schematisation of the system, with potential breaches schematised into these models. However, as mentioned, other processes such as the installation of breaching mitigation measures (sandbags, etc.) could have a significant impact. These are not included in the case study schematisations, but if a model for this behaviour could be inferred, it could be easily

implemented using python functions that 'break' into the model.

The river networks used in both case studies were schematised in 1D, and no significant benefits (that counter the loss of efficiency) are likely to be gained from using higher dimensional routing methods. The software used to implement these 1D numerical schemes are, of course, prone to problems. While the on-going development of Sobek may make it more attractive in the future, other software packages are suggested for future studies. The availability of an existing model for the Rhine, and the legacy and knowledge of Sobek use dictated the software choice for the Netherlands case study. HEC-Ras proved to be highly flexible, useful and powerful when used for the Po River study.

Connected to the 1D river schematisation must be a dike system with the ability to be breached. Some of the problems with the discretisation of the dikes are discussed in section 6.6. Despite these problems, the idea of discretised sections of dike in which a single breach is possible is a practical one, and for this reason it is used in many system behaviour studies. section 6.6 also suggests that the issue of the triggers and development of a breach be addressed as part of a larger conversation (in the Netherlands) in the field of flood risk. If agreement could be reached on the best way to model breach triggering and growth, schematising it in current models would be easily achievable. Although not utilised on the Po, fragility surfaces could be easily implemented to breach the 'lateral structures' that represent dikes in HEC-Ras, and the available growth functions could be better utilised to model the breach development. Furthermore, with more advanced scripting, the location of a breach could be changed dynamically within a section of dike. On the Rhine, special branches at pre-defined breach locations had to be built which could have had a minimal impact on the hydrodynamics of the river. Future Sobek software developments may provide better alternatives than this but are currently unavailable.

For both case studies, a quasi-2D model was utilised to represent flooding, and the limitations of this are discussed in Chapter 3. Problems with overland flow dynamics are even more acute in the Rhine case study, where quasi-2D functionality was not explicitly available, and had to be built and calibrated. Although the calibration was sufficient for purpose, explicit quasi-2D methods may provide better accuracy. In Chapter 5 the accuracy of the inundation patterns was improved in post-processing by the use of predefined flood extents for each breach, but this meant interactions cannot be captured such as breaching of secondary defences in the floodplain, and polder-side breaching. The Quasi-2D and post-processing methods were implemented as computational simplifications, but provide sufficient accuracy to demonstrate the importance of system behaviour interactions in this study.

6.5. OUTPUTS

The final aspect of the basic method shown in Figure 6.1 to be considered is the output. While the outputs themselves are not technically a limitation of the work, the large amount of data and the complexity of the processes used to generate it could limit uptake of the approach by decision makers. For this reason, improved data analysis tools should be developed to display and relate the output information. During this research, initial steps in this process were started by developing GIS platforms (as seen in Fig-

ure 6.3) to easily access the data and explore ideas. These platforms still require further development to be useful for decision-makers and analysts, but were sufficient to explore ideas and general system behaviour concepts during the study.

6.6. RHINE CASE STUDY DISCUSSION: DIKE FRAGILITY AND FLOOD RISK ANALYSIS

6.6.1. BACKGROUND

Flood-risk in the Netherlands is highly sensitive to the failure of the primary defences. The two main reasons for this sensitivity are that failures are often binary in nature (i.e. they usually occur completely or not at all), and that the consequences of failure are likely to be catastrophic. The catastrophic potential of breaches is due to both the significant hazard associated with them (water volume, velocity, etc.) and the large economic and social exposure that the defences protect. For these reasons, protection standards are very strict and dike fragility is one of the most studied flood-risk analysis topics in the Netherlands. The dike fragility data resulting from these studies is a crucial input in the analysis developed in this study.

Despite the depth of this dike fragility research, some issues can be identified that impede the use of dike fragility data in large-scale flood risk analysis (such as the system behaviour method proposed in this research). The issues considered in this study to be most important are disagreement or confusion on the definition of failure, and problems related to spatial, mechanism and duration dependence. Each of these are discussed below, along with some proposed potential solutions to address these issues.

6.6.2. PROBLEMS AND POTENTIAL SOLUTIONS

CONFUSION OR DISAGREEMENT ON THE DEFINITION OF FAILURE

In flood risk analyses, breach failure only becomes relevant if it occurs to such a degree that flow is observed through the breach. The definition of failure often used in the generation of fragility curves in the Netherlands, however, includes any scenario in which the dike geometry has deformed. A macrostability 'failure', for example, could be sliding of the dike body along the line of a stability circle. In reality, unless the dike deteriorates further, it will have a residual strength to prevent inundation. This confusion results in misunderstanding of failure probabilities: while some assume they are related to breach probabilities and link them with breach consequences, they may have been calculated by experts relating to 'just' a little embankment deformation or damage to the embankment only.

One way to address this discrepancy would require altering existing dike stability models that provide information for fragility curves. A possible configuration is that the models recalculate the potential for further movement after an initial 'failure' or change in geometry. This is repeated after each movement, and the threshold to stop these calculations would be if the water can flow freely into the hinterland. The significance of this threshold is that the hydraulics of breach flow become more certain, and existing empirical breach growth models can be used as flow is only geometrically dependent on the increasing width of the breach. The complexities of the growth of the breach from the crest to the base (i.e. the vertical growth) is thus accounted for by the fragility curves

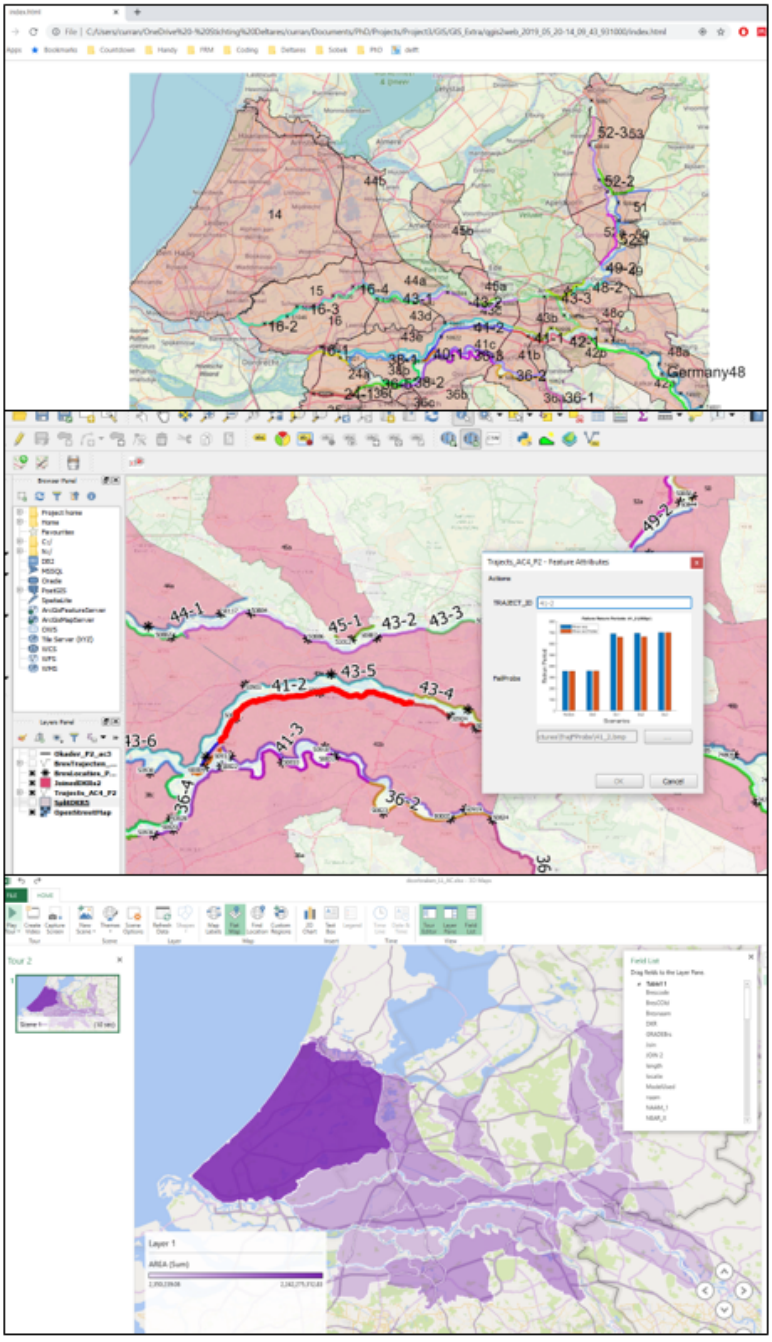

Figure 6.3: Screenshots of data analysis platforms developed as part of PhD. Top – web based, middle – QGIS based, bottom – Microsoft Excel based.

and failure definition, and not through the simplified methods suggested for use in hydrodynamic models by Verheij and der Knaap (2002), for example.

Another possibility is that fragility curves maintain the same format but are instead used to initiate improved breach growth models. These models would be mechanism dependent and could also be probabilistic. An example scenario might be; if the conditions for macrostability 'failure' were reached, a macrostability vertical growth formula would be initiated. Only if this vertical growth resulted in flow into the hinterland would the horizontal growth model be used.

MECHANISM DEPENDENCE

One reason for the breadth of uncertainty in fragility curves is the unknown composition of the dikes. The parameters that describe this composition are usually among the set of variables stochastically sampled in dike stability software to create fragility curves, such as those for macrostability and piping. As both macrostability and piping curves are dependent on the same composition parameters at any given location, they will have some dependence structure. The exact level of that dependence is difficult to quantify, but it can have a major impact on the overall failure probability. For example, suppose a section of dike is calculated as having failure probabilities of 0.01 for both macrostability and piping, given a certain constant water level. The overall failure probability at that water level can vary from 0.01 - 0.02, depending on the correlation / dependence structure assumed. If the mechanisms are considered to be completely independent (i.e. a correlation coefficient of 0 is used), the higher failure probability is obtained. Although choosing this conservative estimate may seem reasonable for risk calculations, over-estimating failure probabilities at a single location in large scale risk calculations may be as problematic as under-estimation, due to system behaviour (De Bruijn et al., 2016). In either case, considering the potential costs associated with large scale measures, accurate estimates are preferable to conservative values.

As well as the composition, failure mechanisms may also be dependent on related sub-processes that occur before a breach. Vorogushyn et al. (2010) include seepage probabilities as a conditional variable for both piping and microstability (failure of the inner slope) fragility functions for the Elbe. This approach arises as a result of analysing a fault tree (top of Figure 6.4) where it is clear that seepage contributes to both failure mechanisms. Fault trees are a useful method of analysing the dependent sub-processes that lead to failures. For example, Slomp (2016) highlights 21 subprocesses (orange subprocesses in fault tree at bottom of Figure 6.4) leading to failure that are used in the computation method of Hydra-ring (Deltares 2017). In Hydra-Ring, the input variables to many of these subprocesses have associated 'α-values' that indicate the sensitivity of the input variable to the reliability index (β). For components where no α-value exists, but a correlation is suspected, expert judgement is used (Deltares, 2017).

While this works well in Hydra-ring, using such programmes to develop fragility curves that can be used in large-scale flood risk assessment causes problems. In the OKADER curves (van der Meij et al., 2016), both the α-values and the expert judgement correlations are lost in calculation due to the separation of the failure mechanisms. Meaning that no dependence can be inferred between fragility curves. One potential method to solve this would be to have combined fragility curves that include all (or at least the

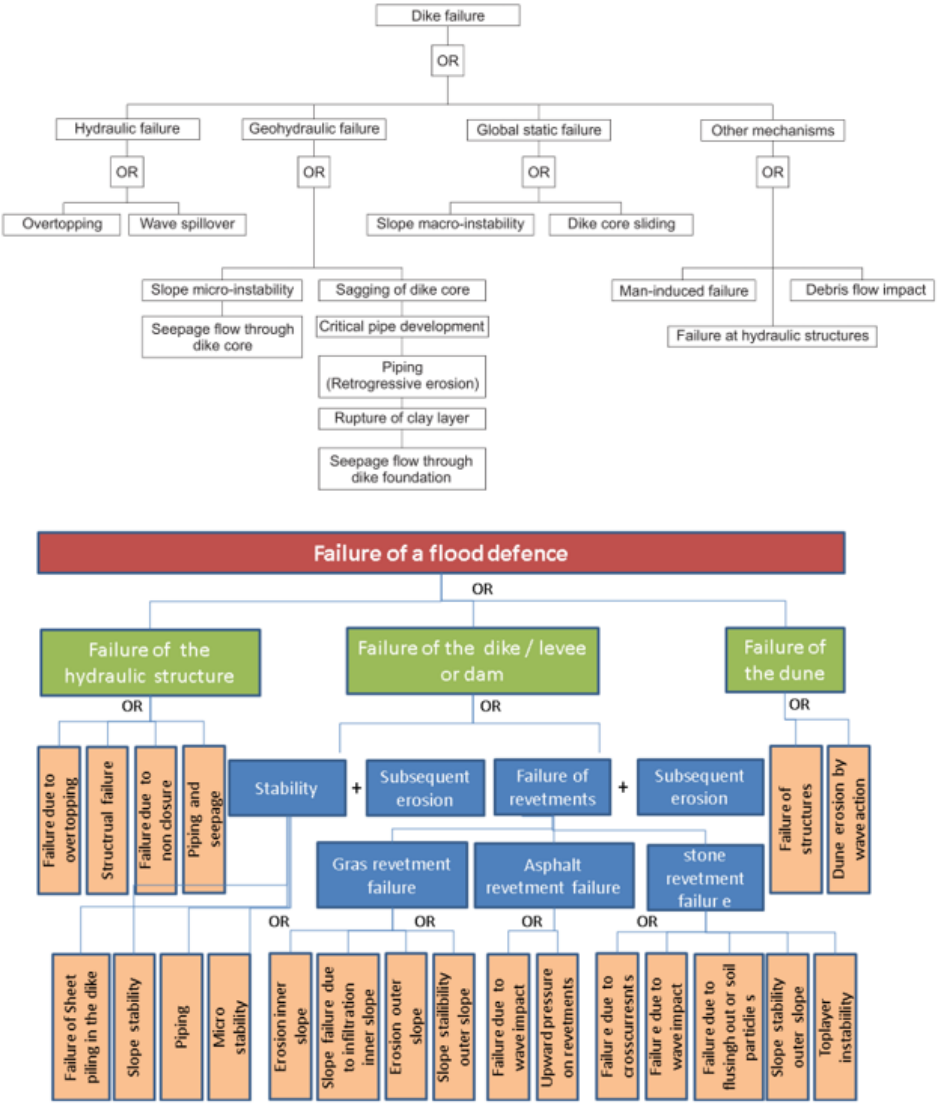

Figure 6.4: Fault trees as developed by Vorogushyn et al. (top) and Slomp (bottom)

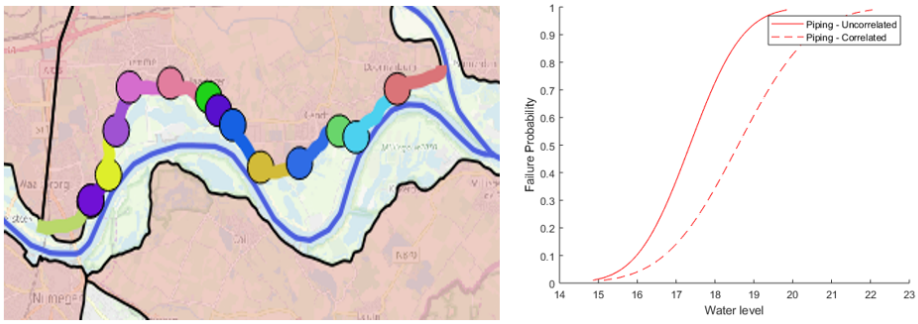

Figure 6.5: (Left), Dike sections discretised in OKADER pertaining to an overall traject. (Right), piping fragility curves for the entire traject when combined independently and with a correlation coefficient of 0.9

main) failure mechanisms. Ideally this would utilise dike stability models that can calculate failure for multiple mechanisms based on the current conditions. This inherently includes the correlation between mechanisms. If this is not possible, stability tests could be also be performed using the same set of conditions for each mechanism, with the resulting failures and successes being used to estimate the correlation. Then the curves could be combined analytically for the specific analysis being done.

In either case, more cooperation is required for the development of the curves. For example, overtopping curves are represented by a table of values in OKADER while macrostability and piping curves are represented as normal distributions, due to their development from different entities.

SPATIAL DEPENDENCE

Another problem when assessing failure probabilities at a large scale is the spatial dependence of failure. One aspect of this is system behaviour, which cannot be accounted for in Hydra-ring (due to the use of pre-defined hydraulic loads) but becomes relevant in the analysis of large systems. This dependence is inherently addressed in system behaviour analyses, but a problem common to both calculation methods is the 'length effect', i.e. the increase of failure probability when calculated over longer dike sections. Hydra-ring includes advanced methods of 'spatial upscaling' of probabilities from one component to the system being investigated, making use of expert judgment to address the length effect.

To illustrate the consequences of this problem, a dike traject on the Waal comprising 15 individual dike sections defined in OKADER is examined, Figure 6.5. The piping fragility curves for each section are combined to create a single curve for the whole traject, using two different assumptions of spatial dependence. The difference between the curves when combined independently and those combined with a (high) correlation coefficient of 0.9 is shown on the right side of Figure 6.5. Although the combination method used is not very refined (for example a decay function could be used in relation to distance), the difference is stark, with failure being roughly three times more likely at water levels of 16 m.

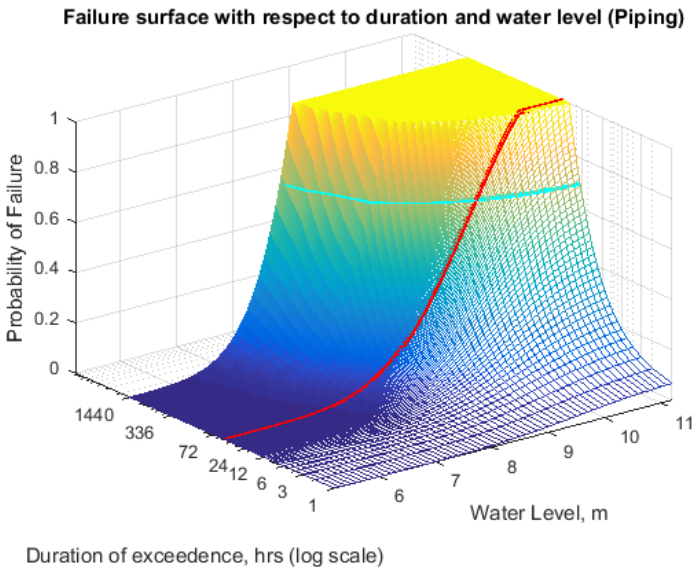

Figure 6.6: Example fragility surface showing a constituent fragility curve (red) and a set of failure conditions from a sampled value of 0.7 (cyan)

DURATION DEPENDENCE

In the macrostability and piping calculations that generate fragility curves in the Netherlands, stochastic simulations of stability are performed at multiple water levels, each of which are considered to be constant over the simulation period. Such static conditions are, however, highly unlikely in a flood-risk event. In most system behaviour flood risk assessments (see, for example, Apel et al. 2009, Bachmann et al. 2013), fragility curves are interpreted so that in any given simulation of the Monte Carlo routine, values are randomly sampled from the fragility curve to represent the strength. This provides a water level as a failure threshold for the simulation, but gives no consideration to the duration of time required for failure to occur. An implication of this approach is that breaches can only occur before or at the peak of the flood wave. This generally makes flood-risk assessments using these curves conservative in terms of the volume of water discharged at any given breach, which is undesirable in the context of the entire system.

Even if the water level conditions during an event are static for a long period, geotechnical characteristics within the dike may still be changing, such as the phreatic surface or backward erosion pipes. Therefore, the failure probability increases the longer this static water level is maintained. To account for this, the duration required for failure can be recorded as another variable in the fragility curves (in this case it is better named a 'fragility surface'). If the impact of the duration on probability is unknown, expert judgement can be used to develop such surfaces as done by Curran et al. (2018), Figure 6.6.

Using fragility surfaces in a similar manner to the curves, sampled values now provide not a single water level failure threshold, but a set of thresholds for failure (e.g. 48 hours above 18 m, 24 hours above 19 m, etc.). An example of a set of these thresholds

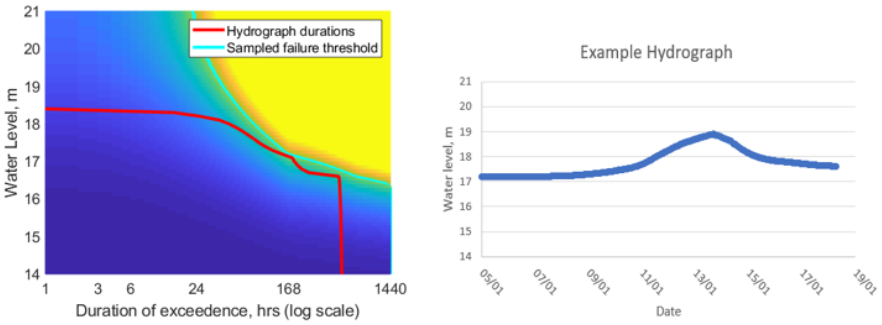

Figure 6.7: (Left) Alternate view of fragility surface with durations of water level exceedances for an example hydrograph superimposed upon it. (Right) Original hydrograph.

are compared against the durations of a hydrograph in Figure 6.7. In this example, failure would occur if the red line that represents the durations of exceedance of the flood-wave were to cross the cyan line at any point. This provides a more accurate estimate of breaching in relation to duration, but it does not take into consideration the 'gradual impoundment' or cumulative effect of the whole flood wave. A method to do so was developed by Vorogushyn et al. (2009), but it requires fragility functions to be developed in multiple dimensions. For example, if the dike height is discretised into just 4 sections, the fragility functions will have 5 dimensions, making them computationally difficult to generate and less easy to communicate.

This problem is highly complex for both the dike stability calculations and risk calculations. Beyond the methods highlighted above, it is not immediately obvious how to bridge the gap between these fields. One option could be a structured expert judgement session to develop new methods and to suggest modifications that could be used for existing data Cooke and Goossens (2004).

6.7. PO CASE STUDY DISCUSSION: FLOOD RISK MAPPING

An aspect of Flood risk management for the Po river case study is the importance placed on flood risk maps in the region. As with all European Union countries, Italy is required to produce such maps as per the 2007 Flood Risk directive. Given that the directive requires maps for events that are well surpassed by current protection standards in the Netherlands (e.g. 1/100 years), the maps are not a vital part of Dutch government policy. In the Po region of Italy, however, they are more significant. As described by Bianchi (2018), the two main tools used by the Po River basin authority in developing flood risk mitigation strategies are the PGRA document (acronym in Italian meaning: plan to manage flood risk; ADBPO 2016) and flood risk maps.

Flood studies have provided detailed maps highlighting areas that are susceptible to flooding as shown on the left side of Figure 6.8. This hazard is indicated in three categories relating to flood probability; frequent (20-50 year return period), less frequent (100-200 year return period) and rare (500 year return period or maximum historical extent). On the right side of the figure these categories are combined with vulnerability to

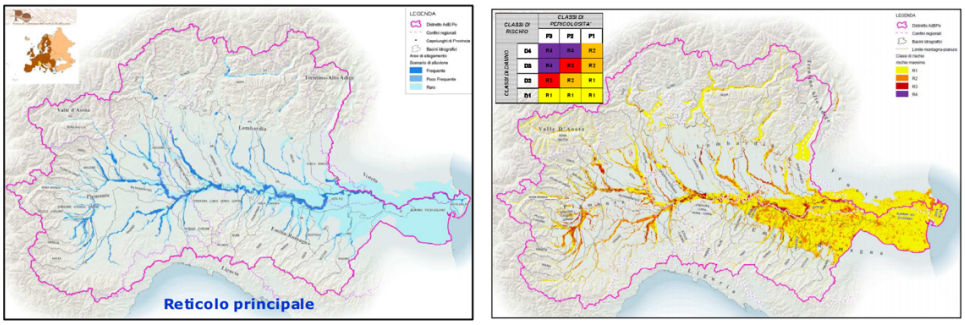

Figure 6.8: (Right) Flood hazard due to river network and (left) combined risk map for the Po catchment

indicate risk.

However, the use of such all-encompassing information has some drawbacks. As shown in Chapter 4, a flood event that causes an extreme discharge value to be obtained at one location is very unlikely to do so at all locations on the main channel of the river, and the relationships between the locations cannot be seen in the maps. Secondly, at locations close to a tributary and the main channel, there is no way to know the source of the inundation from these maps, and thus make sound protection strategies. Finally, the effect of a protection measure at one location on downstream locations cannot be inferred from the maps. Obtaining such information was, in part, a goal of the work done on the Po (Chapter 4).

Figure 6.9 shows recorded events in the region since 1840, and from this it can be clearly seen that the catchments that contribute to major events can vary significantly from one event to the other. This information has been summarised in four 'flood types' for the region, with an example given in Figure 6.10 showing which catchments would contribute to such an event type. However, no information is given on the resulting expected spatial pattern of flooding. Such information would likely be of use for proactive flood management and emergency services.

A more advanced approach would be to create a repository of multiple flood simulations and related characteristic metadata that could be accessed by flood managers. In the case of local flood management, filters could be applied to examine possible events that are pertinent to the region. For flood management at the catchment scale, the repository could be used to prioritise the most effective overall flood management strategies. In both cases, by matching a forecasted rainfall event to a simulation, effective preparation could be enacted without the need for real-time modelling. The work completed in Chapter 4 is a step towards this, and it is hoped that it can provide inspiration for more detailed studies.

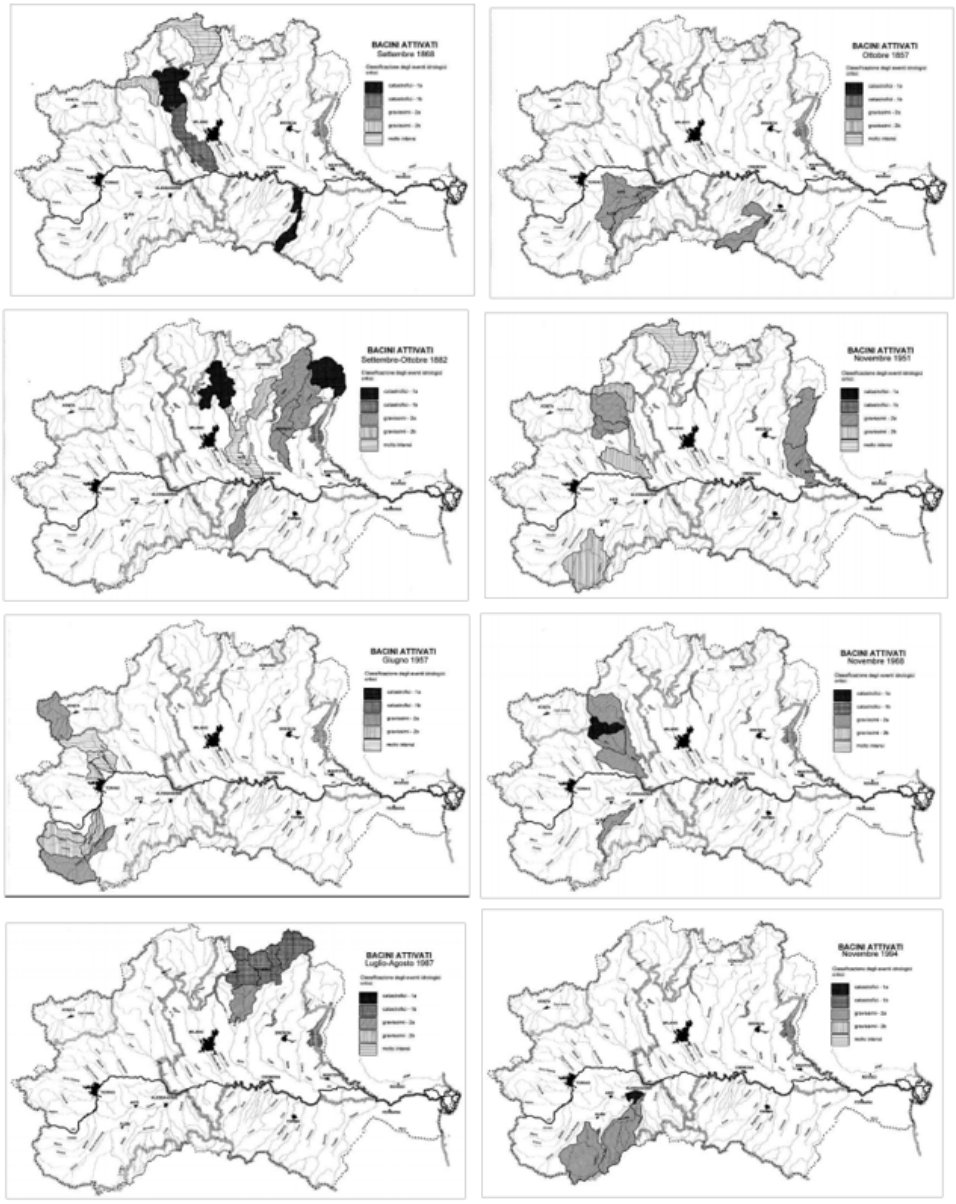

Figure 6.9: Flood events in the Po basin from 1840 to the 1994. The shading indicates the intensity of the discharge in the subcatchments that caused the event (ADBPO, 2016).

Figure 6.10: Example flood type as described in the PGRA document. Example shows 'Lombardo' flood type (ADBPO, 2016).

7

CONCLUSIONS AND RECOMMENDATIONS

7.1. SUMMARY OF OBJECTIVES AND RESEARCH QUESTIONS

The principal aim of this research is to develop a flood-risk analysis method for embanked rivers using a systems approach. The reason for using this approach is to ensure all sources of inundation (dependent tributaries etc.) and pathways for inundation (out of bank flows) are accounted for in the risk analysis. By doing so, flood-risk decision makers receive a more comprehensive estimate of risk, and can derive a better understanding of the interactions in the system that are causing that risk. The application of this systems approach requires modelling the complete area of interest as a system in which different processes can interact. The approach and its limitations are discussed in more detail in Chapters 1 and 6, and the developed methods for each case study are summarised in Figure 7.1.

This systems approach is adopted to address two specific effects of large-scale river systems that are often poorly represented in current analyses: load interdependencies and spatiotemporal dependencies. 'Load interdependency' effects occur when temporal or spatial changes in risk are observed at one location in a system due to flooding that originates at another location. This is especially relevant to systems where breaching of defences can occur, which can significantly reduce the flow downstream in the river network. The second effect is the 'spatiotemporal dependencies' that are observed when the variability of meteorological events causes flows with varying severities and timings in different river channels and tributaries. A systems approach has been utilised in studies by De Bruijn et al. (2014), Merz et al. (2016), Gouldby et al. (2012) and others, but current methods are subject to various limitations and simplifications. Addressing some of the most important limitations are the secondary objectives of this research and doing so contributes to the main goal of developing a systems approach for FRA. The secondary objectives (in the form of research questions) and how they relate to the main goal are given below, alongside a summary of the chapters in which they are addressed.

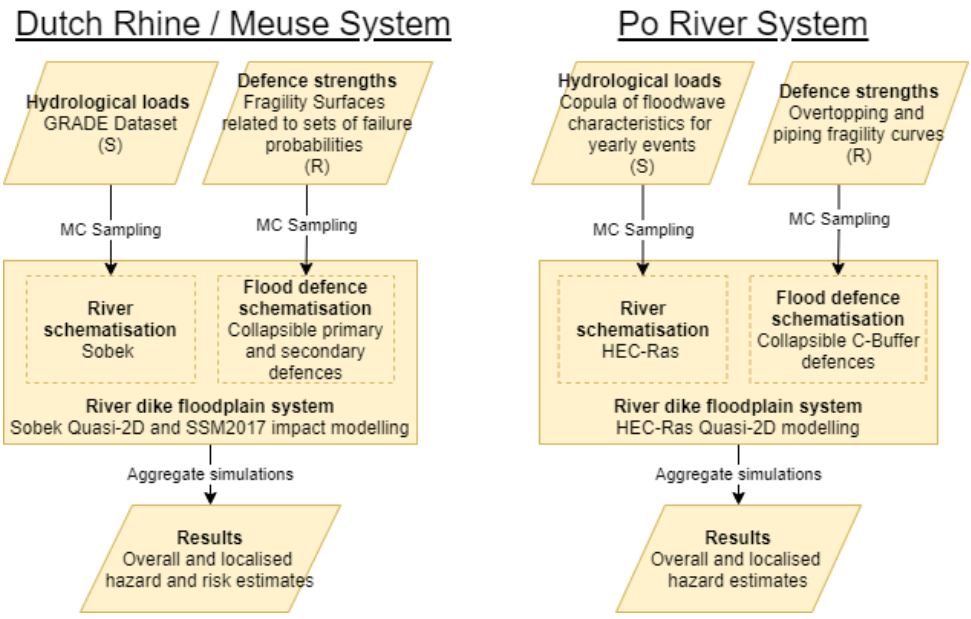

Figure 7.1: Approaches developed for system behaviour hazard/risk assessment in the two case studies, based on basic approach given in introduction.

7

It should be noted, however, that the relationship between research question and chapter is not exclusive, as some chapters contribute (in part) to the answers of other research questions.

7.1.1. RESEARCH QUESTION 1

For system behaviour analysis, how can the resistance to floodwave duration be included in representations of dike defence strengths, and what is the impact of including this component?
Basic answer: By amending existing dike fragility distributions to include duration. Adding this variable is shown to significantly change the results of a risk analysis in the Dutch case study.

In the risk assessments of large-scale river systems, the potential for breaches and the system behaviour effects they produce are a crucial component. In order to take them into account, breaches at a given location are generally considered to occur based on some threshold related to the reliability equation ($Z = R–S$). In other words, if the strength (R) at that dike section is less than the hydraulic load (S) applied to it, failure will occur. To represent this dike strength in a probabilistic distribution, fragility curves are often used, relating the probability of failure to the water levels the dikes are exposed to. This approach does not consider the duration of high water levels in the failure probability, which is known to be relevant for many breaching mechanisms. Thus, the moment of breaching, which may be crucial for system behaviour, is not estimated well in

many traditional methods.

In Chapter 2, expert opinion is utilised to adapt existing fragility curves so that they can include duration as a criterion for failure (creating a 'fragility surface'). The failure probabilities and hazard statistics resulting from system behaviour assessments utilising both fragility curves and surfaces are compared alongside a reference scenario in which no system behaviour is considered at all. As was expected, the hazards downstream are reduced when system behaviour is accounted for due to the 'positive' interdependencies observed in the system. It was also expected that including duration (using the fragility surfaces) might mitigate the effect of system behaviour, as breaches that initiate 'late' (duration dependent) in the floodwave will not reduce downstream flow in the main channel as significantly as 'early' (not dependent on duration) breaches. While this expectation proved true at individual locations, the overall effect on the case study is more complicated.

When applied to the Dutch Rhine system, including duration actually increased the expected number of breaches for a given event, as the 'late' breaches did not reduce flow in the main channel significantly, and diminished their 'positive' effect downstream. Therefore, including duration in the characterisation of dike defence strengths does not significantly reduce the impact of system behaviour overall, as the reduced outflow from breaches is counteracted by more breaches elsewhere in the system. Another unexpected system behaviour phenomenon was also observed in the case study when a large breach in one branch of the system (the Lek, see Figure 7.2) caused a 'drawdown' of flow into that branch. The breach outflow reduced water levels upstream, creating a steeper water profile gradient up to a bifurcation point (Arnhem, Figure 7.2), which pulled (or 'drew down') more water into the branch. For extreme events this drawdown actually increased the discharge into the branch when compared to simulations without breaches. Although this behaviour had been posited for other rivers (Kiss et al., 2015), no other literature has been found in which it is considered in the Dutch river system.

The results from this analysis can be seen as a vindication of using a large-scale modelling approach in risk analysis in general, and of accounting for system behaviour processes. While the 'fragility surface' method introduced to account for duration in breaching is simplified, it provides enough evidence to demonstrate the importance of doing so. As discussed in Chapter 6, methods of schematising breaches in large-scale assessment may need to be part of a larger discussion of flood risk analysis in the Netherlands and elsewhere.

7.1.2. RESEARCH QUESTION 2

How can load interdependencies related to floodplain flows be incorporated into system behaviour risk analyses? What are the results of including them?
Basic answer: Through a schematisation of the system representing floodplain compartmentalisation and potential failures of secondary defences. Including this integrated schematisation affects risk outcomes and improves system understanding.

One of the reasons for employing a systems approach to flood risk analysis is so that potential pathways for flood inundation caused by breaching are accounted for, including all dependencies between regions in the area of interest. While positive interdependencies are a well described feature of system behaviour assessments, less is

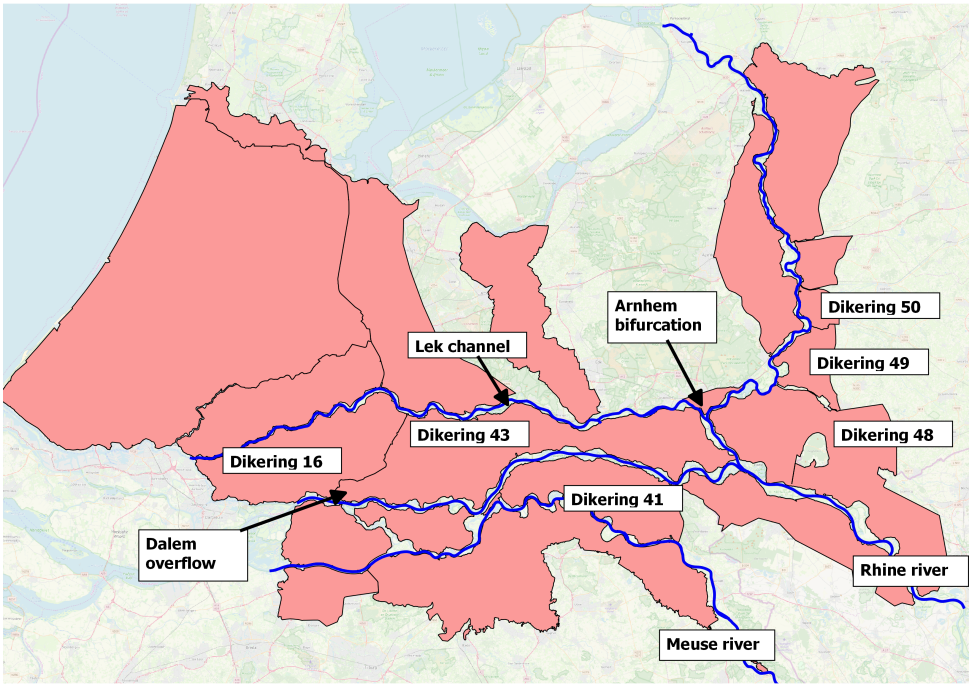

Figure 7.2: Rhine and Meuse case study with locations and dikerings referred to in conclusions

known about negative dependencies. Phenomena such as 'shortcutting' and 'cascading' have been identified as possible negative dependencies in river systems, but are rarely included in large-scale flood risk assessments. Showing the consequence of these effects probabilistically, and in a computationally efficient manner, are key requirements for their inclusion in future flood risk analyses and management decisions.

By considering these dependencies, Chapter 3 is mostly concerned with the flood patterns and timing of flows in the overall system, as opposed to the load and strength inputs. Here, the potential for interdependencies caused by breaches (specifically 'shortcutting' and 'cascading') are included in the system schematisation. This is done by using a quasi-2D model benchmarked on existing breach simulations, allowing for efficient modelling that is representative of potential inundation events. The schematisation of the quasi-2D model also allow for breaching from inundated compartments back into the river and into other compartments.

The model was applied to the Dutch river system (the Rhine branches and the Meuse) and, similar to Chapter 2, the modelling set-up allows hazard metrics to be estimated for the whole system. However, the focus within the case study was on dependencies at three specific locations in the Dutch river system. These had been previously identified as potentially susceptible to system behaviour, but primarily in scenario analyses (as opposed to probabilistic estimates) and in studies where they were isolated from the rest of the system. While the results from these locations are, of course, case specific, they highlight the importance of the method, and are therefore discussed briefly below, with reference to locations given in Figure 7.2.

In a compartment with the potential for cascading effects (dikering 43) the changes in volume introduced by including cascading breaching were minimal. However, the probability of inundation in a connected compartment (dikering 16) increased significantly. At another location (the IJssel valley) the potential for shortcutting of flows from one large river (the German Rhine) to a smaller branch (IJssel river) was demonstrated, after flows had cascaded down through compartments parallel to the river (dikerings 48, 49 and 50). However, increased risk downstream due to flows that had shortcut back into the smaller branch could not be clearly identified. At both these locations, the results of the modelling schematisation made apparent the importance of outflows from inundated compartments back into the river such as those at Dalem.

The third location highlighted shortcutting possibilities across a compartment from one river to another smaller river (flows from Waal to the Meuse across dikering 41 – 'Land van Maas en Waal'). In this case the flows downstream in the smaller river (the Meuse) were noticeably affected by the negative dependency, to the point that it counteracted positive dependencies caused by upstream breaching.

The quasi-2D method proved to be sufficient to model the interdependencies in the system, based on benchmarking results. Although fully 2D models would be preferable in terms of understanding the inundation pathways, they would be at the expense of efficiency. Important outcomes from this study are the various benefits of modelling these interdependencies. Doing so provides significant system understanding and insights when applied to the case study, as demonstrated at the three specific locations of interest. This improvement to the overall systems approach could be used to evaluate large-scale mitigation measures in river systems, such as detention areas, compartmen-

talisation, or locations to discharge inundation back into the river.

7.1.3. RESEARCH QUESTION 3

Research Question: How can the complex spatiotemporal dependencies of systems with multiple rivers or tributaries be accounted for in a system behaviour analysis, and what insights does this bring?
Answer: By developing a dependency model for the hydraulic loading. Doing so will help to identify the causes behind extreme events that occur in the system and methods to mitigate them.

Another objective of using a systems approach in large-scale risk assessments is to accurately model the complete set of sources of inundation. Flood risk maps and other datasets that show synchronous, homogeneous hazard metrics provide little information on these sources and how events manifest in a river system. In river systems with many tributaries, including spatiotemporal dependencies becomes more important in understanding flood dynamics, as it allows the causes of high water levels or inundation to be identified and thus more effective solutions to be made. A systems approach is well-suited to include these dependencies and improve this understanding.

For a systems approach to FRA, the three methods defined in this study to represent the sources (or boundary conditions in a modelling sense) of flooding are: 1) a complete model chain starting with a weather generator, 2) the results of another systems analysis or 3) an extreme value analysis. In the Rhine case (Chapters 2 and 3) another systems analysis (GRADE) is used for the synchronous extreme flows on the Rhine and Meuse, and on the Po (Chapter 4) a simple dependency model is used for the interdependencies between the multiple tributaries. However, in many locations, methods and datasets for the first two methods are not available, so the third option must be used. If this option is implemented in a complex tributary system, a model is required to represent the dependencies between the tributaries. This is one of the principal aims of Chapter 4, which develops a copula to represent dependencies between the various tributaries to the Po River system in Italy.

The basic approach developed here is to 1) estimate a probability distribution for each relevant floodwave characteristic of each tributary, 2) use a synchronous discharge timeseries to infer a relationship (such as a copula) between these distributions and 3) sample events as per the inferred relationship. For the Po River case study, the three dependent floodwave characteristics within each tributary were; peak flow, relative lag in time, and a variable to define volume (duration of time floodwave is above baseflow). A copula was built and sampled to generate multiple events simulated in a 2D model. Despite the use of a simplified dependence model on the Po River, this method provided accurate extreme value flows at various points along the main channel, when compared to distributions inferred directly from observations.

The method is useful for system-wide hazard assessments which allow for a better understanding of high water level events in the main river channel, as well as the dependencies between the inundation sources. This is especially relevant in the Po region, in which multiple hydrological flood 'types' are known to occur from different sources like the Alps or Apennines mountain ranges. Due to these case study dependencies, it is observed that the return periods of peak discharges do not relate directly to the return

periods of inundation levels in the compartmentalised areas of the floodplain. The relevance of this observation is that the deterministic hydrological events currently used to describe floods with exceedance probabilities of 1/500 or 1/200 years will not result in inundation levels of the same exceedance probabilities, and therefore cannot be used to generate flood maps.

It should be noted that a complete systems approach that included breaching and system behaviour effects was also applied to the case study. This required developing dike fragility distributions (overtopping and piping) for the region, which highlighted vulnerable areas and sections of dike. Therefore, this chapter also contributes towards the first two research questions. A stochastic delay was introduced into breaches caused by piping, which is a more simplified version of what was developed in Chapter 2 for the Rhine. The quasi-2D model used to schematise the floodplains allows for cascading similar to what was developed in Chapter 3, but not shortcutting, since this is less relevant in the case study. Finally, the chapter also provides another example of the application of the systems approach, which could contribute to flood-risk management decisions about proposed mitigation measures such as dike strengthening or retention areas.

7.1.4. RESEARCH QUESTION 4

Research Question: How can risk assessments using a systems approach provide useful information and analysis for decision makers? What are the results of such analysis for the Netherlands case study?
Basic answer: Sensitivity, uncertainty and scenario analyses are useful for decision makers, and can be generated by following the developed framework. Doing so for the Netherlands provides important information on expected annual damage both locally and system-wide, and the sensitivities thereof.

While the improved flood risk analysis method developed in this study has the intrinsic benefit of improving system understanding, its principal goal is to help in flood-risk management decision making. The first step of the decision making process is often to simply ascertain what aspects of the system are causing the greatest risk or uncertainty in risk. In this regard, sensitivity and uncertainty analyses are crucial. At later stages of the flood management process when mitigation measures are proposed, scenario analyses become more relevant, helping to determine the effect of the proposed measures on risk. Such scenario analyses are also often used for 'storyline approaches', where possible futures are considered irrespective of their surrounding uncertainty.

Sensitivity, uncertainty and scenario analyses can all be incorporated into risk assessments using a systems approach, but an understanding of the different components and the relationship between them is required. To improve this understanding, and to clearly delineate the components of the assessment method, a framework is developed in Chapter 5. This framework outlines the steps required to incorporate the various analyses used by decision makers into systems assessments. In some cases, the analysis method is trivial. For example, testing the sensitivity of the hydraulic loads only requires rerunning the analysis with changes to this input. However, in other cases the analysis may be more complex. An example of this would be the scenario analysis of a mitigation measure that defines proposed dike failure probabilities. In this case, the dike fragility distributions must be altered to conform to these newly proposed failure probabilities

while considering the hydraulic loads expected in the system.

The framework was applied to the Dutch river system, and various analyses were conducted on features of the system under the general headings of loads, strengths and impacts. In this case study, important sensitivities and uncertainties were observed, such as the change in overall expected annual damage when system behaviour effects are accounted for (EAD of €64 million) and when they are not (EAD of €85 million). The sensitivity analysis methods were also able to highlight potentially unimportant features of the system in terms of risk, such as the dependence between extreme flows on the Rhine and Meuse. Finally, the application of the complete risk assessment method (i.e. including consequences) demonstrates some of the graphics (such as a breakdown of expected annual damage over all probabilities) and datasets that can be generated from such an analysis, both for the entire system and locally. Localised risk estimates will also allow aspects of equity to be incorporated into decision making, by assessing how much risk changes per region due to a proposed measure.

7.1.5. OVERALL OBJECTIVE

The overall objective of this study, in the form of a research question, is:

How can system dependencies and interactions be incorporated into the flood risk analyses of large-scale embanked river systems? What are the outcomes of doing so, in general, and for the Dutch Rhine and Po river case studies?
Answer: Through a systems approach to modelling. The outcomes of doing so are improved system understanding, improved risk estimates and improved graphics and datasets for risk managers.

In summary, the dependencies and interactions examined in this study can be included into flood risk assessments through a systems approach to modelling. The basis of the approach is to create a model of the region of interest that includes the subprocesses relevant to the pathways and sources of inundation, such as the routing network and defences. Then the probability distributions related to defence strengths and hydraulic loading distributions can be applied to the model to account for the complete range of flooding possibilities.

With this approach in place, system behaviour effects can be included through the defence strength distributions and the schematisation of the hydrodynamic model. The spatiotemporal interactions can be introduced by ensuring dependency is built into the hydraulic loading boundary conditions. These analyses can then be made more relevant and useful for decision-makers by estimating the sensitivity of the system and providing scenario analyses. As with any method, the limitations must be carefully considered, and a summary of these for various components, and the method in general, can be found in Chapter 6.

7.2. IMPLICATIONS FOR THE CASE STUDIES

The purpose of this study was to investigate methods for improving flood risk assessment in general, and in section 7.3 suggestions for applications of the method to different locations are discussed. However, the work is (as can be expected) highly influenced

by the issues and dynamics in the two case studies. Therefore, the implications of this study in these regions, and potential follow-on work, is here discussed.

The systems analyses conducted on the Netherlands has shown some noteworthy modelling results, including;

- The possibility for 'drawdown' of flow into branches with breaches, in particular the extreme example of this on the Lek (Figure 7.2).
- Counteracting systems effects on the Meuse due to upstream breaches (positive interdependency) and shortcutting (negative interdependency).
- The importance of outflow points in the dikerings, such as the existing one at Dalem (dikering 43) and potential locations on the right bank of the IJssel.
- The significance (or lack thereof) of different inputs to flood risk analyses in terms of expected annual damage.
- The localised changes in risk observed when different scenarios are tested in the approach.
- A potential ~€20 million annual change in risk when system behaviour is accounted for (32% reduction).

The Netherlands is currently embarking on one the largest upgrades to the river dike system in many years, as a result of new legal protection standards. The development of these standards included some simplified methods to account for system behaviour, and thus may be the first large-scale mitigation measure to consider it. It is very possible that a complete systems analysis, had it been performed, may have had a bigger impact on the protection levels. However, for the time being at least, this is a moot point. The standards have been made law, and required a huge effort in gaining consensus across the stakeholders (the so-called process of 'polderen') that is unlikely to be repeated in the near future, irrespective of potential economies.

Nevertheless, a systems-based approach may yet have applications in the upgrades. The standards are not specific guidelines for the design of the dike sections, but minimum failure probabilities that they should conform to. Currently, the HWBP (in English: High water protection program) is using 'legal assessment tools' to help achieve these new standards. One of the principal tools is Hydra-ring, which uses pre-defined distributions of hydraulic loads for each location. As shown in the present study, new distributions could easily be generated that may be more reflective of the 'true' expected loads at these locations. As the loads expected when system behaviour is accounted for are generally lower, achieving the protection standards would become easier and cheaper.

Although the flood management of the Po River has been examined in less detail in this study than that of the Netherlands, two potential applications of the method appear feasible in the region. The first would be to create a repository of simulations that can accompany the flood maps supplied to regional flood management authorities. Using a method similar to that developed in this study, the simulations would try and capture the variability of flood events in the region. For local flood managers this would provide valuable information on what to expect during an event.

The second application potential application for the Po would be for the cost-benefit evaluation of proposed measures in the region. From the results obtained in Chapter 4, it can already be seen that upstream compartments will likely mitigate downstream inundation, with or without breaching. Understanding these dynamics will allow for effective mitigation measures such as detention areas to be put in place.

7.3. FURTHER RESEARCH AND APPLICATIONS

The systems approach to risk analysis developed in this study can have many more applications besides those examined in the case studies. While some applications may not lead directly to flood risk mitigation measures, they may provide sufficient information to warrant further investigation into a measure or interaction in the system. Some of these applications are listed here.

- Induced dike breaching.

While this study focuses on 'natural' or unanticipated breaching of dikes, the concept of induced breaching has been discussed at many locations worldwide, such as the Mississippi (Olson and Morton, 2012) and the Tigis-Bega river system in Romania (Popescu et al., 2010). Doing so takes advantage of system behaviour effects, but also raises ethical issues about valuing one location over another. In any case, the process requires a thorough understanding of the system to be effective.

Such a strategy is very unlikely to be completely planned during an event, so in the preparation phase of disaster risk management, the first step would be to model the full range of hydrological events that could take place in the system. Then a suitable location could be identified, and the effects on the risk to downstream dikes evaluated. The first steps of such an approach can be seen in the study of Kok et al. (2003). Timing would also be a crucial aspect of such a plan, as the capacity in the flooded area must be used to reduce the peak of the floodwave to be effective. Planning to achieve this timing could also be (partly) achieved in the preparation phase through system modelling. For example, by using statistical data to estimate the likely moment of a floodwave peak for a certain meteorological event.

- Multi-catchment models

Models showing flood risk on the scale of multiple large catchments (e.g. pan-European models) have recently become more popular in scientific literature. This is partly driven by the insurance industry, that seeks to understand the correlations and dependencies of risk for their portfolios. Understanding these dependencies is often sought in relation to different future potential climates or weather patterns for the region of interest. In such models, however, dikes are often poorly represented, either because they are not included at all, or because they do not include the potential for breaching. One approach to account for this would be to run system behaviour analyses in some of the bigger catchments over a broad range of events. Then, when modellers want to look at a certain scenario of weather patterns / climate in the region of a catchment, they select a subset of those simulations that best represents that climate. By doing so, a better estimate of risk can be obtained in these embanked river catchments, presenting a truer estimate of the dependencies between regions.

- Flood simulations database and GIS applications

Many applications of this systems approach will likely be case specific, or simply beyond the imagination of this conclusion. Therefore, perhaps the best use of this approach is to facilitate the development of innovative measures by enabling easily accessible simulation data. Some of the major case-specific outcomes of this study were reached not by trying to model them a priori, but observing them in the results through databases or custom-made GIS (Geographical Information Systems) applications. For example, the possibility of drawdown in the Lek was noticed through GIS analysis, and further research into this phenomenon may show potential mitigation measures that can be derived from it.

One of the best uses of a database in scoping for new mitigation measures and better understanding of processes is to use it to answer queries. Examples of this data mining could be; 'given flooding at location X, how often does it come from a breach at Y?' or 'Given high volumes in the river at X, where is most likely to be flooded?'. If enough data points are collected about the consequences of every event simulated, then the possibilities are enormous.

As suggested by Ferrari et al. (2019) for the Po River, such a database would also have considerable applications in resilience and emergency planning. For example, the statistics of having multiple routes blocked during an event would be of use for evacuation planning.

- Applications in other systems

The methods developed in this study have been tailored for the case studies and the information available within them. The general approach, however, has become more popular worldwide, and it is hoped that this study could contribute to the improvement of understanding at other locations.

As mentioned in the introduction, a number of similar studies have been conducted on the Elbe river, but with perhaps a greater focus on the upstream catchment. The Danube may also benefit from such an approach, but the large number of national stakeholders could mean that measures that result from it are more difficult to implement. Other embanked systems in Europe where the approach would be applicable include the Rhône, the Garonne and the Tisza.

As part of this study, the approach was considered for the Parana river delta in Argentina / Uruguay, but the more fluid nature of the branches of the delta may necessitate a different modelling approach. On rivers systems in the US, the issue of system behaviour is even starting to become a part of the public consciousness, as a major online media stations recently published a piece on the phenomenon (Vox-Media, 2018).

Other major protected systems in Asia such as the Red River and the Mekong would likely benefit from the approach in combination with detailed modelling of the tidal and storm surge influences, which can be more relevant than for the locations examined in this study.

7.4. FINAL REMARKS

It is the author's hope that the methods and approaches developed in this study have contributed to the greater body of knowledge on flood risk analysis, and will perhaps

lead to the implementation of future mitigation measures or further studies. While currently computationally expensive, the methods developed will only become more and more tractable, and perhaps more relevant as the population and assets protected by embanked river systems grow and climate change increases the intensity and severity of flood events.

REFERENCES

ADBPO (2016). Piano per la valutazione e la gestione del rischio di alluvioni. Profili di piena dei corsi d'acqua del reticolo principale.

Ahmadisharaf, E., Bhuyian, M., and Kalyanapu, A. (2013). Impact of spatial resolution on downstream flood hazard due to dam break events using probabilistic flood modeling. *Association of State Dam Safety Officials Annual Conference 2013, Dam Safety 2013*, 1(September).

Alfieri, L., Bisselink, B., Dottori, F., Naumann, G., de Roo, A., Salamon, P., Wyser, K., and Feyen, L. (2017). Global projections of river flood risk in a warmer world. *Earth's Future*, 5(2):171–182.

Alkema, D. and Middelkoop, H. (2005). The Influence of Floodplain Compartmentalization on Flood Risk Within the Rhine-Meuse Delta. *Natural Hazards*, 36(DECEMBER):125–145.

Apel, H., Merz, B., and Thieken, A. H. (2009). Influence of dike breaches on flood frequency estimation. *Computers and Geosciences*, 35(5):907–923.

Arnaud-Fassetta, G. (2013). Dyke breaching and crevasse-splay sedimentary sequences of the rhône delta, France, caused by extreme river-flood of december 2003. *Geografia Fisica e Dinamica Quaternaria*, 36(1):7–26.

Arnold, J. G. and Allen, P. M. (1999). Automated methods for estimating baseflow and ground water recharge from streamflow records. *Journal of the American Water Resources Association*, 35(2).

Assteerawatt, A., Tsaknias, D., Azemar, F., Ghosh, S., and Hilberts, A. (2016). Large-scale and High-resolution Flood Risk Model for Japan. *FLOODrisk 2016 - 3rd European Conference on Flood Risk Management*, 11009:1–5.

Bachmann, D., Huber, N., Johann, G., and Schüttrumpf, H. (2013). Fragility curves in operational dike reliability assessment. *Georisk: Assessment and Management of Risk for Engineered Systems and Geohazards*, 7(1):49–60.

Bates, P. D. and De Roo, A. P. J. (2000). A simple raster based model for flood inundation simulation. *Journal of Hydrology*, 236(1-2):54–77.

Bertrand, N., Liquet, M., Moiriat, D., Bardet, L., and Duluc, C.-M. (2018). Uncertainties of a 1D Hydraulic Model with Levee Breaches: The Benchmark Garonne. In Gourbesville, P., Cunge, J., and Caignaert, G., editors, *Advances in Hydroinformatics*, pages 189–204, Singapore. Springer Singapore.

Bianchi, F. (2018). *Flood hazard spatial distribution along the Po river for different flood types*. PhD thesis, University of Boilogna.

Bishop, A. W. (1955). The use of the slip circle in the stability analysis of slopes. In *The Essence of Geotechnical Engineering: 60 years of G{é}otechnique*, pages 223–233. Thomas Telford Publishing.

Bligh, W. G. (1915). Submerged weirs founded on sand. *Dams and weirs*, pages 151–159.

Bomers, A., Schielen, R. M. J., and Hulscher, S. J. M. H. (2019). How dike breaches affect discharges in a complex river system. *Accepted for publication in: Natural Hazards*, (0123456789).

Bruijn, K. M. D., Diermanse, F. L. M., Doef, M. V. D., and Klijn, F. (2016). Hydrodynamic system behaviour : its analysis and implications for flood risk management. *E3S Web of Conferences*, 11001.

Bubeck, P., Kreibich, H., Penning-Rowsell, E. C., Botzen, W. J., de Moel, H., and Klijn, F. (2017). Explaining differences in flood management approaches in Europe and in the USA – a comparative analysis. *Journal of Flood Risk Management*, 10(4):436–445.

Buijs, F. A., Hall, J. W., Sayers, P. B., and Van Gelder, P. H. A. J. M. (2009). Time-dependent reliability analysis of flood defences. *Reliability Engineering and System Safety*, 94(12):1942–1953.

Castellarin, A., Domeneghetti, A., and Brath, A. (2011). Identifying robust large-scale flood risk mitigation strategies: A quasi-2D hydraulic model as a tool for the Po river. *Physics and Chemistry of the Earth*, 36(7-8):299–308.

Charalambous, J., Rahman, A., and Carroll, D. (2013). Application of Monte Carlo Simulation Technique to Design Flood Estimation: A Case Study for North Johnstone River in Queensland, Australia. *Water Resources Management*, 27(11):4099–4111.

Chen, Y., Syvitski, J. P., Gao, S., Overeem, I., and Kettner, A. J. (2012). Socio-economic impacts on flooding: A 4000-year history of the yellow river, China. *Ambio*, 41(7):682–698.

Ciullo, A., de Bruijn, K. M., Kwakkel, J. H., and Klijn, F. (2019). Accounting for the uncertain effects of hydraulic interactions in optimising embankments heights: Proof of principle for the IJssel River. *Journal of Flood Risk Management*, (March 2018):e12532.

Colucci, A., Larcan, E., and Treu, M. C. (2003). 2 DIIAR Politecnico di Milano, Italy. *Sustainable Planning and Development*, 6:311.

Cooke, R. M. and Goossens, L. H. J. (2004). Expert judgement elicitation for risk assessments of critical infrastructures. *Journal of Risk Research*, 7(6):643–656.

Courage, W., Vrouwenvelder, T., van Mierlo, T., and Schweckendiek, T. (2013). System behaviour in flood risk calculations. *Georisk: Assessment and Management of Risk for Engineered Systems and Geohazards*, 7(2):62–76.

Curran, A., Bruijn, K. M. D., Klerk, W. J., and Kok, M. (2019). Large Scale Flood Hazard Analysis by Including Defence Failures on the Dutch River System. *MDPI Water*, 11(1732):1–13.

Curran, A., De Bruijn, K., Domeneghetti, A., Bianchi, F., Kok, M., Vorogushyn, S., and Castellarin, A. (2020). Large-scale stochastic flood hazard analysis applied to the Po River. *Natural Hazards*, (0123456789).

Curran, A., De Bruijn, K. M., and Kok, M. (2018). Influence of water level duration on dike breach triggering, focusing on system behaviour hazard analyses in lowland rivers. *Georisk: Assessment and Management of Risk for Engineered Systems and Geohazards*.

Dang, N. M., Babel, M. S., and Luong, H. T. (2011). Evaluation of food risk parameters in the Day River Flood Diversion Area, Red River Delta, Vietnam. *Natural Hazards*, 56(1):169–194.

Dawson, R. and Hall, J. (2006). Adaptive importance sampling for risk analysis of complex infrastructure systems. *Proceedings of the Royal Society A: Mathematical, Physical and Engineering Science*, 462(2075):3343–3362.

De Bruijn, K., Beckers, J., and Van Der Most, H. (2010). Casualty risks in the discussion on new flood protection standards in The Netherlands. *WIT Transactions on Ecology and the Environment*, 133:73–83.

De Bruijn, K. M. (2005). Resilience of the lowland part of the Mekong River. *NCR-days 2004*.

De Bruijn, K. M., Diermanse, F. L. M., and Beckers, J. V. L. (2014). An advanced method for flood risk analysis in river deltas, applied to societal flood fatality risk in the Netherlands. *Natural Hazards and Earth System Sciences*, 14(10):2767–2781.

De Bruijn, K. M., Lips, N., Gersonius, B., and Middelkoop, H. (2016). The storyline approach: a new way to analyse and improve flood event management. *Natural Hazards*, 81(1).

De Moel, H., Aerts, J. C. J. H., and Koomen, E. (2011). Development of flood exposure in the Netherlands during the 20th and 21st century. *Global Environmental Change*, 21(2):620–627.

Deltares (2017). Hydra Ring technical reference manual. Technical report.

DHI, D. H. I. (2002). Mike-11: a modelling system for rivers and channels, reference manual.

Dhondia, J. F. and Stelling, G. S. (2004). SOBEK one dimensional–two dimensional integrated hydraulic model for flood simulation–its capabilities and features explained. In *Hydroinformatics*, pages 1867–1874. World Scientific.

Di Baldassarre, G., Viglione, A., Carr, G., Kuil, L., Salinas, J. L., and Blöschl, G. (2013). Socio-hydrology: Conceptualising human-flood interactions. *Hydrology and Earth System Sciences*, 17(8):3295–3303.

Di Baldassarre, G., Viglione, A., Carr, G., Kuil, L., Yan, K., Brandimarte, L., and Blöschl, G. (2015). Debates—Perspectives on socio-hydrology: Capturing feedbacks between physical and social processes. pages 2498–2514.

Diermanse, F., Roscoe, K., Ijmker, J., and Mens, M. (2013). Hydra-Ring : a computational framework to combine failure probabilities. 15:11112.

Diermanse, F. L. M. (2002). Memo samenvallen hoogwaters Rijn en Maas (In Dutch). Technical report.

Diermanse, F. L. M., De Bruijn, K. M., Beckers, J. V. L., and Kramer, N. L. (2014). Importance sampling for efficient modelling of hydraulic loads in the Rhine-Meuse delta. *Stochastic Environmental Research and Risk Assessment*, 29(3):637–652.

Ditlevsen, O., Melcher, R., and Gluver, H. (1990). General multi-dimensional integration by directional 0. *Civil Engineering*.

Domeneghetti, A., Carisi, F., Castellarin, A., and Brath, A. (2015). Evolution of flood risk over large areas : Quantitative assessment for the Po river. *JOURNAL OF HYDROLOGY*, 527:809–823.

Domeneghetti, A., Vorogushyn, S., Castellarin, A., Merz, B., and Brath, A. (2013). Probabilistic flood hazard mapping : effects of uncertain boundary conditions. (2002):3127–3140.

Driessen, A. M. A. J. (1994). *Watersnood tussen Maas en Waal: overstromingsrampen in het rivierengebied tussen 1780 en 1810*. Walburg Pers Zutphen.

Duits-Nederlandse Werkgroep Hoogwater (2009). Risicoanalyse grensoverschrijdende dijk- ringen Niederrhein Risikoanalyse für die grenzüberschreitenden Deichringe am Niederrhein. Technical report.

Dung, N. V., Merz, B., Bárdossy, A., and Apel, H. (2015). Handling uncertainty in bivariate quantile estimation - An application to flood hazard analysis in the Mekong Delta. *Journal of Hydrology*, 527:704–717.

Dunn, C., Baker, P., and Fleming, M. (2016). Flood risk management with HEC-WAT and the FRA compute option. *FLOODrisk 2016 - 3rd European Conference on Flood Risk Managemen*, 11006.

Dupuits, E., Klerk, W., Schweckendiek, T., and de Bruijn, K. (2019). Impact of including interdependencies between multiple riverine flood defences on the economically optimal flood safety levels. *Reliability Engineering & System Safety*, 191(July 2018):106475.

Dupuits, E. J. C., Bruijn, K. M. D., Diermanse, F. L. M., and Kok, M. (2016). Economically optimal safety targets for riverine flood defence systems. *FLOODrisk 2016 - 3rd European Conference on Flood Risk Management*, 20004.

Engelund, S. and Rackwitz, R. (1993). A benchmark study on importance sampling techniques in structural reliability. *Structural Safety*, 12(4):255–276.

Falter, D. (2016). A novel approach for large-scale flood risk assessments : continuous and long-term simulation of the full flood risk chain. (May 2016):96.

Falter, D., Dung, N. V., Vorogushyn, S., Schröter, K., Hundecha, Y., Kreibich, H., Apel, H., Theisselmann, F., and Merz, B. (2016). Continuous, large-scale simulation model for flood risk assessments: Proof-of-concept. *Journal of Flood Risk Management*, 9(1):3–21.

Favre, A. C., Adlouni, S. E., Perreault, L., Thiémonge, N., and Bobée, B. (2004). Multivariate hydrological frequency analysis using copulas. *Water Resources Research*, 40(1):1–12.

Ferrari, A., Dazzi, S., Vacondio, R., and Mignosa, P. (2019). A methodology based on numerical models for enhancing the resilience to flooding induced by levee breaches in lowland areas. *Natural Hazards and Earth System Sciences Discussions*, (May):1–23.

Gouldby, B., Lhomme, J., Mcgahey, C., Panzeri, M., Hassan, M., Burgada, N. K., Orue, C. M., Jamieson, S., Wright, G., Damme, M. V., and Morris, M. (2012). A flood system risk analysis model with dynamic sub-element 2D inundation model , dynamic breach growth and life- loss. *FLOODrisk2012*, (2006):1–13.

Govi, M. and Turitto, O. (2000). Casistica storica sui processi d'iterazione delle correnti di piena del Po con arginature e con elementi morfotopografici del territorio adiacente (In Italian). *Istituto Lombardo Accademia di Scienza e Lettere*.

Gräler, B., van den Berg, M. J., Vandenberghe, S., De Baets, B., Petroselli, A., Verhoest, N. E. C., and Grimaldi, S. (2013). Multivariate return periods in hydrology: a critical and practical review focusing on synthetic design hydrograph estimation. *Hydrology and Earth System Sciences*, 17(4):1281–1296.

Grooteman, F. (2011). An adaptive directional importance sampling method for structural reliability. *Probabilistic Engineering Mechanics*, 26(2):134–141.

Gumbel, E. and Lieblein, J. (1954). SOME APPLICATIONS OF EXTREME- VALUE METHODS. *The American Statistician*, 8(5):14–17.

Hao, Z. and Singh, V. P. (2013). Modeling multisite streamflow dependence with maximum entropy copula. *Water Resources Research*, 49(10):7139–7143.

Heffernan, J. E. and Tawn, J. A. (2004). A conditional approach for multivariate extreme values. *Journal of the Royal Statistical Society. Series B: Statistical Methodology*, 66(3):497–530.

Hegnauer, M. and Becker, A. (2013). Technical Documentation GRADE part II.

Hegnauer, M., Beersma, J., van den Boogaard, H., Buishand, T., and Passchier, R. (2014). Generator of Rainfall and Discharge Extremes (GRADE) for the Rhine and Meuse basins. Final report of GRADE 2.0. page 84.

Hesselink, A. W., Stelling, G. S., Kwadijk, J. C., and Middelkoop, H. (2003). Inundation of a Dutch river polder, sensitivity analysis of a physically based inundation model using historic data. *Water Resources Research*, 39(9).

Horritt, M. and Bates, P. (2002). Evaluation of 1D and 2D numerical models for predicting river flood inundation. *Journal of Hydrology*, 268(1-4):87–99.

Italcopo, C. (2002). Aggiornamento dell'assetto idraulico di progetto del fiume Po dalla confluenza del Tanaro all'incile del Po di Goro me- diante analisi modellistica numerica in moto vario.

Jongejan, R. and Beek, V. V. (2015). ENW-VBG-WTI-15-nov-4.2. 2017:1–11.

Jongejan, R., Maaskant, B., and ter Horst, W. (2013). The VNK2-project: a fully probabilistic risk analysis for all major levee systems in the Netherlands. *Iahs . . .* , 2005:75–85.

Jongejan, R. B., Stefess, H., Roode, N., Horst, W., and Maaskant, B. (2011). The vnk2 project: a detailed, large-scale quantitative flood risk analysis for the netherlands. *International Conference on Flood Management*, (September):27–29.

Jongman, B., Ward, P. J., and Aerts, J. C. (2012). Global exposure to river and coastal flooding: Long term trends and changes. *Global Environmental Change*, 22(4):823–835.

Jonkman, S. and Kok, M. (2008). Risk-based design of flood defence systems-a preliminary analysis for the New Orleans metropolitan area. *4th International Symposium on Flood Defence:Managing Flood Risk, Reliability and Vulnerability*, pages 1–9.

Kalyanapu, A. J., Shankar, S., Pardyjak, E. R., Judi, D. R., and Burian, S. J. (2011). Assessment of GPU computational enhancement to a 2D flood model. *Environmental Modelling and Software*, 26(8):1009–1016.

Kellens, W., Terpstra, T., and De Maeyer, P. (2013). Perception and Communication of Flood Risks: A Systematic Review of Empirical Research. *Risk Analysis*, 33(1):24–49.

Kew, S. F., Selten, F. M., Lenderink, G., and Hazeleger, W. (2013). The simultaneous occurrence of surge and discharge extremes for the Rhine delta. *Natural Hazards and Earth System Sciences*, 13(8):2017–2029.

Khanal, S., Ridder, N., de Vries, H., Terink, W., and van den Hurk, B. (2018). Storm surge and extreme river discharge: a compound event analysis using ensemble impact modelling. *Hydrology and Earth System Sciences Discussions*, (April):1–25.

Kind, J. (2011). Maatschappelijke kosten-batenanalyse Waterveiligheid 21.

Kind, J., Wouter Botzen, W. J., and Aerts, J. C. (2017). Accounting for risk aversion, income distribution and social welfare in cost-benefit analysis for flood risk management. *Wiley Interdisciplinary Reviews: Climate Change*, 8(2):1–20.

Kiss, T., Fehérváry, I., and Fiala, K. (2015). Modelling the Hydrological Effects of a Levee Failure on the Lower Tisza River. *Journal of Environmental Geography*, 8(1-2):31–38.

Klerk, W. J. (2013). *Load interdependencies of flood defences*. PhD thesis, TU Delft, Delft University of Technology.

Klerk, W. J., Pot, R., Van Der Hammen, J. M., and Wojciechowska, K. (2019). A framework for assessing information quality in asset management of flood defences. *Life-Cycle Analysis and Assessment in Civil Engineering: Towards an Integrated Vision - Proceedings of the 6th International Symposium on Life-Cycle Civil Engineering, IALCCE 2018*, (November):673–680.

Klijn, F., Asselman, N., and Van Der Most, H. (2010). Compartmentalisation: Flood consequence reduction by splitting up large polder areas. *Journal of Flood Risk Management*, 3(1):3–17.

Klijn, F., Kreibich, H., de Moel, H., and Penning-Rowsell, E. (2015). Adaptive flood risk management planning based on a comprehensive flood risk conceptualisation. *Mitigation and Adaptation Strategies for Global Change*, 20(6):845–864.

Kok, M., Jongejan, R., Nieuwjaar, M., and Tanczos, I. (2017). *Fundamentals of Flood Protection*. Ministry of Infrastructure and the Environment and the Expertise Network for Flood Protection.

Kok, M., Stijnen, J. W., and Silva, W. (2003). Uncertainty analysis of river flood management in the Netherlands. *Safety and Reliability: Proceedings of the ESREL 2003 Conference, Swets & Zeitlinger, Lisse, the Netherlands. ISBN 90-5809-551-7*, 1:927–935.

Kolen, B., Kok, M., Helsloot, I., and Maaskant, B. (2013). EvacuAid: A Probabilistic Model to Determine the Expected Loss of Life for Different Mass Evacuation Strategies During Flood Threats. *Risk Analysis*, 33(7):1312–1333.

Kreibich, H., Piroth, K., Seifert, I., Maiwald, H., Kunert, U., Schwarz, J., Merz, B., and Thieken, A. H. (2009). Is flow velocity a significant parameter in flood damage modelling? *Natural Hazards and Earth System Science*, 9(5):1679–1692.

Kwadijk, J. (2007). Soil Moisture updating for the Flood Early Warning System of the River Rhine Basin. (December).

Kwakkel, J. H., Walker, W. E., and Haasnoot, M. (2016). Coping with the wickedness of public policy problems: Approaches for decision making under deep uncertainty. *Journal of Water Resources Planning and Management*, 142(3):1–5.

Lammersen, R. (2004). Grensoverschrijdende effecten van extreem hoogwater op de Niederrhein: eindrapport.

Lane, E. W. (1935). Security from Under-Seepage Masonry Dams on Earth. In *Proc. ASCE*, volume 61.

Lendering, K., Jonkman, S., and Peters, D. (2013). Risk based design of land reclamation and the feasibility of the polder terminal. *Proceedings of the 4th International Conference of the Euro-Asia Civil Engineering Forum*, pages 7–14.

Leonard, A. and Beer, S. (1994). The systems perspective: Methods and models for the future. Technical Report 3-4, AC/UNU Project.

Levelt, O., van Vuren, S., Pol, J., van der Meij, R., Nugroho, D., ter Horst, W., Koopmans, R., van der Scheer, P., and de Kruif, A. (2017). Beleidsstudie Kostenreductie Dijkversterking door Rivierverruiming (In Dutch). Technical report.

Lhomme, J., Sayers, P., Gouldby, B., Samuels, P., Wills, M., and Mulet-marti, J. (2008). Spreading Method. (October).

Lindström, G., Pers, C., Rosberg, J., Strömqvist, J., and Arheimer, B. (2010). Development and testing of the HYPE (Hydrological Predictions for the Environment) water quality model for different spatial scales. *Hydrology Research*, 41(3-4):295–319.

Liu, P., Chen, L., Yan, B., Guo, S., and Xiao, Y. (2009). Design Flood Hydrograph Based on Multicharacteristic Synthesis Index Method. *Journal of Hydrologic Engineering*, 14(12):1359–1364.

Loucks, D. and van Beek, E. (2016). *Water resource systems planning and analysis*, volume 4.

Maaskant, B., Jonkman, S. N., and Jongejan, R. B. (2010). The use of individual and societal risk criteria within the Dutch flood safety policy (part 2): Estimation of the individual and societal risk for the dike rings in the Netherlands. *Reliability, Risk and Safety: Theory and Applications Vols 1-3*, (part 2):2099–2104.

Maicu, F., De Pascalis, F., Ferrarin, C., and Umgiesser, G. (2018). Hydrodynamics of the Po River-Delta-Sea System. *Journal of Geophysical Research: Oceans*, 123(9):6349–6372.

Maione, U., Mignosa, P., Tomirotti, M., Maione, U. G. O., Milano, P., and Leonardo, P. (2003). Regional estimation of synthetic design hydrographs. 5124(August).

Mazzoleni, M., Bacchi, B., Barontini, S., Di Baldassarre, G., Pilotti, M., and Ranzi, R. (2014a). Flooding hazard mapping in floodplain areas affected by piping breaches in the Po River, Italy. *Journal of Hydrologic Engineering*, 19(4):717–731.

Mazzoleni, M., Barontini, S., Ranzi, R., and Brandimarte, L. (2014b). Innovative Probabilistic Methodology for Evaluating the Reliability of Discrete Levee Reaches Owing to Piping. *Journal of Hydrologic Engineering*, 20(5):50.

McKay, M. D., Beckman, R. J., and Conover, W. J. (1979). A comparison of three methods for selecting values of input variables in the analysis of output from a computer code. *Technometrics*, 42(1):55–61.

Mediero, L., Jiménez-Álvarez, A., and Garrote, L. (2010). Design flood hydrographs from the relationship between flood peak and volume. *Hydrology and Earth System Sciences*, 14(12):2495–2505.

Merz, B., Apel, H., Dung, N. V., Falter, D., Hundecha, Y., Kreibich, H., and Schröter, K. (2016). Large-scale flood risk assessment using a coupled model chain. 11005:0–4.

Merz, B., Kreibich, H., Schwarze, R., and Thieken, A. (2010). Review article "Assessment of economic flood damage". *Natural Hazards and Earth System Science*, 10(8):1697–1724.

Merz, R. and Blöschl, G. (2008). Flood frequency hydrology: 1. Temporal, spatial, and causal expansion of information. *Water Resources Research*, 44(8):1–17.

Milly, P. C. D., Betancourt, J., Falkenmark, M., Hirsch, R. M., Kundzewicz, Z. W., Lettenmaier, D. P., and Stouffer, R. J. (2005). Stationarity Is Dead: Whither Water Management? *Science*, 319(5863):573–574.

Oliver, J., Qin, X. S., Larsen, O., Meadows, M., and Fielding, M. (2018). Probabilistic flood risk analysis considering morphological dynamics and dike failure. *Natural Hazards*, 91(1):287–307.

Olson, K. R. and Morton, L. W. (2012). The impacts of 2011 induced levee breaches on agricultural lands of Mississippi River Valley. *Journal of Soil and Water Conservation*, 67(1):5A–10A.

Pappenberger, F., Beven, K., Horritt, M., and Blazkova, S. (2005). Uncertainty in the calibration of effective roughness parameters in HEC-RAS using inundation and downstream level observations. *Journal of Hydrology*, 302(1-4):46–69.

Parte, R. (2016). Piano per la valutazione e la gestione del rischio di alluvioni Programma operativo per l ' attuazione e il monitoraggio delle misure del PGRA (POAMM) Parte A a cura di AdbPo e Regioni Parte B a cura di DPCN e Regioni.

Popescu, I., Jonoski, A., van Andel, S. J., Onyari, E., and Quiroga, V. G. (2010). Integrated modelling for flood risk mitigation in Romania: Case study of the Timis-Bega river basin. *International Journal of River Basin Management*, 8(3-4):269–280.

Posner, C. (2015). Historical perspective on structural methods for flood protection in Lower Danube Historical perspective on structural methods for flood protection in Lower Danube. (January):1–12.

Poulin, A., Huard, D., Favre, A. C., and Pugin, S. (2007). Importance of tail dependence in bivariate frequency analysis. *Journal of Hydrologic Engineering*, 12(4):394–403.

Prettenthaler, F., Amrusch, P., and Habsburg-Lothringen, C. (2010). Estimation of an absolute flood damage curve based on an Austrian case study under a dam breach scenario. *Natural Hazards and Earth System Science*, 10(4):881–894.

Rackwitz, R. and Flessler, B. (1978). Structural reliability under combined random load sequences. *Computers and Structures*, 9(5):489–494.

Remo, J. W., Carlson, M., and Pinter, N. (2012). Hydraulic and flood-loss modeling of levee, floodplain, and river management strategies, Middle Mississippi River, USA. *Natural Hazards*, 61(2):551–575.

Renard, B. and Lang, M. (2007). Use of a Gaussian copula for multivariate extreme value analysis: Some case studies in hydrology. *Advances in Water Resources*, 30(4):897–912.

Rijkswaterstaat. Lizard flood simulation repository. https://flooding.lizard.net/. Accessed: 15 July 2019.

Roscoe, K. and Hanea, A. (2015). Bayesian networks in levee system reliability. *12th International Conference on Applications of Statistics and Probability in Civil Engineering, ICASP 2015*, (1).

Salvadori, G. and De Michele, C. (2010). Multivariate multiparameter extreme value models and return periods: A copula approach. *Water Resources Research*, 46(10).

Sayers, P., Mulet-Marti, J., Gouldby, B., Hassan, M. a. a. M., and Benwell, D. (2008). A methodology for national-scale flood risk assessment. *Proceedings of the ICE - Water Management*, 161(3):169–182.

Schmocker, L. and Hager, W. H. (2009). Modelling dike breaching due to overtopping. *Journal of Hydraulic Research*, 47(5):585–597.

Scholvinck, O. (2019). *USE OF SCENARIOS IN PARTICIPATORY ADM*. PhD thesis.

Schweckendiek, T., Kanning, W., and Jonkman, S. N. (2014). Advances in reliability analysis of the piping failure mechanism of flood defences in the Netherlands. *Heron*, 59(2-3):101–127.

Sellmeijer, H., de la Cruz, J. L., van Beek, V. M., and Knoeff, H. (2011). Fine-tuning of the backward erosion piping model through small-scale, medium-scale and IJkdijk experiments. *European Journal of Environmental and Civil Engineering*, 15(8):1139–1154.

Sellmeijer, J. (1988). On the mechanism of piping under impervious structures. *Repository.Tudelft.Nl*, page 116.

Sellmeijer, J. B. (2006). Numerical computation of seepage erosion below dams (piping). *Third International Conference on Scour and Erosion*, pages 596–601.

Slager, K., Burzel, A., Bos, E., de Bruijn, K., Wagenaar, D., Bouwer, L., and van der Doef, M. (2016). User Manual Delft-FIAT version 1.

Slager, K. and Wagenaar, D. (2017). Standaardmethode 2017: Schade en slachtoffers als gevolg van overstromingen.

Slomp, R. (2016). Implementing risk based flood defence standards. Technical report.

Slomp, R., Knoeff, H., Bizzarri, A., Bottema, M., and Vries, W. D. (2016). Probabilistic Flood Defence Assessment Tools. 03015:1–14.

Steenbergen, H. M. G. M., Lassing, B. L., Vrouwenvelder, A. C. W. M., and Waarts, P. H. (2004). Reliability analysis of flood defence systems. *Heron*, 49(1):51–73.

Stelling, G. S. (2012). Quadtree flood simulations with sub-grid digital elevation models. *Proceedings of the Institution of Civil Engineers - Water Management*, 165(10):567–580.

Syme, W. (2001). TUFLOW - Two & onedimensional Unsteady FLOW Software for Rivers , Estuaries and Coastal Waters. *IEAust Water Panel Seminar and Workshop on 2d Flood Modelling*, pages 2–9.

Syvitski, J. P. and Robert Brakenridge, G. (2013). Causation and avoidance of catastrophic flooding along the Indus River, Pakistan. *GSA Today*, 23(1):4–10.

Tanaka, T., Tachikawa, Y., Ichikawa, Y., and Yorozu, K. (2017). Impact assessment of upstream flooding on extreme flood frequency analysis by incorporating a flood-inundation model for flood risk assessment. *Journal of Hydrology*, 554:370–382.

Teng, J., Jakeman, A. J., Vaze, J., Croke, B. F., Dutta, D., and Kim, S. (2017). Flood inundation modelling: A review of methods, recent advances and uncertainty analysis. *Environmental Modelling and Software*, 90(April):201–216.

Ter Horst, W. (2012). Overstromingsrisico van dijkringgebieden 14, 15 en 44. (November).

Thanh, V. Q., Roelvink, D., van der Wegen, M., Reyns, J., Kernkamp, H., Van Vinh, G., and Thi Phuong Linh, V. (2019). Flooding in the Mekong Delta: Impact of dyke systems on downstream hydrodynamics. *Hydrology and Earth System Sciences Discussions*, (February):1–34.

The OFDA/CRED International Disaster Database (2014). Université Catholique de Louvain - Brussels. \url{http://web.archive.org/web/20080207010024/http://www.808multimedia.com/wi

Towler, E., Rajagopalan, B., Gilleland, E., Summers, R. S., Yates, D., and Katz, R. W. (2010). Modeling hydrologic and water quality extremes in a changing climate: A statistical approach based on extreme value theory. *Water Resources Research*, 46(11):1–11.

Tung, Y. K. (2005). Flood defense systems design by risk-based approaches. *Water International*, 30(1):50–57.

UN-DHA (1992). Internationally agreed glossary of basic terms related to disaster management. *UN DHA (United Nations Department of Humanitarian Affairs), Geneva*.

Van, A. M., Koelewijn, A. R., and Barends, F. B. J. (2005). Uplift Phenomenon : Model , Validation , and Design. *International Journal of Geomechanics*, 5(2):98–106.

van Berchum, E. C., van Ledden, M., Jonkman, S., Timmermans, J., and van den Broek, H. (2019). Rapid screening and evaluation of flood risk reduction strategies Exploratory study on the use of the FLORES modelling approach for World Bank projects. (February):75.

van der Meer, J. W., ter Horst, W. L. A., and van Velzen, E. H. (2008). Calculation of fragility curves for flood defence assets. *Flood Risk Management: Research and Practice*, (1):567–573.

van der Meij, R., Levelt, O., and Asselman, N. (2016). Uitwerking methode voor bepaling kostenreductie rivierverruiming. Technical Report November 2017.

Van der Most, H. (2015). Quick scan of options for raising the levels of protection against floods of dike rings in The Netherlands.

Van der Most, H. and Klijn, F. (2013). De werking van het marktmechanisme. Technical report.

van Mierlo, M., Vrouwenvelder, A., Calle, E., Vrijling, J., Jonkman, S., de Bruijn, K., and Weerts, A. (2007). Assessment of flood risk accounting for river system behaviour. *International Journal of River Basin Management*, 5(2):93–104.

Van Mierlo, M., Vrouwenvelder, A., Calle, E. O. F., Vrijling, J. K., Jonkman, S. N., de Bruijn, K., and Weerts, A. H. (2003). Effects of River System Behaviour on Flood Risk (Delft: Delft Cluster). Technical report.

Vaskinn, K., LØvoll, A., and Höeg, K. (2003). Breach formation: Large scale embankment failure. *Projet IMPACT*.

Vergeer, G. J. H. (1990). Probabilistic Design of Flood Defences. *Centre for Civil Engineering Research and Codes, report*, (141).

Verheij, H. J. and der Knaap, F. C. M. (2002). Modification breach growth model in HIS-OM. *WL| Delft Hydraulics Q*, 3299:2002.

Verheij, H. J. and Van der Knaap, F. C. M. (2003). Modification breach growth model in HIS-OM. H.J. Verheij. page 64.

Ververs, M. and Klijn, F. (2004). Werken noodoverloopgebieden? Wat leert ons de overstroming van 1926. *Geografie*, 7:14–17.

Vogel, R. M. and Castellarin, A. (2017). Risk, Reliability, and Return Periods and Hydrologic Design. *Handbook of Applied Hydrology*, pages 78–1 to 78–10.

Voortman, H. G., van Gelder, P. H. A. J. M., and Vrijling, J. K. (2009). *Risk-Based Design of Large-Scale Flood Defence Systems*.

Vorogushyn, S., Apel, H., and Merz, B. (2011). The impact of the uncertainty of dike breach development time on flood hazard. *Physics and Chemistry of the Earth*, 36(7-8):319–323.

Vorogushyn, S., Bates, P. D., de Bruijn, K., Castellarin, A., Kreibich, H., Priest, S., Schröter, K., Bagli, S., Blöschl, G., Domeneghetti, A., Gouldby, B., Klijn, F., Lammersen, R., Neal, J. C., Ridder, N., Terink, W., Viavattene, C., Viglione, A., Zanardo, S., and Merz, B. (2017). Evolutionary leap in large-scale flood risk assessment needed. *Wiley Interdisciplinary Reviews: Water*, (October):e1266.

Vorogushyn, S., Merz, B., and Apel, H. (2009). Development of dike fragility curves for piping and micro-instability breach mechanisms. *Natural Hazards and Earth System Science*, 9(4):1383–1401.

Vorogushyn, S., Merz, B., Lindenschmidt, K. E., and Apel, H. (2010). A new methodology for flood hazard assessment considering dike breaches. *Water Resources Research*, 46(8):1–17.

Vox-Media (2018). How "levee wars" are making floods worse.

Vrijling, J. (2001). Probabilistic design of water defense systems in The Netherlands. *Reliability Engineering & System Safety*, 74(3):337–344.

Vrouwenvelder, A., van Mierlo, M., Calle, E., Markus, A., Schweckendiek, T., and Courage, W. (2010). Risk analysis for flood protection systems. Technical report.

Vrouwenvelder, T. (2006). Spatial effects in reliability analysis of flood protection systems. *International Forum on Engineering Decision Making*, pages 1–12.

Wagenaar, D. J., De Bruijn, K. M., Bouwer, L. M., and De Moel, H. (2016). Uncertainty in flood damage estimates and its potential effect on investment decisions. *Natural Hazards and Earth System Sciences*, 16(1):1–14.

Winsemius, H. C., Aerts, J. C. J. H., Van Beek, L. P. H., Bierkens, M. F. P., Bouwman, A., Jongman, B., Kwadijk, J. C. J., Ligtvoet, W., Lucas, P. L., Van Vuuren, D. P., and Ward, P. J. (2016). Global drivers of future river flood risk. *Nature Climate Change*, 6(4).

Wojciechowska, K., Pleijter, G., Zethof, M., Havinga, F., Van Haaren, D., and Ter Horst, W. (2015). Application of Fragility Curves in Operational Flood Risk Assessment. *Geotechnical Safety and Risk V*, pages 524–529.

Zhang, L. and Singh, V. P. (2019). *Copulas and Their Applications in Water Resources Engineering*. Cambridge University Press.

Zhang, L. M., Xu, Y., Liu, Y., and Peng, M. (2013). Assessment of flood risks in Pearl River Delta due to levee breaching. *Georisk*, 7(2):122–133.

ACKNOWLEDGEMENTS

As part of the EU System-Risk project, this research received funding from the European Union's Horizon 2020 research and innovation programme under the Marie Skłodowska-Curie grant agreement No 676027. I would also like to thank the institutes of TU Delft, Deltares, GeoForschung Zentrum, IHE Delft and the University of Bologna for their role in the completion of the work.

I was brazen enough to 'steal' hours and hours of time from colleagues and friends at these institutions, of whom special mention must be given to Ferdinand Diermanse, Sergiy Vorogushyn, Raymond van der Meij, Anke Becker, Dennis Wagenaar, Rob Brinkman, Frans Klijn, Michal Kleczek, Timo Schweckendieck, Oswaldo Morales Napoles, Hidde Elzinga, Attilio Castellarin, Alessio Domenegetti, amongst others. It has been a pleasure interacting with all of the colleagues from the System-Risk project, but Alessio in particular has been a fantastic friend while we struggled with similar concepts and issues during our PhDs. I have also been incredibly lucky to supervise two fantastic MSc students during this research, and I thank Federica and Odilia for their dedication and inspiration.

The biggest debt of gratitude is owed to my supervsor, Karin De Bruijn. She has shaped, examined and improved every aspect of the dissertation, and has done so with constant support and enthusiasm. Her knowledge and ideas were instrumental in providing content, but just as important were her manner and friendship, for which I am truly grateful. My promoter, Matthijs Kok, has also provided an endless supply of opinions, ideas, reflection and understanding, all washed down with a joyful demeanour and light-hearted laugh. Thank you both for your time, patience and help.

The dedication at the start of this thesis mentions that 'no man is an island'; an important point to remember in relation to both the academic and personal relationships when undertaking a PhD. Those who take your mind off the travails are equally important and I have to thank; football, tennis and volleyball teammates, London legends, Angeliki, my 'taalmaatje' Han, whatsapp jokers, party-goers and anyone that has sat me down for a beer, dinner or chat at some point. My family, of course, supported me since I was doing a crab-walk across the living room, and I owe Mum, Dad, Luke and our dearly missed Shane everything (and more). More recently, Sarah, Milo and Madeleine have been incredible additions to this big pantomine, and my beautiful wife-to-be, Milk, has kept the whole show on the road and done more for me than I ever could asked or imagined. Thank you all so much.

Curriculum Vitæ

Profile

Email: curran.alex@gmail.com
Phone: +31 62 7289688
DOB: 23rd of March 1988

Verwersdijk 100
Delft, 2611NK
Netherlands

I would like to apply the water resources modelling, risk analysis, data analysis and machine learning methods I acquired during my MSc and PhD and at the consultancy BMT WBM. I have good commercial and client experience from WBM and BAM Civil, and more recently at Rijkswaterstaat through my PhD. I have a strong affinity for problem solving, and I am comfortable with both independent and team projects. I think of myself as very social and a quick-learner.

Experience

Researcher at TU Delft
Ref: Roelof Moll
j.r.moll@tudelft.nl

Sep 2019 – Sep 2020: Researcher at TU Delft, working on the BRIGAID and SafeLevee projects.

Researcher at FRM, Deltares
Ref: Dr. Karin De Bruijn
Karin.deBruijn@deltares.nl

Sep 2016 – Sep 2019: While working on my PhD I have been involved with related projects such as KPP and the software developers of SOBEK, Probabilistic Toolkit and FIAT

Engineer at BMT WBM (UK)
Ref: Dr. Matthew Roberts
Mat.Roberts@bmtwbm.co.uk

Dec 2015 – Sep 2016: Worked on FRM, hydraulic and hydrological projects, specialising in modelling, visualisation, report writing and development of the TUFLOW software.

Engineer at BAM Contractors (Ireland)
Ref: Darren Devane
ddevane@bamcontractors.ie

Aug 2012 – Sep 2013: Engineer and Quality Manager for a large PPP project, communicating and developing procedures for the companies involved in the project: PPP company, contractor, client's representative and designer.

Volunteer at Ecological Sanctuary (Brazil)
Ref: David Hassett
davidh@digi.com

2006 – 2007, 2012: Over two 6-month periods I worked on ecological, administrative and design projects. I taught myself Portuguese and worked with a sea turtle project based in the region.

Education

PhD from TU Delft, (expected graduation: Oct 2020) **2016 - Current**

PhD in large-scale flood risk analysis, with publications in the fields of;

- Dike breach triggering in river system behaviour *Published*
- 2D schematisations in river system behaviour *Published*
- System behaviour applied to Po River, Italy *Published*
- Economic analysis of Dutch river system *Under review*

Prof. Matthijs Kok (Promoter) Matthijs.Kok@tudelft

MSc in Flood Risk Management, (overall grade: 8.6) **2013-2015**

I studied various hydroinformatics and water resource topics at the institutes of TU Dresden, IHE-Delft, UPC Barcelona, University of Ljubljana.

- The topics included; climatology, ecology, data-driven modelling, real-time control, river-basin modelling, fluvial morphodynamics and debris flow, drought, RADAR, spatial planning and socio-economic aspects of floods.
- MSc thesis on *'Representing model uncertainty in rainfall-runoff model pools for use in real-time forecasting'*.

Prof. Dimitri Solomatine (Academic Supervisor) d.solomatine@un-ihe.org

BEng in Civil Engineering, National University of Ireland, Galway **2007 - 2011**
(1st class honours)

Skills and achievements

Languages

- English as mother-tongue with courses in report-writing and presentation
- B1 level Dutch. Currently attending weekly meetings and planning new lessons.
- Spoken Portuguese and basic Spanish.

Other

- Awarded scholarships to high school, MSc and PhD programs.
- Class representative for my bachelor's degree, and vice-captain for the university tennis team.
- Captain of department football team
- Well-organised and efficient worker, with strong interpersonal skills.
- Paper published related to Machine learning in disaster-risk management.

Modelling	
Sobek	*****
HEC-Ras	****
TUFLOW	*****
GIS	
QGIS	*****
ArcGIS	***
Programming	
Python	****
Matlab	*****
XML	***
HTML	***

Interests

I am enjoying life in Delft, where I live with my girlfriend (who is also undertaking a PhD in water resources). We like travelling, board games, sport and of course evenings with friends.

List of Publications

Journal publications related to thesis

- **Curran, A.**, De Bruijn, K. M. and Kok, M., *Evaluating flood risk with a systems approach: a framework for scenario and sensitivity testing applied to the Netherlands*, in review. Submitted to *Risk Analysis* June 2020.

- **Curran, A.**, De Bruijn, K. M., Domeneghetti, A., Bianchi, F., Kok, M., Vorogushyn and S., Castellarin, A., *Large-scale stochastic flood hazard analysis applied to the Po River*, Natural Hazards, 2020

- **Curran, A.**, De Bruijn, K. M, Klerk, WJ. and M., Kok, *Large Scale Flood Hazard Analysis by Including Defence Failures on the Dutch River System*, Special issue on Flood Risk Analysis and Management from a System's Approach, Volume 8, Issue 11 (2019).

- **Curran, A.**, De Bruijn, K. M. and Kok, M., *Influence of water level duration on dike breach triggering, focusing on system behaviour hazard analyses*, Georisk: Assessment and Management of Risk for Engineered Systems and Geohazards, Volume 14 (2018).

Other publications

- Wagenaar, D., **Curran, A.**, Balbi, M., Bhardwaj, A., Soden, R., Hartato, E., Mestav Sarica, G., Ruangpan, L., Molinario, G. and Lallemant. D., *Invited perspectives: How machine learning will change flood risk and impact assessment*, Natural Hazards and Earth System Sciences, (2020).

- **Curran, A.**, De Bruijn, K. M. and Kok, M., *Influence of water level duration on dike breach triggering, focusing on system behaviour hazard analyses*, NCR Days 2018 - Book of abstracts.